DEPARTMENT OF ENGINEERING SCIENCE

UNIVERSITY OF WARWICK

A PRELIMINARY STUDY OF THE ANALYSIS OF REINFORCED CONCRETE PLANE FRAMES UNDER SUSTAINED SERVICE LOADS

A Thesis for the Degree of Doctor of Philosophy

by

Christopher S. Lewsley, BSc

April 1971

CONTAINS

PULLOUTS

ACKNOWLEDGEMENTS

This thesis is based on work which forms part of the research programme of the Building Research Station, Watford and is prepared by permission of the Director. The author wishes to thank his supervisor Dr R H Wood DSc, PhD, MICE, MIStructE for his constant help and encouragement during the course of this investigation. Thanks are also due to the Head of the Structural Engineering Division of the Building Research Station, Dr S C C Bate, BSc, PhD, FICE, FIStructE and the other members of staff who have shown an interest in the work.

A PRELIMINARY STUDY OF THE ANALYSIS OF REINFORCED CONCRETE PLANE FRAMES UNDER SUSTAINED SERVICE LOADS

ABSTRACT

Owing to developments in materials and in structural analysis, the control of deflection under service loads has recently begun to play a large part in the design of reinforced-concrete structures.

Creep and shrinkage of plain concrete has been the subject of a considerable amount of research during the last fifty years and there have been several studies of the behaviour of statically-determinate beams under sustained load. However, most reinforced concrete structures are statically indeterminate and the behaviour of this type of structure under sustained load has received very little attention. It is important to establish the main differences in time dependent behaviour of statically determinate and indeterminate structures under sustained load so that the validity of extending existing methods of calculation of long term deflection (developed with limited success for determinate structures) to indeterminate structures may be assessed.

This investigation is an experimental and theoretical study of the behaviour of statically-indeterminate structures under sustained service loads. All the experimental work was performed in a laboratory where the temperature and humidity were maintained constant. Concrete of the same mix proportions and strength was used throughout the programme and control shrinkage and creep tests were performed on the plain concrete. A theoretical study of the behaviour of plain concrete was made and compared with the experimental results.

The sustained moment-curvature relationships of two reinforced concrete cross sections was investigated experimentally over eighteen months. The investigation was limited to the service moment range. A typical beam cross section, whichwas 200 x 380 mm and reinforced with approximately 1.5%

of tensile steel, was studied using seven specimens each subjected to a different value of sustained pure moment. The curvature of each specimen was measured at intervals over eighteen months so that sustained moment curvature diagrams could be plotted. A typical column cross section, which was 200 mm square and reinforced with approximately 1% of steel symmetrically distributed was studied under combined sustained axial load and moment. Each specimen was subjected to the same value of axial load but a different value of sustained moment. The curvature and axial strain of each specimen was measured at intervals over eighteen months and sustained moment curvature diagrams plotted.

Computer programs were developed for the analysis of continuous beams and two storey single bay reinforced concrete portal frames under sustained service loads. The programs are based on a finite difference treatment of the basic equations of bending and include the effects of cracking in flexure and redistribution of moments under sustained load.

The behaviour of the individual cross sections of the frame is defined by moment-curvature data input to the computer which calculates the force and deformation fields at various times after loading.

Three full scale structures were tested under sustained service loads so that the results of the computer analysis could be compared with experimental results. Each member of each frame had one of the two cross sections tested under sustained load.

CONTENTS

PART 1. Introduction.

A. A Brief Review of British Standard Codes of Practice for Reinforced Concrete Design 1

B. General Discussion of the Problem 5

C. A Review of Previous Work 17

D. Object and Scope of Investigation 29

PART 2. Experimental Programme

A. General 31

B. Creep and Shrinkage Specimens 37

C. Sustained Moment Curvature Specimens 44

D. Full Scale Structures 66

PART 3. Theoretical Studies

A. Creep in Plain Concrete 96

B. Analysis of Reinforced Concrete Continuous Beams under Sustained Service Loads 105

C. Analysis of Reinforced Concrete Plain Frames under Sustained Service Loads 126

PART 4. Discussion

A. Creep in Plain Concrete 143

B. Moment-Curvature Relationships 158

C. Full Scale Structures 161

D. General Conclusions and Comments on Future Research 174

BIBLIOGRAPHY 180

PART 1 : INTRODUCTION

A. A Brief Review of British Standard Codes of Practice for Reinforced Concrete Design

The reasons for undertaking research into the behaviour of reinforced concrete under sustained service loads can best be seen in the light of the developments in Codes of Practice that have occurred since the publication of the DSIR Code in 1934 (1).

Under this Code, the structure was analysed elastically with 15% redistribution of moments in continuous beams. The basis for design of sections was also elastic for beams and slabs with variable modular ratio and permissible stresses. For axially loaded columns only an ultimate load method was used but with permissible stresses to give the service load. The permissible tensile stress in steel reinforcement in beams was limited to the smaller of 140 N/mm^2 and 0.45 of the yield strength. At that time the most commonly used reinforcing steel was mild steel with a yield strength of about 250 N/mm^2. The permissible compressive stress in concrete in bending was limited to 11 N/mm^2 for concrete with nominal mix proportions of 1:1:2. There was no direct reference to cracking or deflection under service loads although there were certain minimum depth requirements for flat slabs. Basically, this was a conservative design against collapse using materials of about half the strength of modern concretes and reinforcing steels. Consequently the permissible stresses were sufficiently low that strains under service loads need not be considered explicitly by the Code.

CP 114:1948 - The Structural Use of Normal Reinforced concrete in Buildings (2) contained the same methods of analysis of structures and design of sections. However, the limit on the permissible tensile stress in steel reinforcement in beams was increased to the smaller of 190 N/mm^2 and 0.5 of the yield strength.

The limit on the permissible compressive stress in concrete in bending was increased to 11.5 N/mm^2 for concrete with nominal mix proportions of 1:1:2. The Code contained a warning against excessive deflection and against cracking. However no limits on deflection or crack width were specified and no methods were given by which they could be calculated.

With the introduction of the current Code CP 114:1957 and the amendments of 1965 and 1967 (3), the ultimate load method of design of sections, previously only used for axially-loaded columns, was extended to beams and eccentrically loaded columns. The elastic design method was retained as an alternative. Also yield-line analysis of slabs was permitted. The limit on the permissible tensile stress in steel reinforcement in beams was increased to the smaller of 210 N/mm^2 and 0.5 of the yield strength. At present, the most commonly used reinforcing steel has a yield strength of about 415 N/mm^2. The limit on the permissible compressive stress in concrete in bending was increased to 19 N/mm^2 for designed concrete mixes. The Code defines maximum span/depth ratios for beams and slabs for several combinations of concrete and steel strength. These ratios were intended to prevent undesirable deflections occurring under service loads. In short, the stage had been reached where although a structure may have an acceptable factor of safety against collapse it could still become unserviceable due to excessive deflections under service loads and span/depth ratios were introduced to prevent this. Excessive deflection under service loads had come to be recognised as failure. The Code retained the warning against excessive cracking. No methods were given by which deflections or crack widths could be calculated.

Consequently, refinements in design against collapse, a gradual reduction in factors of safety, and an increase in material strengths by a factor of about 2 without corresponding increases in modulii of elasticity have combined to lead to an increase in the importance of the behaviour of reinforced concrete under sustained service-loads.

The realisation that the design of reinforced concrete to provide an adequate factor of safety against collapse no longer largely guaranteed serviceability is reflected in the Limit State approach to design which has been developed in Europe since about 1955 (4), (5). In Limit State Design the design process must ensure the achievement of an acceptable probability that the structure does not become unfit for use during its specified life. In any structure, unfitness for use may arise in three principal ways; they are collapse, excessive deflection or excessive cracking.

The latest draft of the Unified British Standard Code of Practice for Structural Concrete, which will replace CP 114:1957, is written along Limit State lines and contains a more detailed span/depth ratio approach for control of deflection and formulae for the calculation of crack width under sustained service-loads. The span/depth ratios are based on experience of structures in service and an appraisal of experimental data (6) relating mainly to simply-supported beams. The experience of structures in service was gained partly abroad where structures are designed by other Codes and are in service under different climatic conditions and partly in Britain where structures were designed to a Code of Practice more conservative than the draft Unified Code. The formulae for the calculation of crack width are largely based on experimental data relating to crack widths under pure bending moment (ie in the absence of shear) (7). The draft Unified Code limits the final deflection of beams (including the effects of temperature, creep and shrinkage) measured below the as cast level of the supports to span/250. However it concedes that greater deflections may be acceptable provided the appearance and efficiency of the structure is not impaired and that for particular structures span/250 may be too large. The draft Code also suggests a limit of the lesser of span/350 or 20 mm to the part of the deflection which occurs after construction of the partitions and application of the finishes.

In addition the draft Code contains a warning regarding lateral deflections particularly of tall slender structures. Cracking is considered in some detail and a general limit on surface crack width of 0.3 mm is recommended. Where members are exposed to particularly aggressive environments surface crack widths at points nearest the main reinforcement should not exceed 0.004 times the minimum cover to the main reinforcement. Consequently, when the Unified Code comes into force designers will be required to pay considerable attention to the serviceability limit state. In many cases serviceability will govern design.

A further point emerging from the draft Unified Code is that permissible deflection depends very much on the use to which the structure is to be put, the finishes used and the location on non-loadbearing partitions. Clearly therefore, a blanket span/depth ratio approach must be conservative but cannot guarantee freedom from deflection problems. In a great many cases it will be unnecessarily conservative.

Steels with yield strengths of 550 N/mm^2 and 690 N/mm^2 are now being introduced into use in reinforced concrete; these steels have the same modulus of elasticity for design purposes as mild steel. Concrete strengths continue to increase; the modulus of elasticity of concrete is approximately proportional to the square root of its cube strength. Design against collapse continues to be further refined. There is no doubt that the importance of design against excessive deflection under service loads will increase (8).

B. General Discussion of the Problem

The behaviour of a reinforced concrete structure under sustained service loads is greatly influenced by the force and deformation fields which exist immediately after loading. Consequently the response of reinforced concrete to the application of load is an important part of the problem.

In order to clarify some of the main points a brief discussion of the behaviour of plain concrete is given. This is extended through the behaviour of reinforced concrete cross sections to reinforced concrete plane frames. The discussion is limited to the service load range and to structural members whose size and reinforcement are typical of those found in a reinforced concrete frame.

(a) Behaviour of Plain Concrete

The response of plain concrete to compressive stress is normally taken to be linear up to about one third to one half of the crushing strength and the modulus of elasticity is roughly proportional to the square root of the crushing strength. For most practical purposes the modulus of elasticity in tension can be taken as equal to the value in compression. Failure in tension is more brittle than failure in compression. Thus the response to tensile stress is linear up to a higher fraction of the failure stress and the departure from linearity is less marked. The tensile strength of concrete is only about one tenth of the crushing strength.

Concrete under sustained load is subject to a time-dependent deformation which can be somewhat artificially but quite often usefully divided into two parts which are known as shrinkage and creep. Shrinkage is a shortening which is independent of externally applied stress and is associated with the

drying out of the concrete. The most important source of shrinkage is the drying which follows casting as the concrete seeks to achieve hygral equilibrium with its environment. This may occur over a period of years although for normal size structural members in sheltered summer time conditions in Britain about half the shrinkage will occur in the first month and three quarters in the first six months. If dried out concrete is saturated and re-dried, the expansion and contraction will be substantially equal but will only be about one half to two thirds of the shrinkage on first drying. The amount and rate of shrinkage due to first drying out are most influenced by member size, mix proportions, environmental conditions and occasionally aggregate type. Shrinkage is of considerable importance, not only as a source of unacceptable deformations, but also, under conditions of restraint, as a potential cause of cracking in concrete.

Creep in dependent upon externally applied stress. Concrete under a stress suddenly applied and then kept constant will exhibit, besides the immediate strain, a further time-dependent strain or creep which may continue for several years and become several times greater than the original immediate strain. For stresses up to about one third to one half of the crushing strength the creep strain at any time after loading is approximately proportional to the sustained stress. On removal of load after a period of sustained load concrete exhibits, in addition to the immediate strain, a small amount of time-dependent recovery. A typical creep-time curve is shown in diagram 1. In normal size structural members in sheltered summer time conditions in Britain about half the creep will occur in the first month and three quarters in the first six months. The amount and rate of creep are most influenced by mix proportions, environmental conditions and stress-strength ratio. Creep is of considerable importance in reinforced concrete design not only as a cause of unacceptable deformations but also, under conditions of restraint, as a

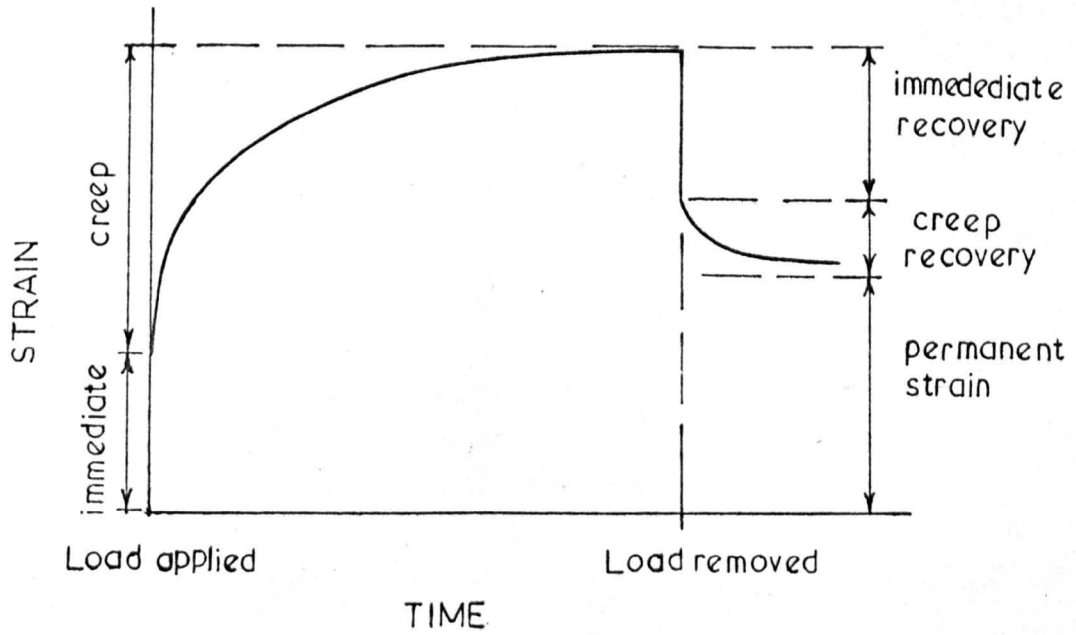

DIAGRAM 1: Typical Creep - Time Curve

mechanism that relieves stress.

It is usual in investigating the deformation of plain concrete under sustained load to measure the deformation of "identical" unloaded specimens. The deformation of the unloaded specimens is taken as the shrinkage and this is subtracted from the deformation of the loaded specimens in order to obtain the creep deformation. This approach certainly leads to a great simplication and is of great value from the design point of view. However creep will affect internal stresses developed in externally unrestrained plain concrete during drying out and curing and it is accepted that a large proportion of both creep and shrinkage is due to various forms of moisture movement. Consequently in considering the fundamental aspects of time strains it is at least as false to divide the deformation in this way as it is to consider the total strain.

(b) Behaviour of Reinforced Concrete Sections

For a reinforced concrete cross section in pure bending the strain distribution both before and after cracking is approximately linear as shown in diagram 2. The strain distribution referred to is measured over a gauge

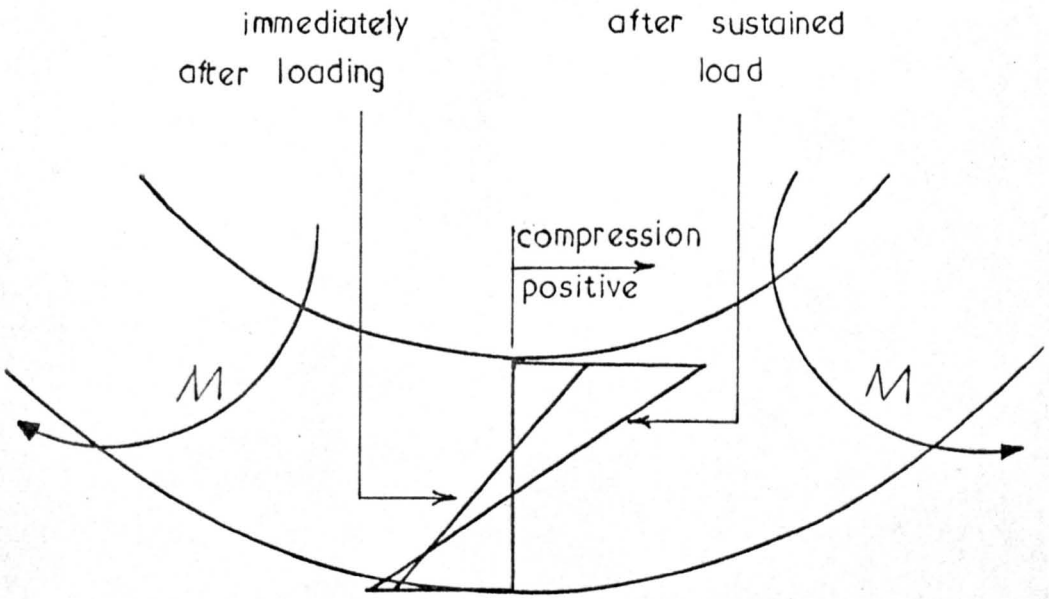

DIAGRAM 2: Strain Distribution in a Cracked Reinforced Concrete Beam

length of several centimetres and thus is an average of cracked and uncracked sections. The moment curvature relationship in the service moment range can be taken for most practical purposes to be bi-linear; the discontinuity is caused by cracking of the tensile concrete. There is no doubt that there is a degree of non-linearity associated with the moment-curvature relationship since the tensile concrete is stressed into its non-linear range and in addition bond slip between tensile reinforcement and the concrete occurs. Also cracking does not lead to a simple "point" discontinuity but occurs

over a small range of bending moment. However for practical purposes these complications can be neglected. Before cracking most of the tensile force is provided by the concrete. After cracking the tension at the cracked section is supplied almost entirely by the reinforcement and between the cracks a large part of the tension is supplied by the reinforcement due to bond breakdown. As the bending moment is increased after cracking most of the increase in strain appears in the cracks. For beams with modern steel percentages the cracking moment is normally about one fifth to one third of the service moment. Cracking produces a sudden decrease in the stiffness of the tensile part of the beam whilst leaving the compression part largely unaltered. It is true that the stiffness of the compression part will also decrease as the neutral axis rises but this decrease is small relative to the large change which occurs in the tensile part. The reduction in beam stiffness which occurs on cracking is thus mainly due to a reduction in stiffness of the tension part and consequently tensile-steel percentage plays a dominant part in defining the after cracking stiffness. In cracked members therefore tensile-steel percentage is a major influence on the deflection immediately after loading.

When a cracked length of beam is subject to sustained moment there is an increase in strain in the compression zone due to concrete creep but a much smaller increase in strain in the tension zone as much of the tension is provided by the steel reinforcement which is not subject to significant time-strains in the service stress range. There is however a small increase in tension strain owing partly to creep in tension in concrete and partly to creep in bond. Thus the strain distribution will change as shown in diagram 2. Notice the increase in the depth of the strain neutral axis; it frequently moves below the tops of the cracks. The curvature of the section is equal to the gradient of the strain diagram with respect to the line of zero strain and can be seen to have increased. However it can be seen that the dominant

influence on the time dependent part of the deflection of a cracked reinforced concrete beam is exerted by the compression part of the beam. This is in sharp contrast to the situation regarding deflection immediately after loading.

In an uncracked length of beam much more of the tensile force is borne by the concrete and consequently under sustained moment there is a greater increase in tensile strain, per unit moment, than for the cracked case. This is reflected in a much greater increase in curvature per unit moment in an uncracked beam than in a similar cracked beam. There is no precise information available on this but it appears that the benefit which uncracked lengths of beam may have on deflection is only temporary.

The argument regarding uncracked lengths of beam can also be extended to columns in combined axial load and bending. Under full service loads columns are usually uncracked in flexure and beams are usually cracked over most of their length. Thus under sustained service loads it can be expected that column curvatures will increase more rapidly than beam curvatures per unit moment. In other words column stiffnesses will decline with time relative to beam stiffnesses. Stiffness is here intended to mean the stiffness with regard to the sustained loads and no comment is intended regarding the stiffness of members under sustained load to further load changes.

The presence of reinforcement in the compression zone of a member will reduce creep of the concrete by reducing the stress on the concrete. As creep occurs the stress on the concrete will reduce and the stress on the steel will increase. Thus the increase in curvature of a beam containing reinforcement in the compression zone is generally less than a similar beam reinforced in tension only subjected to the same moment.

On removal of load after a period of sustained load reinforced concrete exhibits, in addition to the immediate strain, a small amount of time-dependent recovery. Thus for a reinforced concrete cross section an axial strain-time or a curvature-time curve can be plotted which is similar in form to the strain-time curve for plain concrete under axial load.

Shrinkage of concrete will produce a shortening of a member and if unsymmetrical reinforcement or unsymmetrical environmental conditions are present shrinkage will lead to warping. The shrinkage warping of a structural member due to unsymmetrical reinforcement usually produces a curvature of the same sign as that due to load. However the most important influence of shrinkage is frequently the apparent reduction in tensile strength of concrete which results from the build up of tensile stress due to restraint. This can lead to a serious reduction in the cracking moment.

The response of a reinforced concrete cross-section to moment can be conveniently defined in the form of the moment-curvature relationship. The response after any period of sustained moment can be defined by a sustained moment-curvature relationship.

(c) Behaviour of Reinforced Concrete Structures

(i) Statically Determinate. In a statically determinate structure the force field can be calculated by simple statics and is not influenced by the properties of the member cross sections. Consequently the force field is time independent.

If the sustained moment-curvature response of the cross sections is known then the curvature distribution at any time can be found and since deflections are the double integral of curvatures the deflection profile can be computed.

(ii) Statically Indeterminate. The majority of structures are statically indeterminate. This means that the force field depends upon member properties and thus to some extent the force field is time dependent.

Two causes of time dependent moment redistribution may be seen in the light of the simple "moment distribution" method of structural analysis as applied to reinforced concrete frames. The analysis procedure is to work out the fixed-end moments for every member and then to distribute any out of balance moment at the joints according to the relative stiffnesses of the members framing into the joint. Member stiffness depends upon cross section properties and consequently the relative stiffnesses may be time dependent. For example, it has already been explained that column stiffnesses are likely to decline relative to beam stiffnesses. This will clearly lead to a change in relative stiffnesses at a joint and consequently to time-dependent moment redistribution. Also, if two beams frame into a joint and one contains steel in the compression zone and one does not, then the stiffness of the first member will increase with time relative to the stiffness of the second member and again moment redistribution will result. The magnitude of the moment redistribution from this source will depend upon the magnitude of the change in relative stiffnesses and the magnitude of the out of balance moment. Analysis of a reinforced concrete frame during design against collapse is often performed elastically as this is known to approximate to a lower bound solution provided secondary (ie buckling) effects are small. In doing this relative stiffnesses are usually calculated on the concrete section throughout. It is realised that as collapse is approached, beams will generally be cracked and columns uncracked and the relative stiffnesses assumed during design will not apply. However for the type of frame geometry and loading distributions usually met in practice the errors introduced by the approximations during design are generally small and easily covered by the factor of safety. It

is worth bearing in mind that this may not be the case especially since the estimation of stiffness on the concrete section throughout tends to lead to an under-estimation of the moments in columns, which are the more critical elements of a frame. In calculating deflection a much more accurate determination of the distribution of moments is required. It should be remembered that in calculating the downward deflection of a beam the procedure is usually to calculate the downward deflection due to the free moment and subtract the upward deflection due to the continuity moments. Consequently the deflection of a beam is often the difference of two much larger quantities; in short, an error of 10% in estimating the continuity moment can easily produce an error of 30% - 40% in the calculation of downward deflection. Thus the relative stiffness changes produced by cracking and time strains are very important if a realistic estimate of deflection is to be made. In order to clarify the influence of stiffness and initially out-of-balance moment on the final moment distribution diagram 3 contains a graph showing the influence of these factors on a simple frame. A second cause of moment redistribution affects the fixed end moments. The formulae used to calculate fixed-end moments have become so well known that they themselves tend to be regarded as "fixed". It should be remembered that if, for example, the stiffness of the support zone of a member differs from the stiffness of the midspan zone (quite a common situation in practice) then the fixed end moment will be a function of the relative stiffness of these zones. If the midspan zone is cracked and the support zone is uncracked, this again will affect the value of the fixed-end moment. If the time properties of one zone are different to the other zone, owing for example to the presence of compression steel in one zone but not the other, the fixed-end moments will be functions of time. Again, in order to clarify this point diagram 4 contains a graph showing the influence of the relative stiffness of support and midspan zones on the value of the fixed-end moment. Since an accurate estimation of the continuity moment is necessary in the calculation of deflection, this point must be borne in mind.

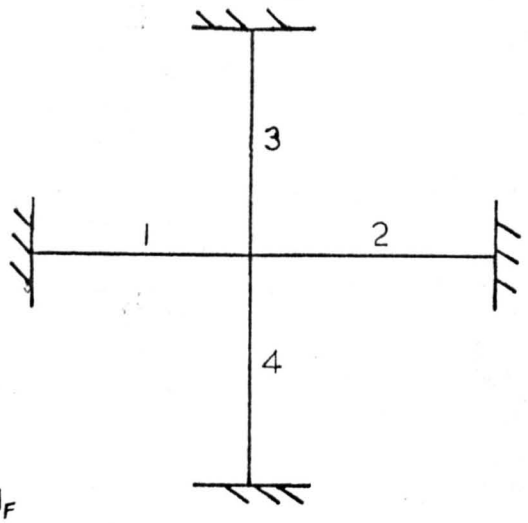

$M = \alpha M_F$

where, M = bending moment at joint in any member
M_F = fixed-end moment of same member
ΔM = initially out of balance moment
K = member stiffness
α is a factor defined below

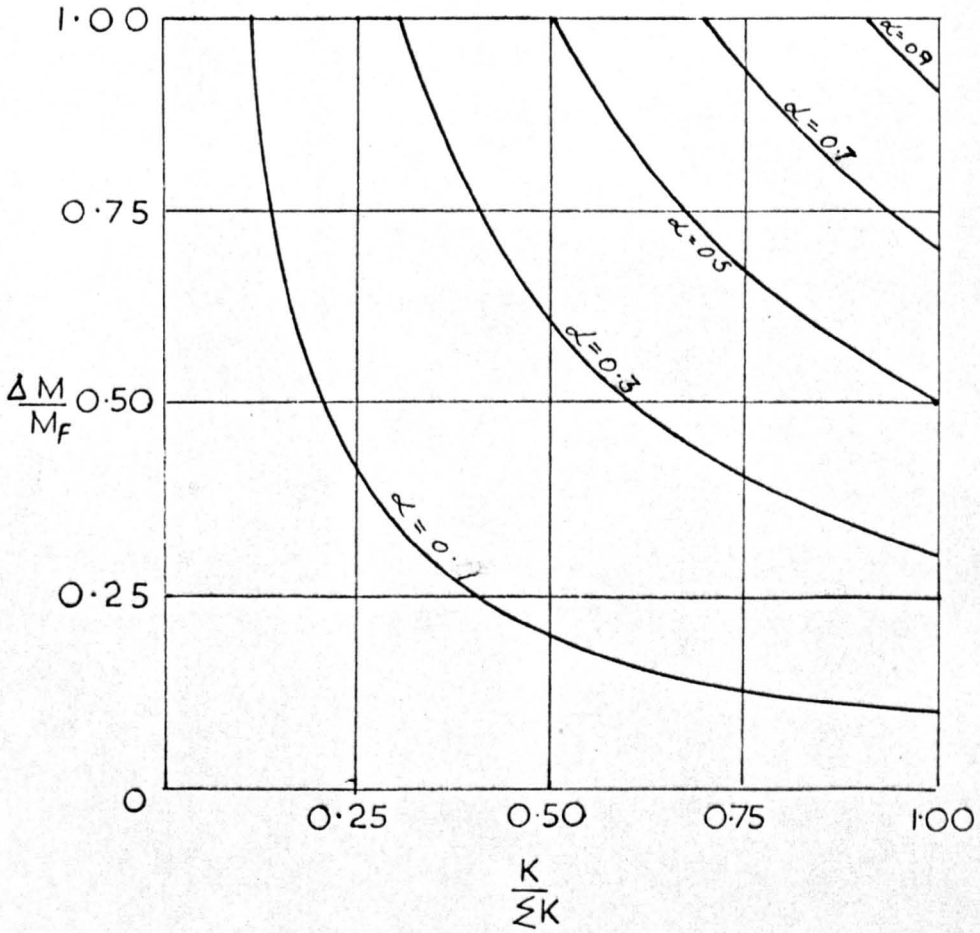

DIAGRAM 3: Bending Moments in a Simple Frame

Beam under uniform load

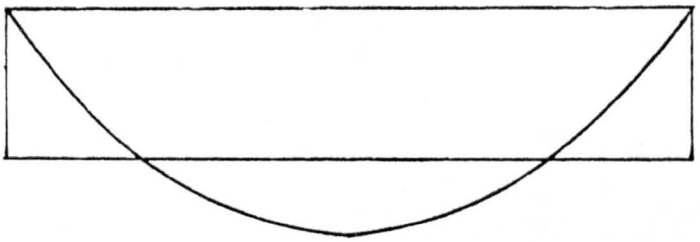

Bending moment distribution

η_1 = flexural rigidity in negative moment zones
η_2 = flexural rigidity in positive moment zone
M_F = free bending moment
M_S = support moment

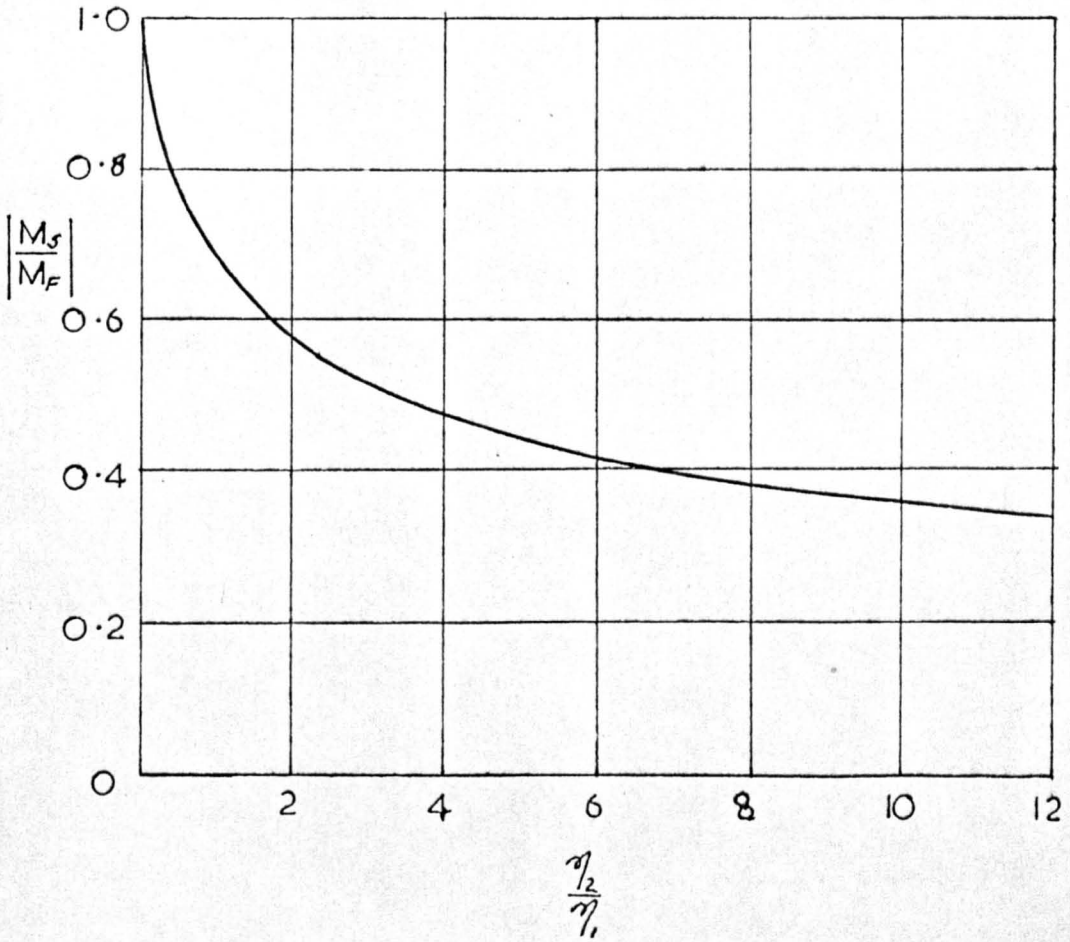

DIAGRAM 4: Fixed-end Moments in Non-uniform Members

There are several other causes of time-dependent moment redistribution but their effects are usually small. For example restraint to shrinkage warping leads to the generation of a secondary force field; in columns the moments due to lateral deflection increase with time as the deflections increase and the effects of this are transmitted to beams.

C. A Review of Previous Work

The problem of creep and shrinkage in plain and reinforced concrete has been investigated since the early part of this century. Plain concrete has received the greater amount of attention partly because it is the logical starting place to understanding the whole problem and partly due to the difficulty of testing full-scale reinforced concrete members under sustained load. There have been a considerable number of publications concerning creep and shrinkage and it is not possible to discuss them all. However, sufficient number will be reviewed to show the developments in understanding since the early part os this century and the extent of knowledge to-day.

One of the first major investigations was conducted at the Building Research Station by Glanville (9), (10) and later by Glanville and Thomes (11). This work, which was published in the early 1930's, established some of the basic facts concerning shrinkage and creep. For example they recognised that during shrinkage of reinforced concrete restraint would be exerted on the cement paste by inert pieces of aggregate and by reinforcing steel leading to the development of stresses which would be continuously moderated by creep. Shrinkage warping due to the presence of unsymmetric reinforcement was discussed and the significant compressive stresses which can be induced in reinforcing steel by shrinkage of concrete were measured. Sustained load tests on plain concrete were also performed and an approximately linear relationship between creep strain and stress was observed for stresses up to about one third of the crushing strength. The influence of cement type was investigated and the conclusion reached that the more rapid hardening the cement the smaller the creep. It was observed that the creep is considerably lower for specimens of Portland cement concrete maintained wet than for similar specimens stored in air and that creep decreased as the age at loading increased. Glanville and Thomas also investigated the behaviour of small reinforced concrete columns

under sustained load and measured the time-dependent increase in compressive stress in the reinforcement due to concrete creep.

Glanville and Thomas published a further paper in 1939 (12) which contained results relating to the possible limiting values of creep and proposed a relationship between creep strain and time, which is essentially exponential in form and thus gives a finite limiting value for creep at infinite time. They also investigated creep in tension and concluded that for practical purposes creep is the same for compressive and tensile stresses of the same magnitude. Lateral creep was also measured and it was concluded that loading a specimen in compression may cause considerable longitudinal creep without any appreciable lateral creep.

At about this time thought was being given to the mechanisms of creep and to devising a mathematical relation to fit creep data. Glanville and Thomas's view was that concrete is composed of two distinct constituents, one of which flows under load, but in which the rate of flow or viscosity changes with time, and the other of which is solid, and undergoes elastic changes only.

In 1937, Ross (13) discussed the mechanisms of creep as well as reviewing previously proposed mathematical relationships for creep and suggesting his own. Ross considers that the major part of creep is due to colloidal seepage in the gel with some crystalline creep in the aggregate and viscous flow of the gel. A mathematical expression for creep suggested by Shank (14), which was in fact a linear relationship between log creep-strain and log time, was discussed by Ross who criticised the expression on the grounds that it shows deformation under stress to increase progressively for all time. Ross preferred an equation which showed a limit to creep and pointed out that this could only be achieved by Shank's expression if a revision of the constants were made as time increased. There does not appear to have been any

experimental data to support the idea of a discontinuous log creep - log time plot and, after disposing with Thomas's expression on the grounds that it was too complicated, Ross suggests a hyperbolic relation. A hyperbolic form is simple, mathematically continuous and has a limiting value for creep strain; it therefore has many advantages from the practical point of view. Theoretically, however, there is no reason why creep should be mathematically continuous or have a limiting value. This is the first example of a theme which is recurrent throughout creep and shrinkage literature, namely that there is a conflict between producing expressions of practical value and producing expressions which reflect an understanding of the behaviour of concrete.

In 1946, Ross began to consider the effects of creep on indeterminate structures (14). He pointed out the effect creep would have on instability in columns and demonstrated this using plastic models. With regard to indeterminate beams Ross states "If the supports of an externally redundant structure are rigid, then the analysis can proceed without any knowledge of Young's modulus. For this reason it was thought that moments and forces in such a structure would not alter because of creep and tests on continuous beams and two-pinned arches demonstrated this quite clearly." This statement does not apply to reinforced concrete statically-indeterminate structures. As discussed earlier a change in the moment field in a continuous beam can most certainly occur under sustained load in certain fairly common circumstances; presumably Ross is referring to tests on plastic model beams which were homogeneous throughout.

In 1943, McHenry (15) emphasised the importance of creep recovery and stated a Principle of Superposition as "The strains produced in concrete at any time t by a stress increment applied at any time t_0 are independent of the effects of any stress applied earlier or later than t_0". Thus the state of strain

of concrete at any time is a function not only of the forces acting at that time, but of the entire past stress history. The influence of moment history is important when considering the effects of time-dependent moment redistribution in statically indeterminate structures.

In 1946 a review paper was published by Lea and Lee (16) which described the then current knowledge of creep and shrinkage and discussed theories regarding the underlining mechanisms. The use of dashpot and spring models to visualise creep and to obtain equations for creep strain was considered. However, it was recognised even then that, in order to produce a model which fitted most aspects of creep behaviour, quite complicated combinations would be required.

By the 1950's there were three principal theories regarding the mechanisms of creep. The first of these, termed the plastic theory of creep, suggested that creep was due to crystalline flow, ie slipping along planes within the crystal lattice, as is the case with metals. There was some support for this but two main objections which were that there appears to be no stress below which creep does not occur (there is with metals), and, most important, concrete exhibits considerable volume change during creep whereas metals do not. Also the marked influence of humidity on creep is difficult to explain in terms of crystalline flow. However, crystallographic work indicated the possibility of both inter- and intra crystalline movement. The second mechanism was termed viscous flow and involves the movement of particles one over the other. It was thought that viscous flow of the more fluid phase of the concrete lead to a general increase in stress on the more solid phase of the concrete. A principal objection to this is that viscous flow would imply constant volume whereas creep of concrete includes substantial volume change. The third mechanism is seepage of water from the cement gel. This explained well creep under compression but clashed badly with experimental evidence regarding creep in tension. The seepage theory would

lead one to expect that creep in tension would involve the concrete taking in water and therefore that creep in tension in water would exceed creep in tension in air. However experimental evidence showed tensile creep in water to be about ten times smaller than tensile creep in air.

The main theories of creep which existed in 1955 were discussed by Neville (17). There had been a growing feeling that creep had more than one mechanism, and Neville came out strongly in favour of this, stating that creep is due to viscous flow and seepage. Crystalline flow he considered to be negligible, at least under service stresses. It is not clear what proportion of creep Neville attributes to viscous flow and what proportion to seepage (presumably this would depend upon the mix proportions and environmental conditions) but he gives the impression that viscous flow is at least as important as seepage. This is a slightly different view to that held by Ross in 1937 who stated that the major part of creep is due to seepage. However, there is a great similarity between seepage and viscous flow. When seepage produces removal or rearrangement of internal moisture the "structure" of concrete deforms, presumably by a mechanism similar to viscous flow. In other words, viscous flow in the usual sense is deformation under external loading whereas seepage can be seen as viscous flow caused by the removal of internal supports.

In the 1950's also, reports of major investigations on the influence of sustained load on full-scale beams and columns began to emerge. Voist, Elstner and Hognestad investigated the influence of sustained load on the strength of eccentricially loaded columns (18) and Washa and Fluck investigated the creep of reinforced concrete beams under sustained service-loads (19), (20). Washa and Fluck measured the long term strains of simply supported beams under uniformly distributed sustained service-load for two and a half years. They concluded that, at the end of the loading period, the average creep compressive strain for beams with no compression steel was slightly more

than four times the immediate elastic strain, while the average for beams with an area of compression steel equal to the area of tensile steel was slightly more than twice the immediate elastic strain. The compression steel was undesigned, that is it was not included in the ultimate load or service-load calculations. Washa and Fluck also investigated the behaviour of two span continuous beams under sustained load for two and a half years. They measured the central reaction and showed that it increased with time. All the beams they tested were symmetric about the central support with respect to geometry, load and reinforcement and all beams contained reinforcement in the compression zone at the support. It was in the midspan reinforcement that the beams differed; some had no steel in the compression zone, some had an amount equal in area to half the tensile steel area and some had an amount equal in area to the tensile steel area. The beams with no steel in the midspan compression zone showed an increase in central support reaction of about 5%; the beams with an area of steel in the midspan compression zone equal to half the midspan tensile steel showed an increase in central support reaction of about 3%; the beams whose midspan compression zone contained reinforcement equal in area to the midspan tensile steel showed an increase in central support reaction of about 2%. An increase of 1% in the central support reaction implies a decrease of about 3.5% in the maximum positive moment (at midspan) and an increase of about 4.5% in the maximum negative moment (at the central support). Clearly this time-dependent moment redistribution could not be ignored if an accurate assessment of long-term deflection is required. The reason for the moment changes with Washa and Fluck measured can be understood with reference to the simple "moment distribution" method of structural analysis. The redistribution was due to a change in the relative stiffness of the midspan and support zones which produces a change in the fixed-end moment; this is why the effect was more marked with the beams having no steel in the midspan compression zone since in all beams the support region contained steel in the compression zone.

The fact that a change in support moment produces a much smaller change in support reaction is one of the difficulties of measuring the magnitude of time-dependent moment redistribution.

In 1958 Ross considered three methods of computing creep strains under variable stress from constant stress data (21). The principles embodied in these methods are relevant to the calculation of creep curvatures under variable moment from constant moment data. The first of these techniques is called the "effective modulus method" and involves the normal procedures of structural mechanics but the elastic modulus is replaced by a reduced value called the effective modulus which allows for both elastic and creep strains. This method is simple and easy to use but disregards stress history; the ultimate strain predicted depends only on the ultimate stress and consequently in situations where the stress decreases with time the effective modulus method will underestimate the strain after long periods. However if stress changes are known to be small, the simplicity of this technique makes it preferable to the other two. Ross calls the second technique the "rate of creep method" and this is based on the assumption that the amount of creep in a small increment of time is a function only of the stress at the beginning of that time. Thus the rate of creep method neglects stress history; under a declining stress the strain is overestimated. Ross concludes that under large changes of stress the rate of creep method gives more accurate results than the effective modulus method and consequently the extra work involved is justified. The third method is an application of the principle of superposition stated by McHenry in 1943. It is the most accurate method but involves a considerable amount of work and requires a great deal of experimental data.

Also in 1958 a paper by Freudenthal and Roll (22) appeared which was concerned with creep and creep recovery of concrete under high compressive stress.

The approach used differs from those used in the papers discussed so far. Freudenthal and Roll collected experimental data relating to creep and creep recovery and devised a spring and dashpot model (consisting of a Maxwell element in series with three Kelvin elements) whose behaviour was a close approximation to that of the concretes they had tested. The eight constants defining the behaviour of the model were then deduced from the experimental data and the differential equation derived from the model was integrated and compared with the experimental data. The equation they arrived at is remarkable in its complexity.

A paper presenting experimental data relating to creep and shrinkage and collected over a period of 30 years was published by Troxell, Raphael and Davis in 1958 (23). They investigated a wide range of variables and showed that creep was still occurring in measurable amounts after twenty years of sustained load.

In 1959, Neville investigated the creep of mortar (24) and made an important conclusion. He emphasised the influence of the stress-strength ratio on creep and some other variables (ie fineness of cement and cement type) appeared to Neville only to influence creep of mortar in so far as they influenced strength. Neville also investigated creep recovery (25) and showed that while the principle of superposition of strains represents a convenient working assumption, the principle is not strictly true, and creep recovery may be influenced by factors other than those discussed by McHenry. An important result of Neville's work is that he showed that creep of mortar could occur in significant amounts without moisture loss to the environment. This he considered to be due to the internal rearrangement of moisture. It had been recognised earlier by Neville (17) that part of creep of concrete was due to viscous flow of mortar with a gradual transfer of load to the aggregate. He now recognises a component of creep in mortar as being due

to moisture movement internally, presumably with a transfer of load to a more solid phase. This action of the movement of a more fluid phase shedding load on to a more solid phase thus occurs at several levels in concrete. In other words, what is at one level the more fluid phase (ie mortar is more fluid than aggregate) can itself be broken down into fluid and solid phases.

Methods of calculating deflections of reinforced concrete beams were reviewed by Yu and Winter in 1960 (26). For estimating deflection immediately after loading two techniques were discussed which were both based on elastic theory but differed in the method of calculation of the second moment of area. The first method calculated the second moment of area in the cracked transformed section and made no allowance for tensile concrete. The second method included a correction factor (largely empirical) which allowed for the effects of the tensile concrete between cracks. In continuous beams the average of the second moment of area at the support and midspan zones is taken. For the calculation of long-term deflection the effective modulus method is used and compared with a table of coefficients for multiplying instantaneous deflection. The source of the table of coefficients is not given. Despite the many limitations of these methods (these were discussed earlier), most of the test results available to Yu and Winter differ by less than $\pm$ 20% from the calculated values. However, since the calculation procedures were developed empirically using the experimental data, this agreement is not surprising but the general applicability of these methods must be uncertain in view of their theoretical limitations.

In 1962, Gesund investigated the influence of sustained moment on the curvature of a cracked cross section of a reinforced concrete beam including the effects of creep and shrinkage but assuming zero tensile strength of concrete (27). He arrives at the conclusion that the sustained moment curvature relationship is slightly non-linear but that the non-linearity

is small. Gesund emphasises the importance of shrinkage warping especially under loads which are just large enough to crack the concrete on the tensile side of the member. This is the first of several similar investigations which will be reviewed here. In 1966, Arutyunyan considered the deformation on an uncracked cross section of a reinforced concrete beam reinforced in tension only (28); he assumed the concrete to behave as a linear visco-elastic material. Sackman and Nickel (29) using similar techniques, examined the long-term deformation of a cracked cross section of beam; they neglected shrinkage and the tensile strength of concrete. In 1969, Leong and Warner (30) also investigated the long-term deformation of a cracked cross-section of beam but included shrinkage effects; they use a slightly different differential equation to represent the behaviour of concrete. Leong and Warner concluded that for a cracked reinforced concrete beam the assumption of a linear relationship between moment and curvature at all times is satisfactory for most purposes. All these investigations involve assumptions which simplify the problem but are questionable. For example, for cracked sections the tensile strength of concrete is neglected both below the neutral axis at the cracked section and between cracks and stress concentrations around cracks are ignored. A very approximate equation is used to represent concrete behaviour and stress history is not considered. Also, it is well known that the curvature of a cracked reinforced concrete section at any bending moment depends very much on whether it is the first application of load or whether the section had been cracked under previous loading; in the investigations just discussed it is not clear which situation is being considered. Consequently, experimental tests provide the most reliable means of obtaining the long-term moment curvature response of a reinforced concrete cross section.

In 1965, England and Illston (31) introduced a new method of computing creep under variable stress from constant stress data. This work was basically an extension of that published by Ross in 1958. The new technique is called the rate of flow method and is based on a consideration of two components of creep (32), (36). The first component is called flow and is a time-dependent irrecoverable strain so that its rate of occurrence at any particular time after loading is independent of the previous stress history. The rate of occurrence is proportional to the applied stress and under constant stress it diminishes as the concrete ages. The second component is a delayed elastic strain which is fully recoverable on removal of the applied stress. Its properties are the same regardless of whether it is developing, following the application of stress, or being recovered, following the removal of stress. The delayed elastic component is further divided into rapid and slow elastic strains. The constants defining the contribution of each of these components of creep is determined experimentally. The technique of the rate of flow method is then very similar to the method of superposition (Ross, 1958) except that the rheological treatment outlined above greatly reduces the required experimental data. England and Illston present experimental data to which the rate of flow method gives slightly better agreement than the method of superposition.

In 1965, Branson presented a review of existing methods of deflection calculation and some data from long-term service load tests on reinforced concrete simple and continuous beams (33). He concluded that most of the methods reviewed provide rough estimates of reinforced concrete beam deflections but owing to the complex behaviour of reinforced concrete a great deal of judgement is required in many cases. This conclusion can also be drawn from the tests of Hajnal-Konyi (34) and Corley and Sozen (35). The continuous beams tested by Branson were two span beams, symmetric about the centre support and having the same (inverted) section at support and midspan.

Consequently moment redistribution effects were negligible.

In 1967, England, wording under the direction of Ross at Kings College (37), published a paper concerned with creep in concrete structures in which he states in the first paragraph "At uniform temperatures the effective modulus method provides a suitable method of analysis for structures under sustained loads, where strains continue to change with time but stresses are constant. Such conditions apply to statically determinate and indeterminate structures where supports are rigid and no imposed displacements exist." This is the view put forward by Ross in 1946 (14). It must be emphasised that England's statement is not true for reinforced concrete structures (perhaps he intended his remarks to be limited to plain concrete). Apart from the internal stress redistributions which occur at a cross-section in any reinforced concrete beam, it has been discussed earlier how time-dependent moment redistribution occurs in some common structures and Washa and Fluck (20) have measured it.

D. Object and Scope of Investigation

Nowadays, serviceability plays a large part in the design of reinforced concrete structures and its importance is likely to increase in the future.

The control of deflection by specifying limiting span/depth ratios which are necessarily conservative will lead to uneconomic use of both steel and concrete and yet cannot prevent serviceability failure in all cases. The value of deflection which produces serviceability failure is not the same for all types of structures or, indeed, for all parts of the same structure, and considerable saving would result if deflections could be accurately assessed in advance.

According to the draft Unified Code, the designer faced with a deflection problem can either comply with span/depth ratios which he knows may be uneconomic or may not prevent serviceability failure or calculate the magnitude of the deflection and judge for himself whether this is acceptable.

Existing methods of calculation are crude and likely to produce unreliable results. This is because they are based on an incomplete understanding of the behaviour of reinforced concrete structures under service loads. The only experimental results available to check the accuracy of these methods are results from tests on simply supported beams and a few two span continuous beams whereas most reinforced concrete structures in service are statically indeterminate.

There is a real need for more fundamental understanding of the behaviour of statically-indeterminate structures and more experimental data relevant to full-scale structures.

The object of this investigation is to make a fundamental study of the behaviour of reinforced concrete statically-indeterminate structures under sustained service-load.

Since there is no reliable method of calculating the sustained moment-curvature relationship of a reinforced concrete cross-section from the basic properties of steel and concrete this is obtained experimentally for two particular cross sections. The first of these is a typical beam cross-section and its sustained moment-curvature behaviour is investigated in the absence of axial load; the second is a typical column cross section and its sustained-moment curvature behaviour is investigated under one particular value of sustained axial load.

Computer programs are developed which compute the deflections of reinforced concrete continuous beams and plane frames under sustained service-loads using the long-term moment-curvature relationship of each cross-section. The computer program for continuous beam analysis is general but the plane frame analysis program is limited to frames of one bay with a maximum of two storeys. Both programs include the effects of cracking during loading and time-dependent moment redistribution during sustained load.

As a check on the results of the computer work, two plane frames and a pair of continuous beams are tested under sustained service-load for eighteen months. The members of these structures have the cross-sections investigated under sustained moment.

The same concrete mix proportions, one type of reinforcing steel and one age at loading are used throughout the experimental programme. Tests to determine the elastic, creep and shrinkage properties of the concrete are performed. All experimental work is done under controlled environmental conditions.

PART 2: EXPERIMENTAL PROGRAMME

A. General

All the experimental work was performed in the controlled environment of the New Structures Laboratory at the Building Research Station. The temperature in the laboratory is maintained at 19°C (± 1°C) and the humidity is maintained at 65% (± 2%).

G.K. 60 high-tensile ribbed bars were used for main reinforcement throughout the programme. For design purposes, the characteristic strength in both compression and tension was taken as 413 N/mm^2 and the modulus of elasticity was taken as 207 KN/mm^2. Mild steel bars were used for stirrups and the characteristic strength was taken as 247 N/mm^2.

The concrete used throughout the programme had the following mix proportions by weight:
1 part cement: 3.5 parts of sand (less than 4.75 mm) : 1 part of gravel (greater than 4.75 mm but less than 9.5 mm) : 2.25 parts of gravel (greater than 9.5 mm but less than 19 mm).
The water/cement ratio was 0.69. Ordinary Portland cement and Ham river aggregates were used. The concrete was cast in wooden formwork and was cured for three days under damp sacks and polythene sheets before demoulding. The plane frames and continuous beams were cast in the laboratory but the smaller specimens were cast in a separate casting bay and transferred to the laboratory immediately after demoulding. During casting external ('Kango') and internal ('poker') vibrators were used to ensure good compaction of the concrete.

It was specified that the crushing strength of water stored 100 mm cubes tested at 28 days should be 30 N/mm^2 and this was taken as the characteristic compressive strength of the concrete for design purposes. Eight castings

were necessary to obtain the specimens on which the moment-curvature data was collected. With each casting three 100 mm cubes were taken for water store and were tested by crushing at 28 days. One 100 x 100 x 500 mm beam and three 120 x 120 x 250 mm cylinders were also taken with each casting. They were air stored with the moment-curvature specimens and tested at 28 days; the cylinders were used to determine the static modulus of elasticity and the beam was used to determine the flexural tensile strength. The results are shown in table 1.

All specimens were loaded at 28 days and it is assumed that the parameters which define the instantaneous moment curvature response are thereafter independent of time. This assumption greatly reduces the amount of basic data required. In order to obtain an estimate of the error involved in making this assumption under the conditions of this investigation it was decided to measure the strength development of 100 mm cubes stored in air with the moment-curvature specimens. The results are shown in table 2.

Cubes for water store were taken during the casting of the plane frames, the continuous beams and the creep and shrinkage specimens. These were tested at 28 days in order to confirm that the correct mix proportions had been used and the results are shown in table 3. In the case of the shrinkage specimens, the curing and testing instructions were not obeyed and the cubes were treated incorrectly in that three were water stored and tested at 7 days and the remainder were air stored and tested at 28 days. The results are shown in table 4.

Compression load cells of 300 KN capacity were used in part of the experimental work; these cells had been in general laboratory use and were known to be very reliable under short term load and sustained load of a few months duration. They were calibrated before and after use and no significant

TABLE 1: Concrete Properties at 28 days

Ref	Crushing strengths of water stored 100mm cubes tested at 28 days N/mm^2	Flexural tensile strengths of air stored 100 x 100 x 500mm specimens tested at 28 days N/mm^2	Static modulus of elasticity values of air stored 120 x 120 x 250mm cylinders tested at 28 days KN/mm^2
1	24.9 27.4 24.3	2.16	28.6 27.8 30.8
2	29.1 30.9 28.3	2.95	29.1 28.0 30.3
3	27.3 29.1 31.5	3.22	28.9 26.6 31.4
4	21.1 28.5 25.0	2.22	30.5 30.3 30.4
5	29.0 31.5 29.1	2.99	30.2 30.9 30.6
6	30.7 29.9 28.0	2.76	29.5 26.5 29.0
7	30.4 30.6 30.3	3.01	25.6 29.6 28.1
8	35.2 30.5 26.2	2.91	24.7 26.3 28.6
Mean	28.7	2.78	28.8
Std Devn	2.84	0.36	1.8

TABLE 2 : Influence of Age on the Crushing Strength of Dry Stored 100 mm Cubes

Ref	Crushing Strength of Air Stored Cubes N/mm^2								
	28 days	30 days	33 days	40 days	54 days	88 days	164 days	410 days	576 days
1	17.2	19.7	16.6	18.2	18.1	20.1	18.5	22.8	20.4
2	22.2	22.2	27.2	21.5	22.0	28.7	28.2	23.5	29.6
3	27.6	25.8	28.1	27.9	25.5	26.3	30.3	23.2	27.1
4	24.1	16.9	22.7	19.3	25.8	28.0	25.8	28.6	21.9
5	28.9	32.5	32.6	30.7	32.2	30.4	36.3	30.8	35.7
6	23.7	20.9	23.5	25.3	22.9	25.7	23.8	30.4	30.9
7	21.5	23.5	23.0	24.9	24.4	21.3	27.1	26.7	30.1
8	26.7	28.5	28.8	22.6	24.7	30.7	25.6	24.6	23.6
Mean	24.1	23.7	25.3	23.8	24.4	26.4	26.8	26.3	27.4
Std Devn	3.55	4.70	4.62	3.95	3.82	3.69	4.68	3.07	4.84

TABLE 3: Control Cube Crushing Results

Ref	Water stored 100m cubes tested at 28 days		
	No. Tested	Mean Crushing strength N/mm^2	Standard Deviation N/mm^2
Frame 1	21	29.5	1.54
Frame 2	6	29.3	4.93
Continuous beams	30	29.3	1.87
Creep Specimens CB1 and CC1	6	32.5	1.70
Creep Specimens CB3 and CC3	6	32.4	1.71

TABLE 4: Shrinkage Specimens CB2 and CC2, Control Cube Crushing Results

	No. Tested	Mean Crushing strength N/mm^2	Standard Deviation N/mm^2
Water Stored 100mm cubes tested at 7 days	3	17.4	0.44
Air Stored 100mm cubes tested at 28 days	3	19.5	0.63

change had occurred in their characteristics. Tension load cells of 180 KN capacity were also used. These cells had been used extensively under short term load and their reliability had been excellent. Since these tension cells had not been used under sustained load they were subjected to rigorous testing before use. This included approximately 30 hours during which the cells were subjected to a continuous cycling of load between 30 and 180 KN. The cycle time was approximately 60 secs. This was followed by about 67 hours during which the cells were subjected to a continuous cycling between 110 and 130 KN; the machine used is incapable of sustaining a constant load but cycling over a small range is a fairly close approximation to a sustained load. When in use in the experimental arrangements the most highly loaded cell was under a sustained load of 120 KN. Calibrations were performed before, during and after this testing procedure and any cells which showed signs of instability were rejected. During the experimental work, significant change in tension load cell characteristics occurred on only one occasion and this is discussed later.

Throughout the programme strains were measured using a demountable mechanical strain gauge ('demec') which read on punched targets fixed to the concrete surface by a quick setting resin cement. The gauge length of the instrument was 200 mm. Deflections of the full-scale structures were measured using mechanical dial gauges reading to 0.025 mm. Cracking patterns were observed on all specimens using an illuminated magnifier with a magnification factor of 2.

The design of the experimental specimens was performed using a draft of the Unified Code of Practice for Structural Concrete (38) which was current in 1968. This draft has subsequently been modified but the changes affect only a small part of the calculations and the designs remain valid.

B. Creep and Shrinkage Specimens

Creep and shrinkage strains were measured on six plain concrete specimens; three specimens had dimensions of 100 x 190 x 600 mm and the remainder had dimensions of 100 x 100 x 600 mm. The ends of each specimen were sealed with peridite about 7 days after casting to prevent drying through the ends producing non uniform shrinkage. One specimen of each type remained unloaded and the surface free shrinkage strains were measured from 28 days after casting. One specimen of each type was loaded at 28 days to a uniform stress of 4.1 N/mm^2 and the remaining pair were loaded at 28 days to a uniform stress of 8.3 N/mm^2. Both these stresses are in the service stress range. The loaded specimens were maintained under sustained load for approximately 18 months.

Strains were measured immediately after loading and at roughly equal intervals of log time up to a maximum time between observations of just over one month. 24 gauge lengths were provided on each plain concrete specimen. Further strain readings were taken after unloading and observations were continued for 100 days in order to investigate the magnitude of creep recovery.

The experimental results are shown in table 5 and a typical strain-time curve is shown in diagram 5.

The experimental arrangement is shown in diagram 6 and plate 1. Loading was performed by inserting the ram of a hydraulic jack and a compression load cell in the locations shown in diagram 6. Load was applied by the ram until the reading on the load cell indicated that the required stress had been reached. The nuts labelled A in diagram 6 were then tightened, the load applied by the ram was let off and the nuts maintained the load on the concrete. Tests were performed earlier to determine the amount of load

TABLE 5: Strains in Plain Concrete under Axial Load

Specimens CB1 (100 x 190 x 600mm) and CC1 (100 x 100 x 600mm)

Sustained stress = 8.3 N/mm^2 Age at loading = 28 days

Time* days	Total strain** $x10^{-6}$	
	CB1	CC1
0	325	322
3	491	542
5	526	607
7	560	667
12	654	791
26	796	957
60	1000	1200
74	1100	1340
89	1190	1430
108	1270	1500
136	1360	1580
157	1430	1640
179	1490	1680
195	1520	1710
216	1550	1750
248	1600	1800
273	1640	1820
304	1670	1850
340	1680	1860
381	1710	1900
423	1720	1920
465	1740	1930
507	1760	1950
550	1810	1990
load removed		
550	1440	1540
551	1410	1520
552	1410	1510
553	1390	1510
557	1380	1500
559	1380	1490
564	1410	1520
571	1380	1490
578	1400	1500
592	1360	1470
608	1360	1470
650	1360	1470

*measured from loading

**elastic+shrinkage+creep; compression positive

TABLE 5: continued

Specimens CB2 (100 x 190 x 600mm) and CC2 (100 x 100 x 600mm)

Time*	Shrinkage Strain** x 10^{-6}	
days	CB2	CC2
0	0	0
2	0	4
4	-3	8
7	15	24
11	15	56
25	84	112
43	118	134
74	169	168
88	183	187
107	180	172
136	203	203
157	216	214
179	219	197

Time*	Shrinkage Strain** x 10^{-6}	
days	CB2	CC2
196	230	223
218	251	235
248	272	258
273	280	264
302	243	237
315	254	241
340	255	244
386	252	243
427	265	246
464	175	157
506	257	245
552	245	232

* 28 days from casting taken as zero

** shrinkage positive

TABLE 5: continued

Specimens CB3 (100 x 190 x 600mm) and CC3 (100 x 100 x 600mm)

Sustained stress = 4.1 N/mm^2 Age at loading 28 days

Time* days	Total Strain** x10^{-6}	
	CB3	CC3
0	146	165
1	204	244
2	211	260
11	288	362
25	334	427
42	430	560
60	500	644
74	540	680
88	590	730
107	630	770
136	670	820
157	690	850
178	710	880
198	744	909
219	747	913
248	780	941
298	794	954
345	809	974

Time* days	Total Strain** x10^{-6}	
	CB3	CC3
382	824	996
427	871	1060
464	824	1010
506	786	977
548	852	1050
load removed		
548	668	819
549	657	803
550	656	809
553	660	810
555	680	817
560	680	815
562	670	810
569	640	790
576	640	788
590	644	790
605	640	781
681	673	807

*measured from loading

** elastic+shrinkage+creep; compression positive

DIAGRAM 5: Strain - Time Curve for Specimen CB1

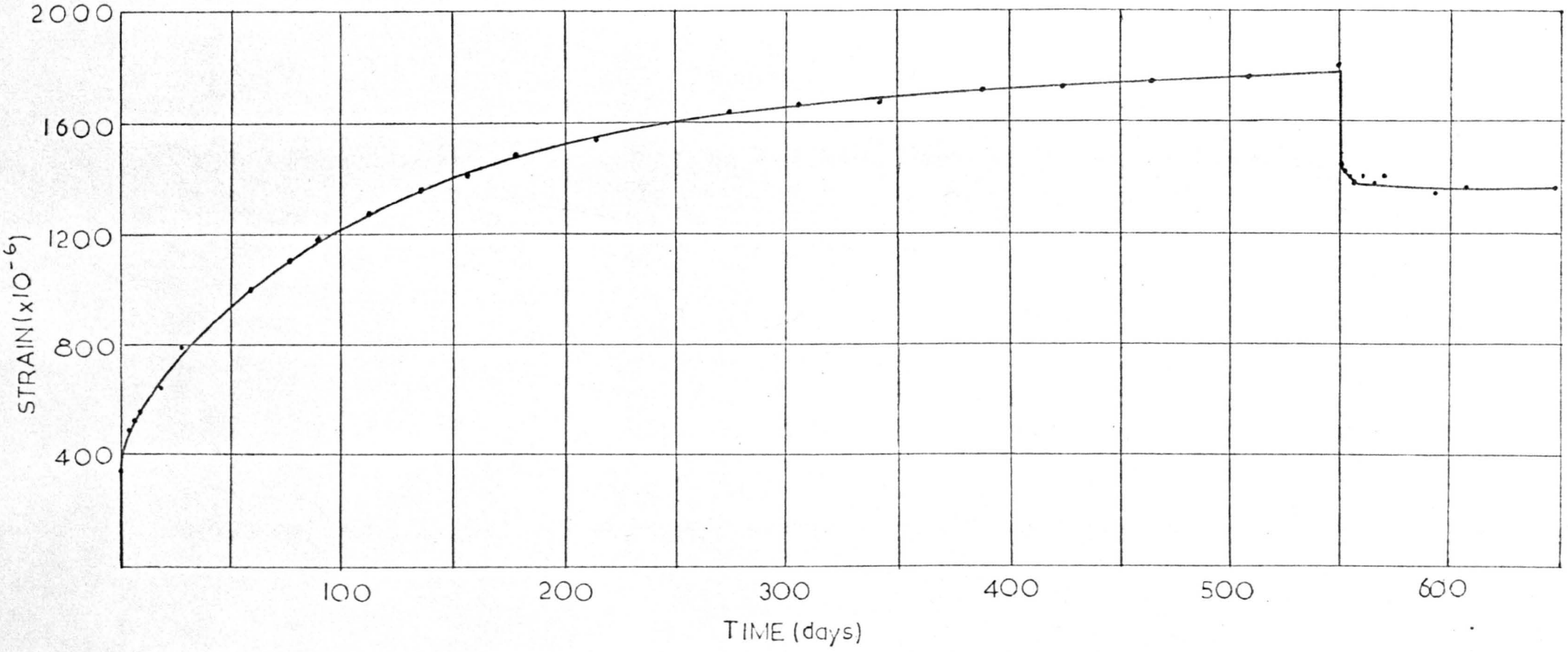

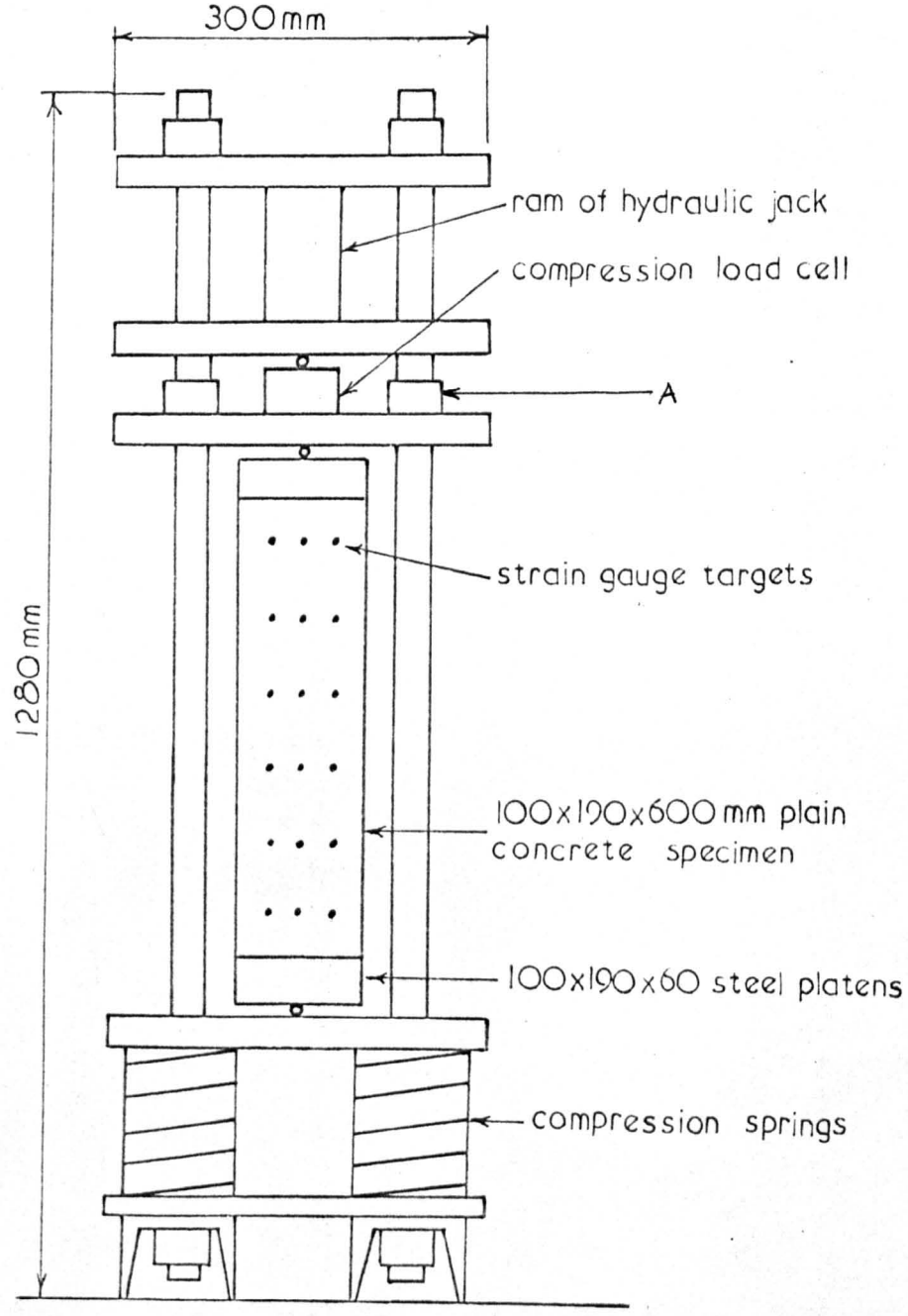

DIAGRAM 6: Experimental Arrangement for Specimen CB1

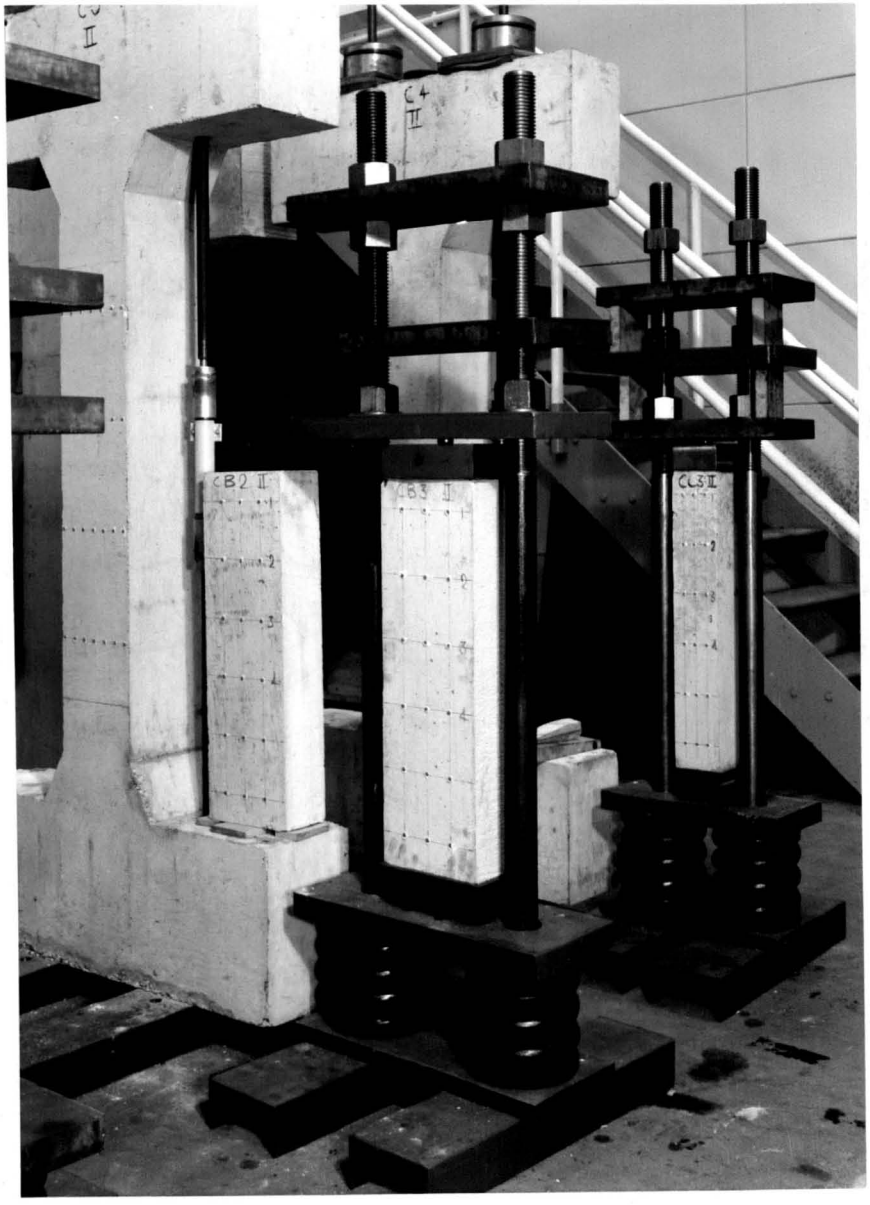

PLATE 1: Creep and Shrinkage Specimens.

"drop-off" during transfer of the load from the ram to the nuts; this was found to be very small and was allowed for during loading of the concrete specimens. Owing to the presence of the springs, the amount of load reduction during creep was small. However, the load was "topped up" (using a procedure similar to the initial loading method) daily during the first fortnight after loading, then weekly until 3 months after loading and thereafter monthly.

C. Sustained Moment Curvature Specimens

The behaviour of two cross sections was investigated under sustained moment.

(a) A rectangular (200 x 380 mm) beam section reinforced with approximately 1.5 per cent of tensile steel. Calculations based on the draft Unified Code gave the service moment of this section as 66 KNm. The type of specimen used and the loading arrangement are shown in diagram 7 and plate 2.

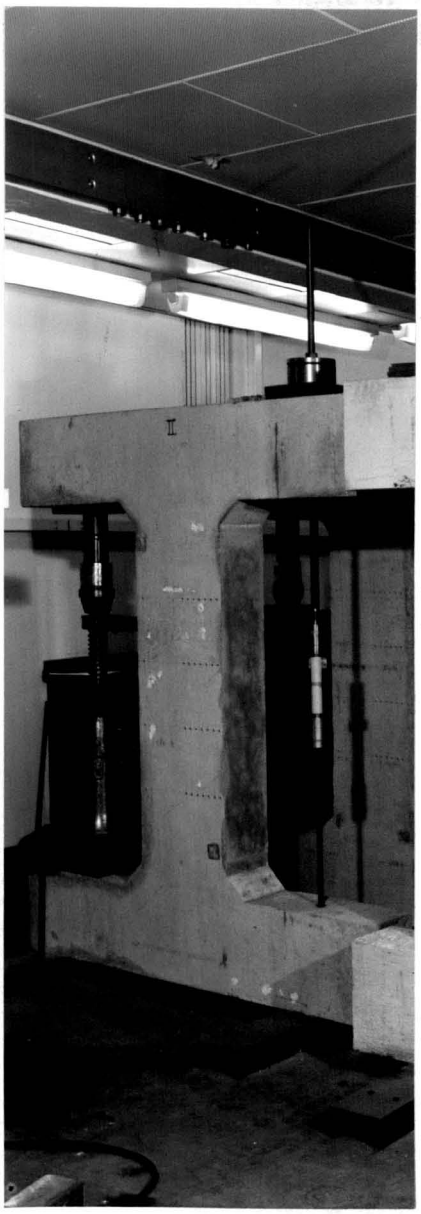

PLATE 2: Beam Section Moment-Curvature Specimen

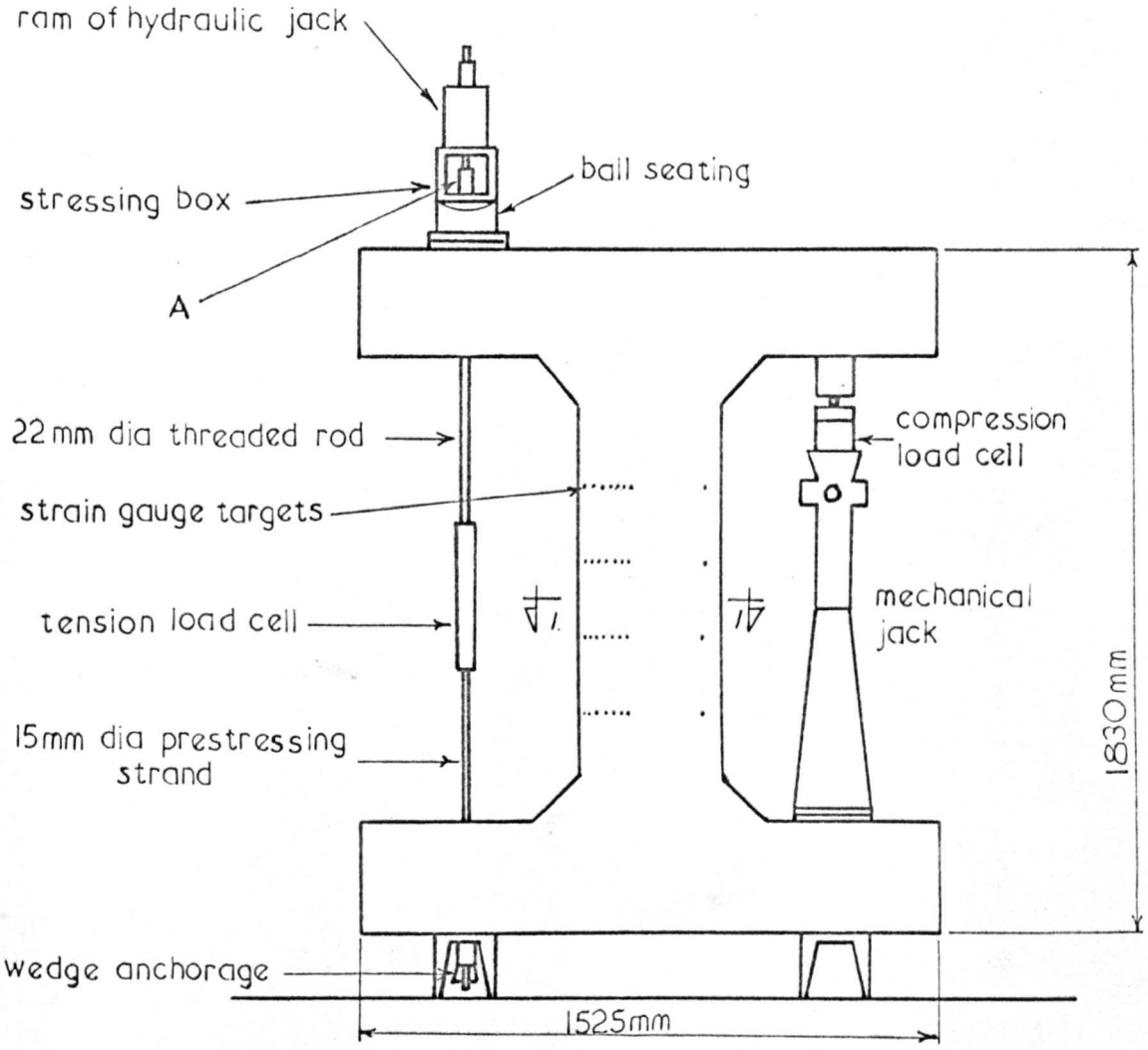

Elevation of loading arrangement

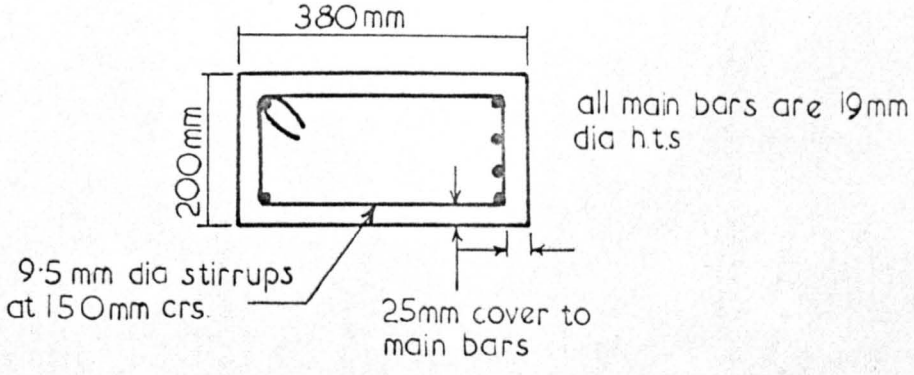

Section 1 : Beam cross section

DIAGRAM 7: Beam Section Moment-Curvature Specimen

Six specimens were placed under sustained moment; each specimen was subjected to a different magnitude of moment as defined in table 6. A seventh unloaded specimen was used to measure the influence of shrinkage.

Loading was performed in a step by step manner by inserting the ram of a hydraulic jack in the locations shown in diagram 7. A fraction (say about one sixth) of the final load was then applied by the ram. The same amount of load was next applied by the mechanical jack using a lever. Further load was then applied by the hydraulic ram and so on until the required final load was reached. The nuts, labelled A in diagram 7 were then tightened, the load applied by the ram was let off and the nuts maintained the load. The amount of load "drop off" during transfer of the load from the ram to the nuts could be observed using the tension load cell and was found to be negligible. During creep the reduction in load could be observed using the load cells and by "topping up" operations the loads were maintained in the range $\pm$ 2.5% of the required values.

Strains were measured immediately after loading and at roughly equal intervals of log time up to a maximum time between observations of approximately three months. The location of the targets is shown in diagram 7; 48 gauge lengths were provided on each specimen. Further strain readings were taken after unloading and observations were continued for up to 100 days in order to investigate the magnitude of creep recovery.

All the experimental results were processed by computer and the values obtained for curvature, depth of strain neutral-axis and surface strain at the level of the tensile reinforcement are given in table 7. The curvature data was then plotted in the form of moment-curvature diagrams for various times after loading. Three typical moment-curvature plots are shown in diagram 8. The relationship can be seen to be bi-linear for

TABLE 6: Loading Schedule for Beam Section Specimen

Specimen Reference	Applied moment KNm	Value of P_1*
B1	11.0	11.0
B2	22.0	22.0
B3	33.0	33.0
B4	44.0	44.0
B5	55.0	55.0
B6	66.0	66.0
B7	0	0

*see diagram 7

practical purposes; the cracking moment was assumed to be independent of time. Consequently the relationship at any time may be defined by

$$M = \eta_o \phi + \rho_o \qquad M \leq M_c$$

$$M = \eta_c \phi + \rho_c \qquad M > M_c$$

where M is the applied bending moment, ϕ is the curvature of the cross section and η_o, η_c, ρ_o, ρ_c are constants for a particular concrete and cross section. The time dependence of the quantities η_o, η_c, ρ_o and ρ_c is shown in table 8.

The extent of cracking on each specimen was investigated and is shown in diagram 9.

(b) A square (200 mm) column section reinforced with 1.25% of steel symmetrically distributed. The section was subjected to a sustained axial load of about half the service value permitted by the draft Unified Code. The sustained moment-curvature relationship, in the presence of this axial load, was obtained experimentally; the type of specimen used and

DIAGRAM 8: Typical Beam Section Moment Curvature Diagrams

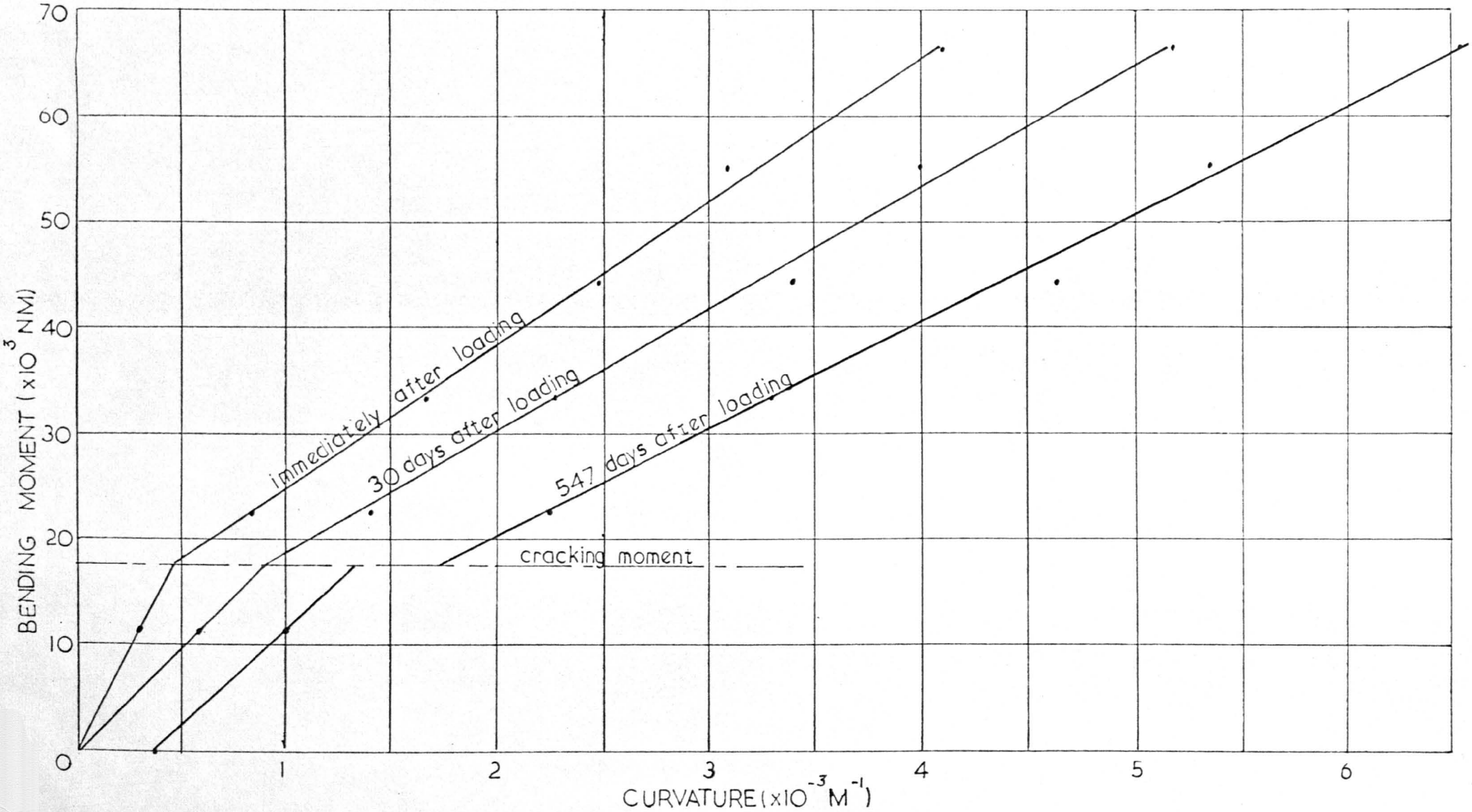

B 2

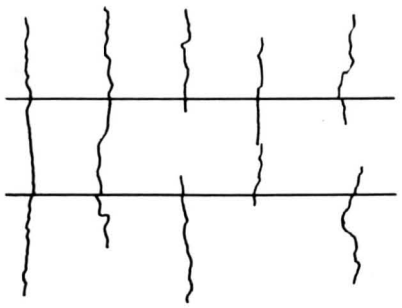

B 3

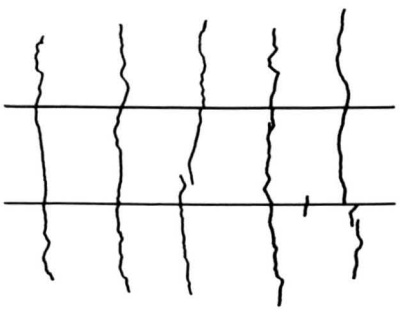

B 4

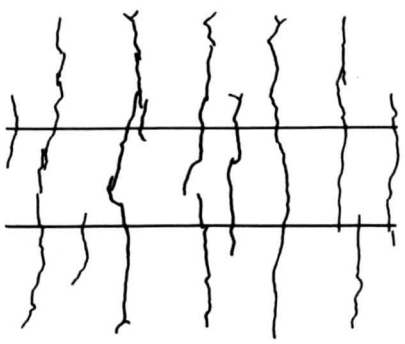

B 5

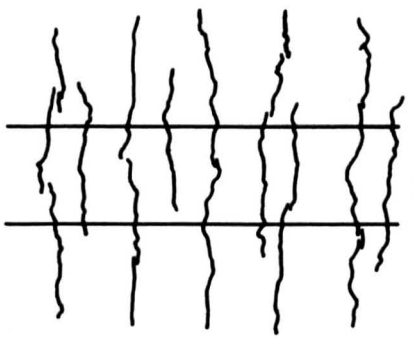

B 6

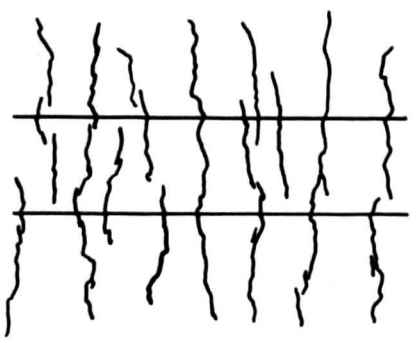

DIAGRAM 9: Cracking Patterns in Beam Section Moment Curvature Specimens

TABLE 7 : Beam Section Experimental Results

All results are total values ie elastic + creep + shrinkage

B1				B2			
Time* days	Curvature mm^{-1} x10^{-6}	Depth of neutral axis of strain mm	Surface*/ strain at tension steel level x10^{-6}	Time* days	Curvature mm^{-1} x10^{-6}	Depth of neutral axis of strain mm	Surface*/ strain at tension steel level x10^{-6}
0	0.336	196	57	0	0.827	166	135
2	0.464	209	53	3	1.043	172	180
5	0.517	201	67	5	1.083	185	173
12	0.538	235	70	12	1.167	176	197
26	0.591	250	68	26	1.293	198	183
60	0.710	303	33	60	1.450	213	188
134	0.760	328	27	138	1.733	239	170
218	0.845	342	8	217	1.871	261	140
296	0.897	355	-8	299	2.069	260	157
380	0.987	387	-38	382	2.205	252	180
463	1.003	390	-42	493	2.245	261	165
551	0.999	450	-103	548	2.233	262	168
	Load removed				Load removed		
551	0.642	584	-148	548	1.324	317	22
552	0.608	577	-140	549	1.264	327	7
553	0.622	553	-128	550	1.255	318	17
534	0.609	567	-133	551	1.233	321	18
535	0.607	571	-135	552	1.221	323	12
558	0.621	579	-143	555	1.231	312	20
560	0.617	512	-102	557	1.200	328	5
562	0.612	543	-120	559	1.183	332	3
565	0.614	503	-95	562	1.146	343	0
567	0.613	502	-93	564	1.169	335	2
569	0.616	514	-102	566	1.179	333	2
572	0.615	521	-107	569	1.160	333	5
579	0.627	513	-103	576	1.124	378	-40
593	0.595	530	-68	590	1.045	367	-28
				608	1.089	358	-17
				652	1.078	375	-35

* Measured from loading

*/ Tension positive

TABLE 7 : continued

All results are total values ie elastic + creep + shrinkage

B3

Time* days	Curvature mm^{-1} $X10^{-6}$	Depth of neutral axis of strain mm	Surface*/ strain at tension steel level $X10^{-6}$
0	1.657	150	242
2	1.861	151	282
5	1.914	149	307
12	2.060	165	288
26	2.238	170	293
60	2.493	181	307
135	2.788	193	305
218	2.874	207	288
299	3.074	215	293
382	3.171	226	275
467	3.288	226	263
552	3.276	226	273
Load removed			
552	1.695	280	32
553	1.581	287	15
554	1.543	293	10
555	1.557	281	18
558	1.296	356	-30
559	1.298	338	-7
561	1.275	335	-2
566	1.266	338	-7
568	1.455	300	13
573	1.236	344	-13
580	1.238	333	0
594	1.203	341	-10
610	1.177	342	-10
652	1.177	365	-40

B4

Time* days	Curvature mm^{-1} $X10^{-6}$	Depth of neutral axis of strain mm	Surface*/ strain at tension steel level $X10^{-6}$
0	2.482	145	535
5	2.975	156	567
12	3.177	159	592
26	3.381	170	600
60	3.676	182	608
138	4.041	196	625
216	4.231	206	613
299	4.391	219	583
382	4.529	218	612
467	4.602	229	583
550	4.671	223	615
Load removed			
550	0.860	306	92
551	0.674	333	68
552	0.641	334	67
553	0.591	336	67
554	0.591	342	62
557	0.514	373	60
559	0.536	362	52
561	0.507	338	68
564	0.502	365	57
566	0.505	337	70
568	0.505	334	65
571	0.471	364	55
578	0.448	351	66
593	0.419	370	50
604	0.338	391	62
650	0.250	311	97

* Measured from loading
*/ Tension positive

TABLE 7 : continued

All results are total values ie elastic + creep + shrinkage

B5

Time* days	Curvature mm^{-1} x10^{-6}	Depth of neutral axis of strain mm	Surface*/ strain at tensile steel level x10^{-6}
0	3.080	139	577
2	3.501	143	625
4	3.585	148	635
11	3.745	150	652
26	3.930	162	647
60	4.245	168	663
136	4.533	180	663
218	4.805	188	665
297	5.079	191	687
382	5.212	196	682
465	5.264	197	695
553	5.352	198	705
Load removed			
553	1.064	248	150
554	0.814	234	137
555	0.747	224	140
556	0.743	184	163
557	0.671	177	162
560	0.501	186	163
562	0.552	194	140
567	0.529	270	102
569	0.536	277	97
571	0.560	232	117
574	0.502	253	110
581	0.429	170	155
596	0.448	210	128
609	0.412	235	120

B6

Time* days	Curvature mm^{-1} x10^{-6}	Depth of neutral axis of strain mm	Surface*/ strain at tension steel level x10^{-6}
0	4.103	141	785
2	4.539	154	808
12	4.956	156	861
26	5.071	161	848
61	5.402	171	867
135	5.686	182	855
218	6.067	184	890
299	6.241	192	862
383	6.310	203	805
464	6.488	198	853
551	6.674	196	880
Load removed			
551	1.700	238	155
552	1.419	238	130
553	1.412	248	113
555	1.341	235	123
558	1.338	211	150
560	1.281	229	133
565	1.262	244	103
573	1.238	241	103
579	1.210	244	100
601	1.117	225	130
615	1.093	265	87
659	1.074	268	55

* Measured from loading
*/ Tension positive

TABLE 7: continued

B7: Shrinkage curvature

Time* days	Curvature $mm^{-1} \times 10^{-6}$
0	0
2	0.034
26	0.049
61	0.100
135	0.149
218	0.198
299	0.261
342	0.261
383	0.275
422	0.270
459	0.313
505	0.316
551	0.326

*28 days from casting taken as zero

the loading arrangement are shown in diagram 10 and plate 3. The value of axial load selected was 178 KN and the service moment in the presence of this load was calculated using the draft Unified Code and was found to be 11.5 KNm.

Six specimens were placed under sustained axial load and moment; each specimen was subjected to the same value of axial load but a different magnitude of moment as defined in table 9. A seventh unloaded specimen was used to measure the influence of shrinkage.

Loading was performed in a step by step manner by inserting the rams of two hydraulic jacks in the locations shown in diagram 10. A fraction (say about one sixth) of the final load was then applied by the ram of one jack. The same amount of load was next applied by the other ram. This

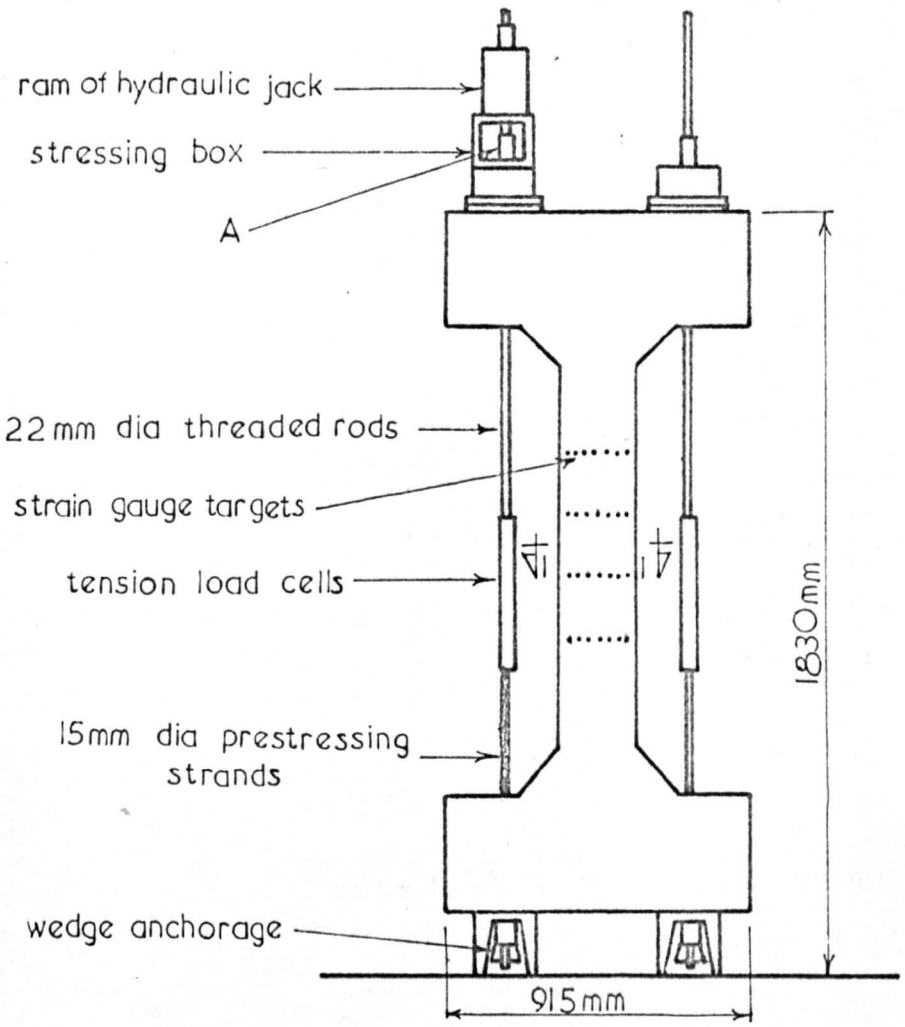

Elevation of loading arrangement

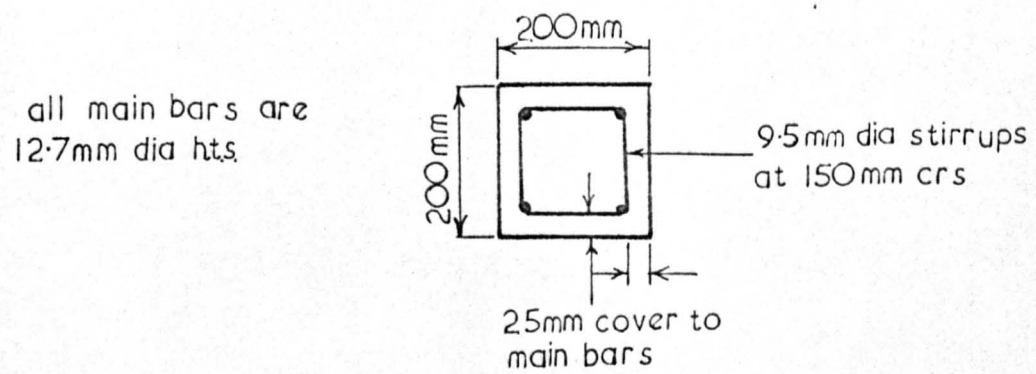

Section 1 : Column cross section

DIAGRAM 10: Column Section Moment-Curvature Specimen

TABLE 8: Beam Section Moment Curvature Parameters

Time* days	MNM^2	KNM	MNM^2	KNM
0	31.80	-0.00	13.80	10.00
1	26.66	-0.05	13.13	9.00
2	23.80	-0.12	12.92	8.00
3	23.20	-0.14	12.55	9.00
4	21.90	-0.18	12.90	8.00
5	21.30	-0.21	12.85	7.50
6	21.82	-0.26	12.60	8.00
7	21.20	-0.30	12.55	7.80
8	20.25	-0.32	12.40	8.00
9	20.90	-0.38	12.65	7.20
10	20.70	-0.41	12.10	7.80
12	20.80	-0.50	12.00	7.20
14	20.60	-0.58	11.75	7.70
16	20.15	-0.60	12.12	7.00
18	19.60	-0.67	12.40	6.20
20	19.20	-0.76	12.15	6.00
25	20.30	-0.94	11.60	7.00
30	19.40	-1.09	11.62	6.50
35	18.65	-1.16	11.55	6.50
40	18.80	-1.24	11.60	5.50
45	19.15	-1.42	11.35	6.00
50	18.30	-1.46	11.60	5.50
65	18.20	-1.71	11.22	5.00
80	17.75	-1.77	11.25	4.40
100	17.50	-2.10	11.35	4.00
125	17.50	-2.37	11.28	2.00
150	17.65	-2.70	11.00	3.00
200	16.20	-3.50	10.90	2.00
250	17.50	-4.00	10.45	2.00
300	16.42	-4.00	11.25	-0.75
350	16.00	-4.25	10.77	-0.75
400	16.36	-4.50	10.78	-1.50
450	15.29	-4.50	10.53	-1.75
500	15.71	-5.25	10.52	-2.00
547	17.14	-6.25	10.30	-1.50

*measured from loading

PLATE 3: Column Section Moment-Curvature Specimen

process was continued until one ram reached the required load and then the necessary additional load was applied by the other ram. The nuts labelled A in diagram 10 were then tightened, the load applied by the rams was let off and the nuts maintained the load. The amount of load "drop off" during transfer of the load from the ram to the nuts could be observed using the load cells and was found to be negligible. During creep the reduction in load could be observed using the load cells and by "topping up" operations the loads were maintained in the range $\pm$ 2.5% of the required value.

TABLE 9: Loading Schedule for Column Section Specimen

Specimen Reference	Sustained moment KNm	Sustained axial load KN	Value of P_2* KN	Value of P_3* KN
C1	7.67	178.0	107.70	70.30
C2	1.92	178.0	93.80	84.20
C3	2.88	178.0	96.01	81.99
C4	9.59	178.0	113.50	64.50
C5	4.80	178.0	101.00	77.00
C6	11.50	178.0	117.20	60.80
C7	0	0	0	0

* see diagram 10

Strains were measured immediately after loading and at roughly equal intervals of log time up to a maximum time between observations of approximately three months. The location of the targets is shown in diagram 10; 42 gauge lengths were provided on each specimen.

All the experimental results were processed by computer and the values obtained for curvature, axial strain and, where relevant, neutral axis depth are shown in table 10. The curvature data was then plotted in the form of moment-curvature diagrams for various times after loading. Three typical moment curvature plots are shown in diagram 11. The relationship can be seen to be linear to cracking and then non-linear. However, a bi-linear form is a convenient simplification for practical purposes. Consequently the relationship may be defined by a relationship identical to that used for the beam section. The time dependence of the quantities η_o, η_c, ρ_o and ρ_c is shown in table 11. The extent of cracking on each specimen was investigated and is shown in diagram 12.

DIAGRAM 11: Typical Column Section Moment Curvature Diagram

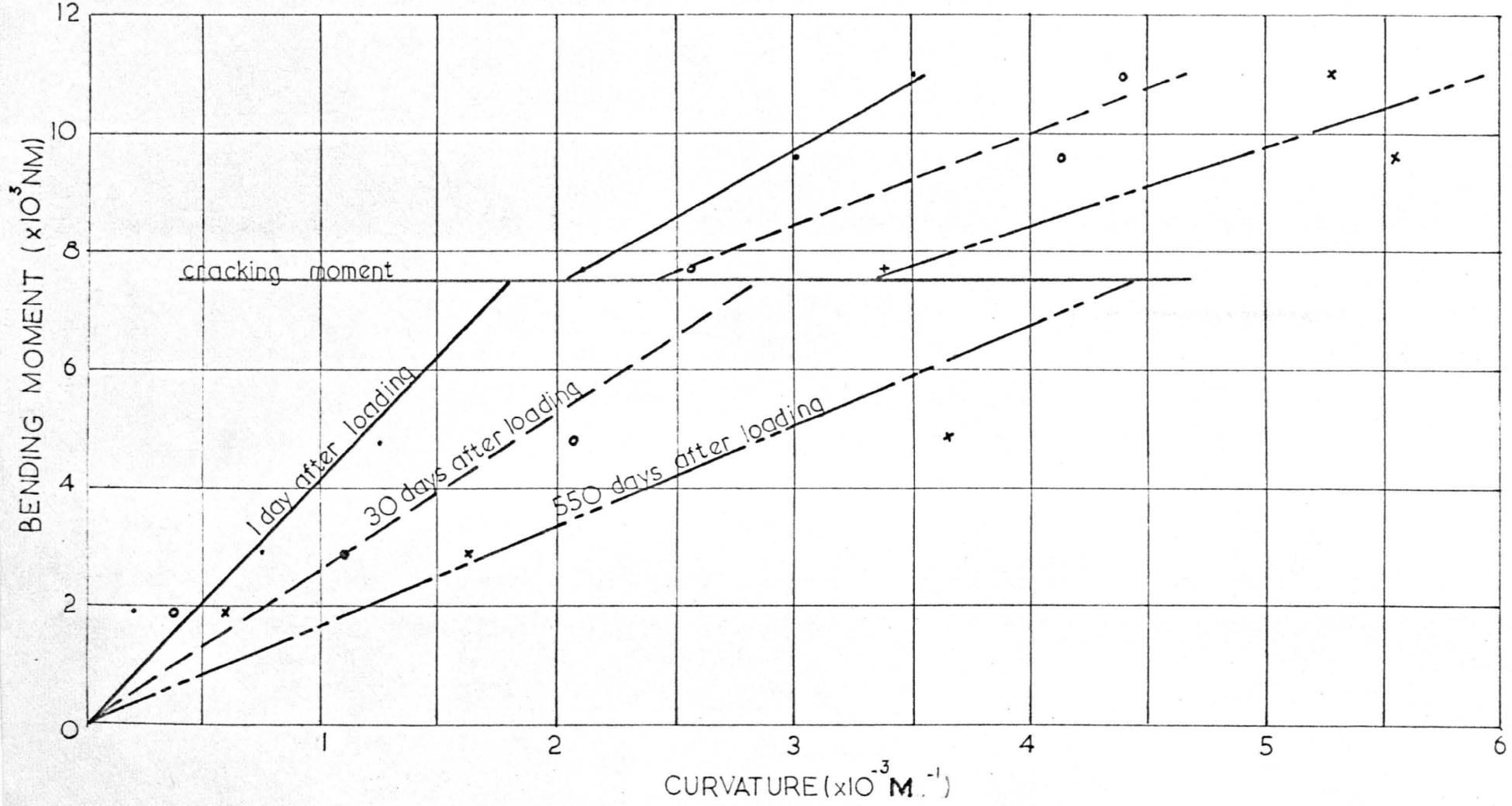

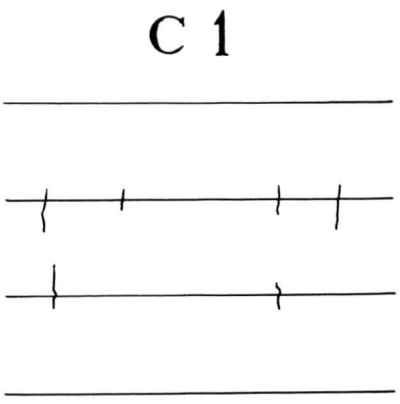

DIAGRAM 12: Cracking Patterns in Column Section Moment Curvature Specimens

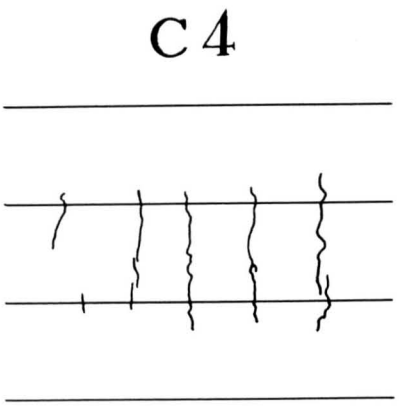

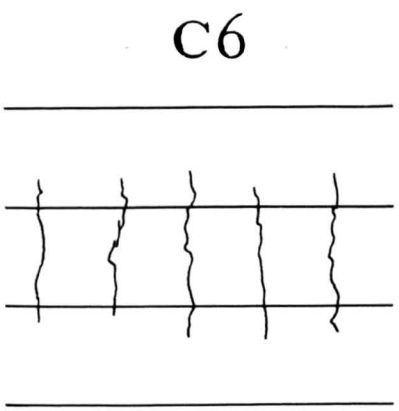

The column section specimens subjected to the lower values of moment were set up in the laboratory and there was a short delay (2-3 months) before the remaining specimens could be cast. During this time a failure of the laboratory humidity control plant (located in the roof of the laboratory) caused water to drip almost directly onto three of these specimens and, in particular, onto their tension load cells. One load cell on each of these specimens showed marked signs of instability in the

days that followed. Those three specimens were consequently unloaded and the suspect load cells replaced. They were then reloaded to the high moment values and the specimens which were cast later were subjected to the lower moments. Thus the experimental results for the specimens labelled C1, C4 and C6 in table 10 must be interpreted in the light of this.

TABLE 10: Column Section Experimental Results

All results are total values ie elastic+creep+shrinkage

C1				C2		
Time* days	Curvature mm^{-1} $x10^{-6}$	Depth of neutral axis of strain mm	Mean strain** over cross section $x10^{-6}$	Time* days	Curvature mm^{-1} $x10^{-6}$	Mean strain** over cross section $x10^{-6}$
0	1.894	169	127	0	0.165	150
2	2.284	160	134	2	0.296	151
4	2.340	166	151	5	0.383	151
11	2.437	161	144	12	0.341	216
25	2.581	161	154	27	0.532	235
60	2.786	160	165	61	0.466	298
136	2.852	167	189	135	0.423	390
183	3.014	161	181	218	0.556	470
218	3.022	163	186	299	0.522	494
302	3.140	178	240	382	0.575	535
385	3.205	167	211	467	0.609	553
457	3.321	165	214	552	0.593	555
547	3.398	176	254			
load removed				load removed		
547	1.872	119	31	552	0.611	396

* measured from loading

** compression positive

The neutral axis of C2 lies so far outside the section that the depth values are meaningless.

Specimen C1 had been loaded previously (see text).

TABLE 10: continued

All results are total values ie elastic+creep+shrinkage

C3

Time* days	Curvature mm^{-1} $x10^{-6}$	Mean strain** over cross section $x10^{-6}$
0	0.625	137
2	0.804	168
5	0.976	193
12	1.010	223
26	1.056	261
61	1.258	378
135	1.389	466
218	1.593	522
299	1.587	563
342	1.593	607
383	1.611	566
422	1.579	591
468	1.548	610
551	1.649	605
load removed		
551	0.033	416

C4

Time* days	Curvature mm^{-1} $x10^{-6}$	Depth of neutral axis of strain mm	Mean strain** over cross section $x10^{-6}$
0	2.928	155	162
2	3.728	146	171
4	3.872	149	187
11	4.022	146	185
25	4.083	148	197
60	4.400	145	199
136	4.756	150	235
183	4.811	153	254
218	4.806	151	243
302	5.106	153	271
385	5.239	148	247
457	5.450	146	251
547	5.578	152	290
load removed			
575	1.630	46	83

* measured from loading

** compression positive

The neutral axis of C3 lies so far outside the section that the depth values are meaningless.

Specimen C4 had been loaded previously (see text).

TABLE 10: continued

All results are total values ie elastic+creep+shrinkage

C5

Time* days	Curvature mm^{-1} $\times 10^{-6}$	Mean strain** over cross section $\times 10^{-6}$
0	1.077	149
2	1.464	182
4	1.544	191
11	1.730	208
28	2.054	287
60	2.435	318
136	2.720	402
218	3.101	473
297	3.268	507
382	3.454	548
465	3.569	555
556	3.641	525
load removed		
556	2.775	302

C6

Time* days	Curvature mm^{-1} $\times 10^{-6}$	Depth of neutral axis of strain mm	Mean strain** over cross section $\times 10^{-6}$
0	2.789	142	114
2	4.217	129	120
6	4.222	132	131
13	4.317	133	142
24	4.428	134	146
59	4.528	140	176
135	4.700	148	224
183	4.828	147	228
218	4.900	148	234
273	5.017	157	286
384	5.217	154	281
456	5.239	152	271
546	5.267	161	317
load removed			
556	0.730	88	8

* measured from loading

** compression positive

The neutral axis of C5 lies so far outside the section that the depth values are meaningless.

Specimen C6 had been loaded previously (see text).

TABLE 10: continued

C7: Mean Shrinkage Strain

Time* days	Mean shrinkage strain $x10^{-6}$
0	0
12	30
26	70
60	116
136	164
218	217
300	221
346	256
382	228
423	226
465	258
506	170
548	218

* 28 days from casting taken as zero

TABLE 11: Column Section Moment Curvature Parameters

Time* days	MNM^2	KNM	MNM^2	KNM
0	4.40	0	1.95	4.21
1	4.12	0	2.45	2.35
2	3.83	0	1.95	3.25
3	3.70	0	1.90	3.30
4	3.45	0	2.00	3.25
5	3.30	0	1.80	3.15
6	3.25	0	1.93	2.80
7	3.40	0	1.45	4.25
8	3.35	0	1.35	3.90
9	3.20	0	1.70	3.60
10	3.20	0	1.80	3.35
12	3.10	0	1.68	3.52
14	3.05	0	1.85	3.00
16	2.95	0	1.75	3.35
18	2.95	0	1.70	3.40
20	2.90	0	1.70	3.35
25	2.80	0	1.70	3.30
30	2.60	0	1.80	3.00
35	2.55	0	1.60	3.40
40	2.50	0	1.63	3.35
45	2.40	0	1.60	3.40
50	2.40	0	1.70	3.10
65	2.30	0	1.73	2.80
80	2.20	0	1.70	2.90
100	2.20	0	1.90	2.25
125	2.10	0	1.70	2.80
150	1.95	0	1.60	2.90
200	1.90	0	1.66	2.40
250	1.85	0	1.70	2.20
300	1.80	0	1.55	3.65
350	1.80	0	1.55	2.60
400	1.75	0	1.60	2.30
450	1.70	0	1.50	2.70
500	1.70	0	1.50	2.50
550	1.70	0	1.40	2.90

*measured from loading

D. Full Scale Structures

Three full scale structures were investigated under sustained load of 18 months duration.

(a) Frame 1, a rectangular frame whose members have the beam section throughout. The geometry of the frame and the loads which were applied are shown in diagram 13. The loads were applied by making use of the strong floor of the laboratory with its grid of holes at 760 mm centres. It was decided to load the lower beam of the frame by means of a steel spreader beam spanning from one loading point to the other. The spreader beam was then loaded by a second steel beam, crossing it obliquely, with two cables passing from it down through the laboratory floor to hollow ram jacks in the basement, plate 4. The loading cables consisted of 15 mm diameter prestressing strand with a short length of 22 mm diameter Macalloy threaded bar at the lower end. The bar passed through the floor and maintained the load by means of a nut bearing against a plate, with a rubber pad between this plate and the underside of the floor. The nut can be seen inside the stressing box in plate 5 which shows the ram of the jack in place ready to apply load. The loads were measured by means of tension load cells incorporated into the loading cables. A dense rubber pad 25 mm thick was placed between the top surface of the concrete beam and the steel load spreader; a similar pad was provided between the underside of the laboratory floor and the ram of the jack. These pads were used to distribute the load evenly over the concrete surface and also to introduce a bit more "spring" into the loading system. The uniformly distributed load was applied to the top beam in the form of 10 separately applied point loads 760 mm apart. Each point load was applied using a ratchet type of hoist and the load was measured by the extension of tension springs incorporated into the system, see plate 4. The top load spreader applied the load through a hardwood half-round section bearing on a flat steel plate.

DIAGRAM 13: Frame 1

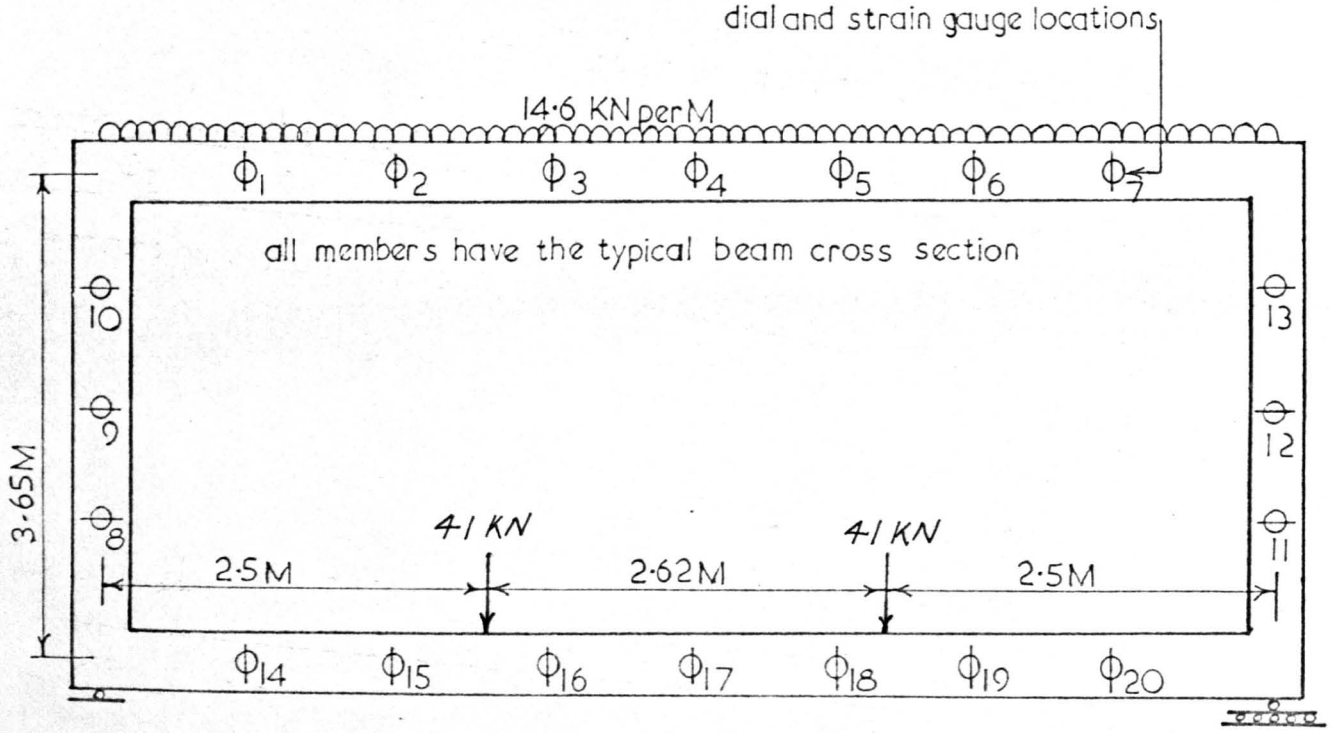

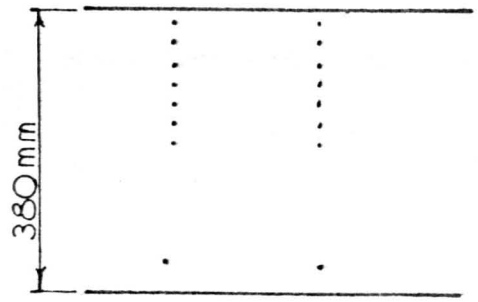

typical arrangement of strain gauge targets

A dense rubber pad was inserted between the steel plate and the concrete. Loading was performed incrementally, that is a fraction of the final load was applied to the lower beam, then the same fraction of the final load was applied to the upper beam and so on until the final values were reached. By "topping up" operations the loads were maintained in the range $\pm$ 2.5% of the required values.

Strain and deflection observations were made at the locations shown in diagram 13; readings were taken immediately after loading and at roughly equal intervals of log time up to a maximum time between observations of approximately three months. Further readings were taken after the removal of the loads and for a subsequent period of 100 days in order to measure the creep recovery. The position of the targets is shown in diagram 13; 16 gauge lengths were provided at each location.

The readings were computer processed and the values of curvature, neutral axis depth and deflection at each location are shown in table 12.

The extent of cracking was observed and is shown in diagram 14.

(b) Frame 2, each member of this frame has one of the cross sections investigated under sustained load. The geometry of the frame and the loads which were applied are shown in diagram 15. Each load was applied using two cables, one each side of the frame, passing through the laboratory floor to the jacks beneath. The load was transmitted to the specimen through a spreader beam and steel half round section, rubber pads were again included in the system. During the test the tops of the two columns were fixed in position (but free to rotate) so that significant sidesway was prevented. This frame can be seen in plate 4, behind and to the right of frame 1. Loading was performed incrementally, that is a fraction of the

DIAGRAM 14: Cracking Patterns on Frame 1

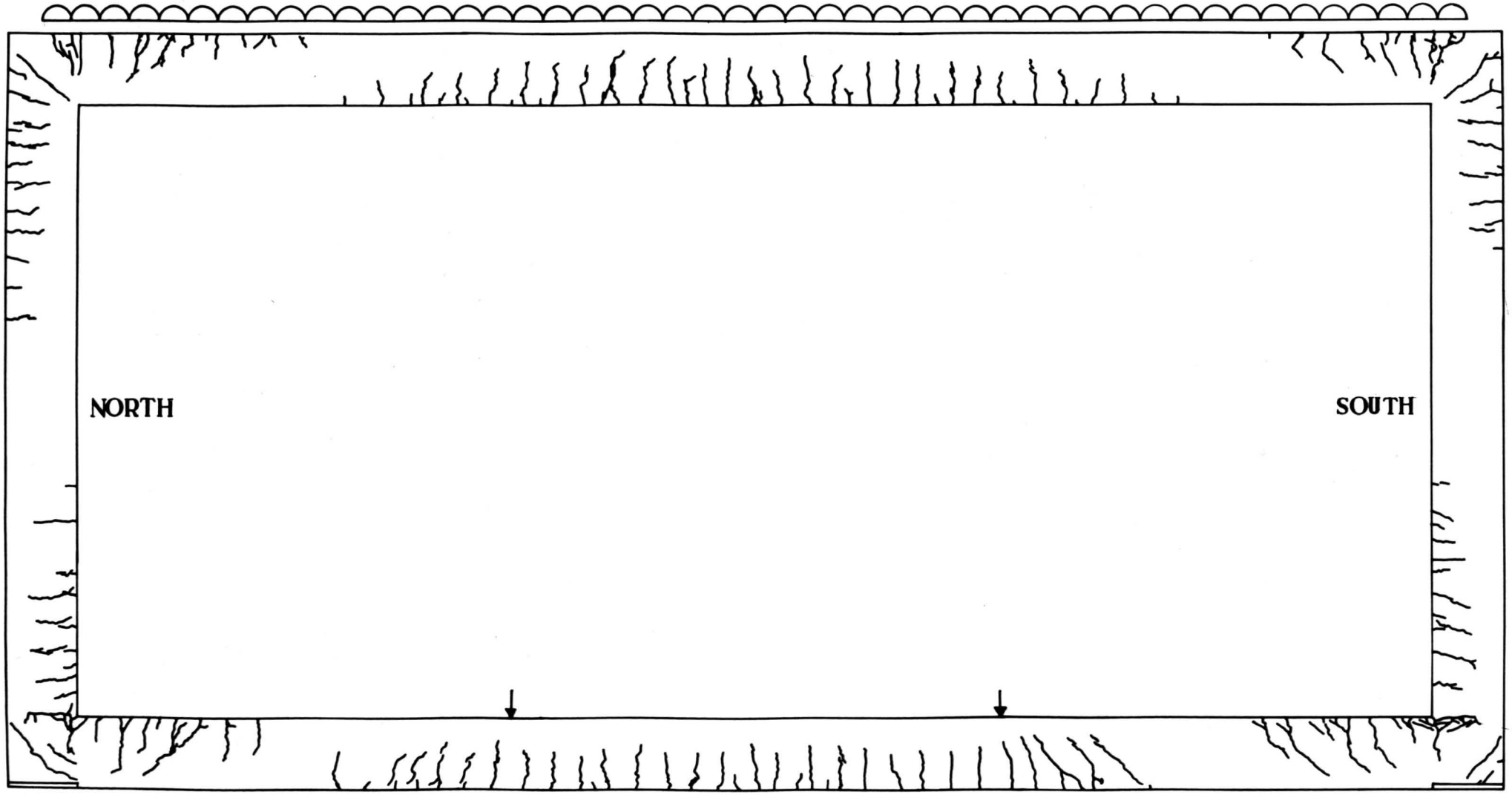

DIAGRAM 14: Continued

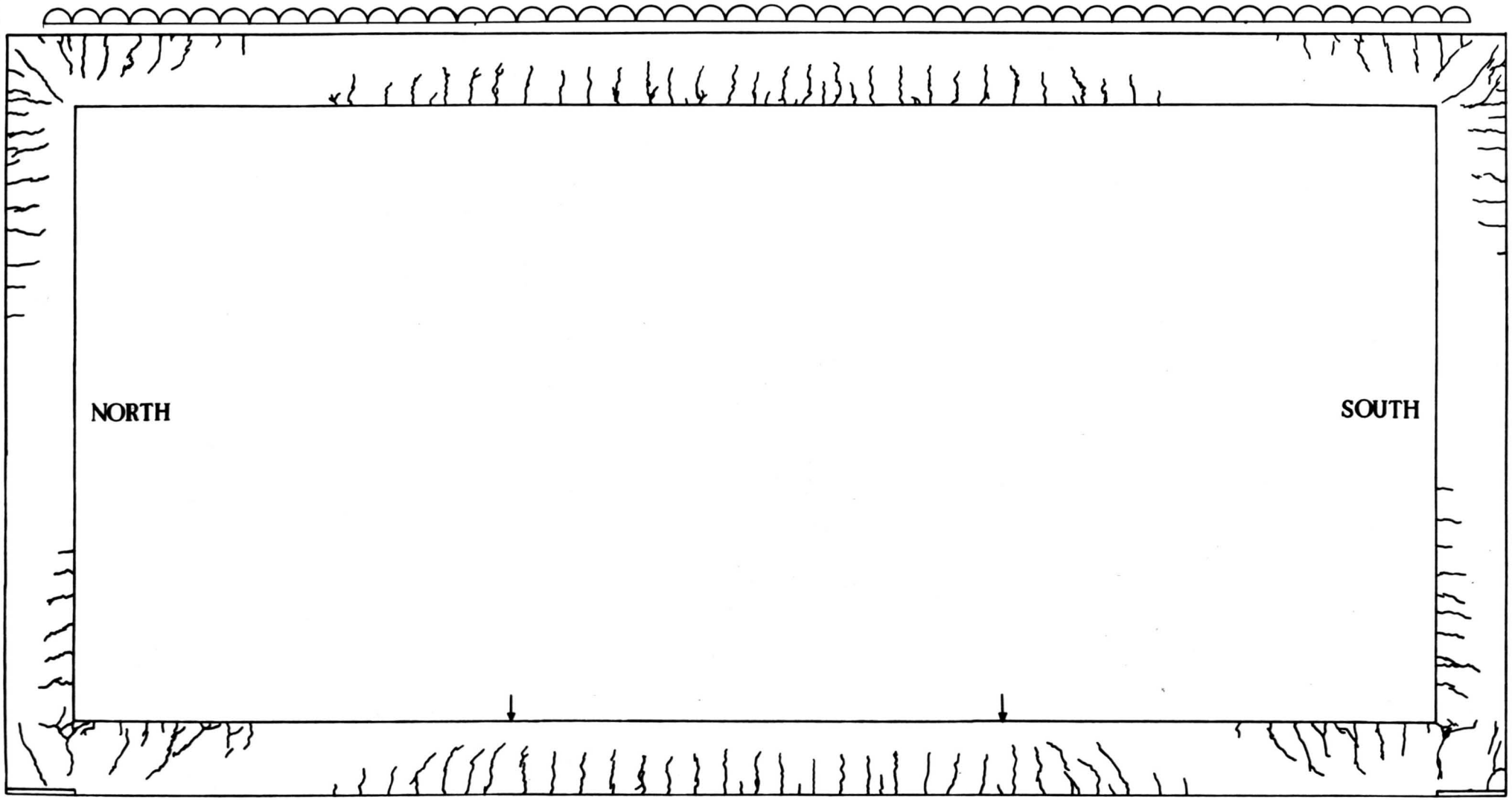

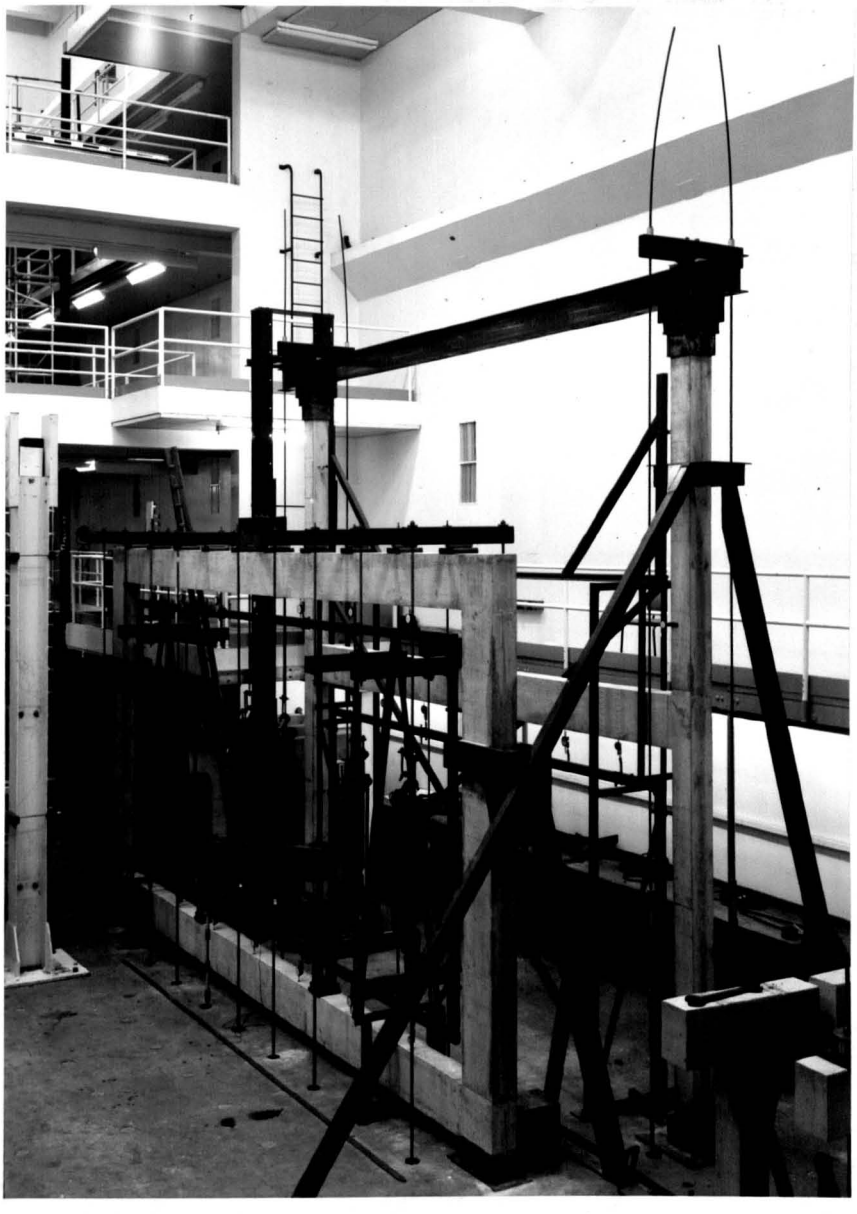

PLATE 4: Loading Arrangements for Plane Frames

final load was applied to the beam and then the same fraction of the final load was applied to each column and so on until the final values were reached. By "topping up" operations the loads were maintained in the range $\pm$ 2.5% of the required values. The loads were measured by means of tension load cells incorporated into the loading cables.

Strain and deflection observations were taken at the locations shown in diagram 15; readings were taken immediately after loading and at

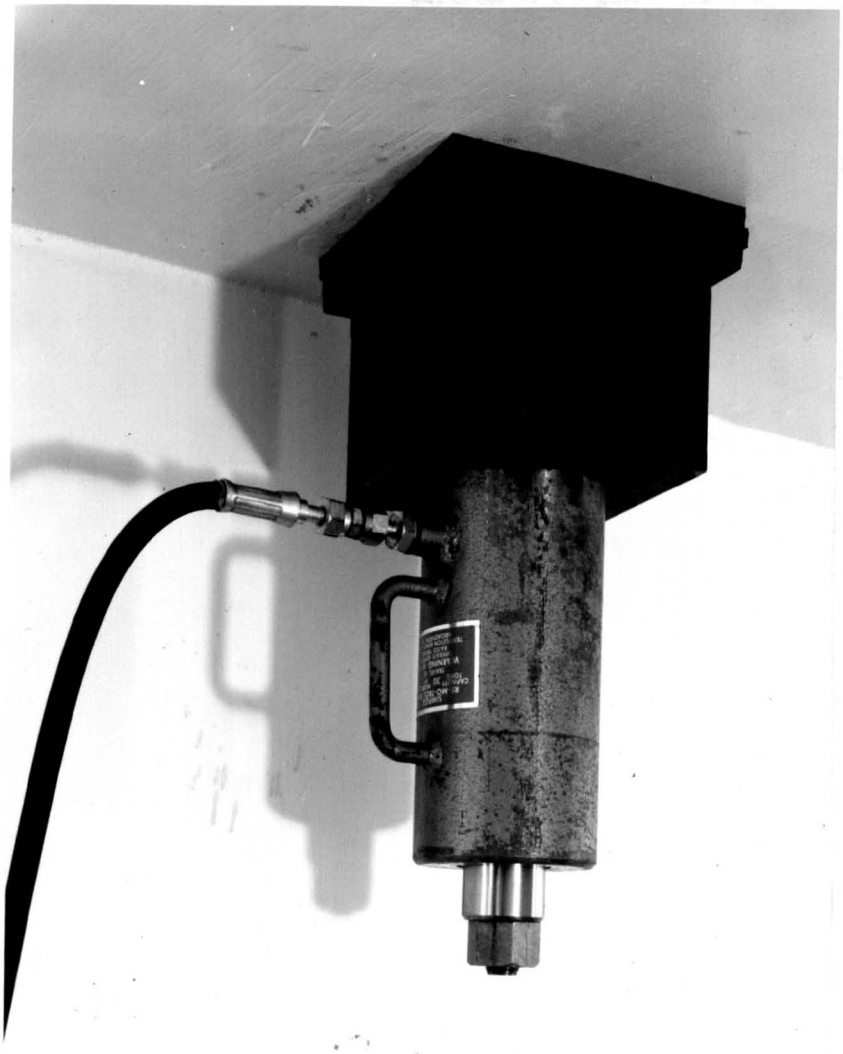

PLATE 5: Application of load by jacking against the underside of the laboratory floor.

roughly equal intervals of log time up to a maximum time between observations of approximately three months. Further readings were taken after the removal of the loads and for a subsequent period of 100 days in order to measure the creep recovery. The position of the targets is shown in diagram 15; 16 gauge lengths were provided at each beam location and 14 gauge lengths at each column location. The readings were computer processed and the values of curvature, neutral axis depth, column mean strain and deflection at each location are shown in table 13. The extent of cracking was observed and is shown in diagram 16.

DIAGRAM 15: Frame 2

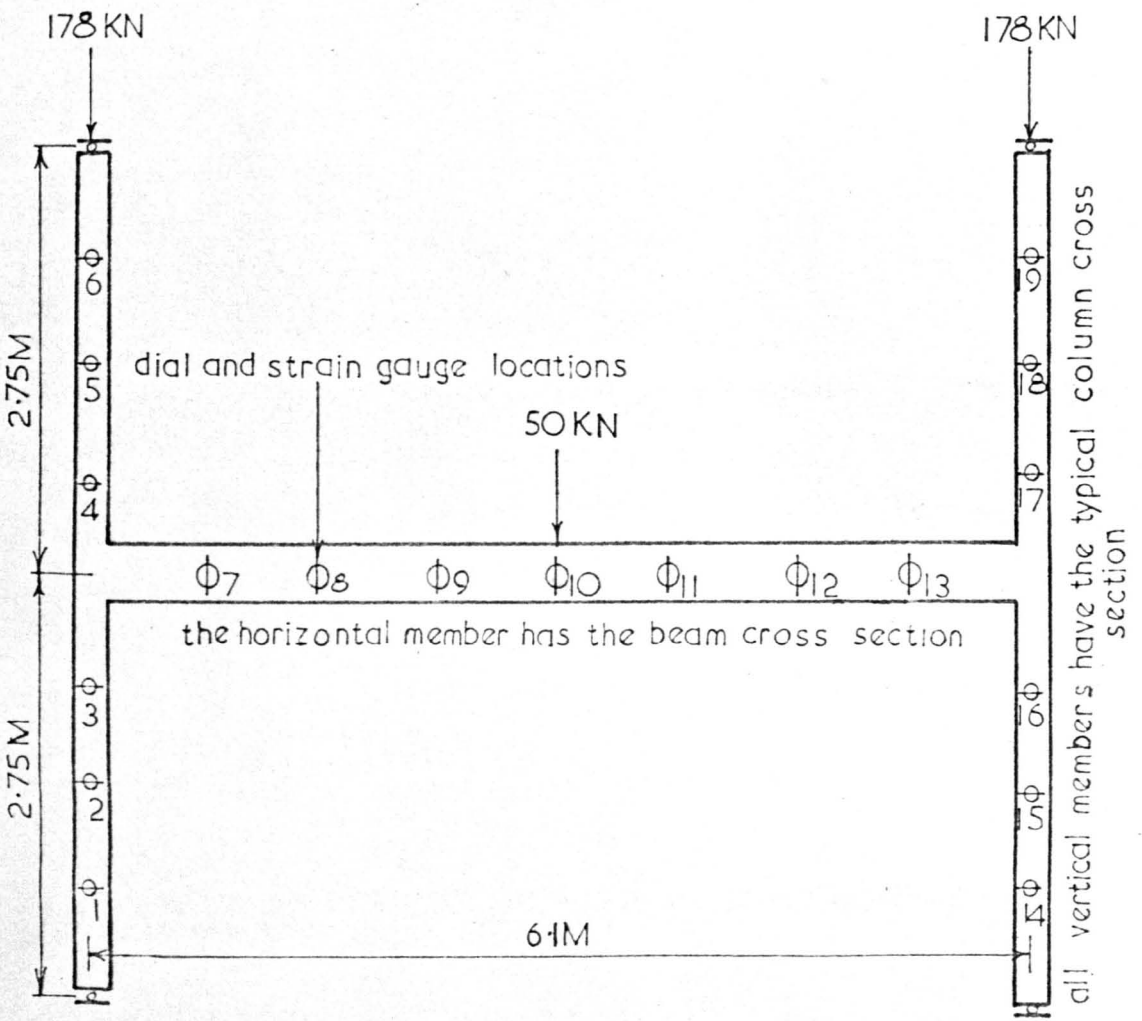

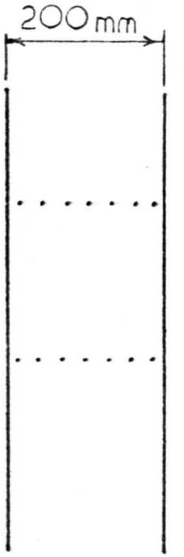

typical arrangement of strain gauge targets at column locations

DIAGRAM 16: Cracking Patterns in Frame 2

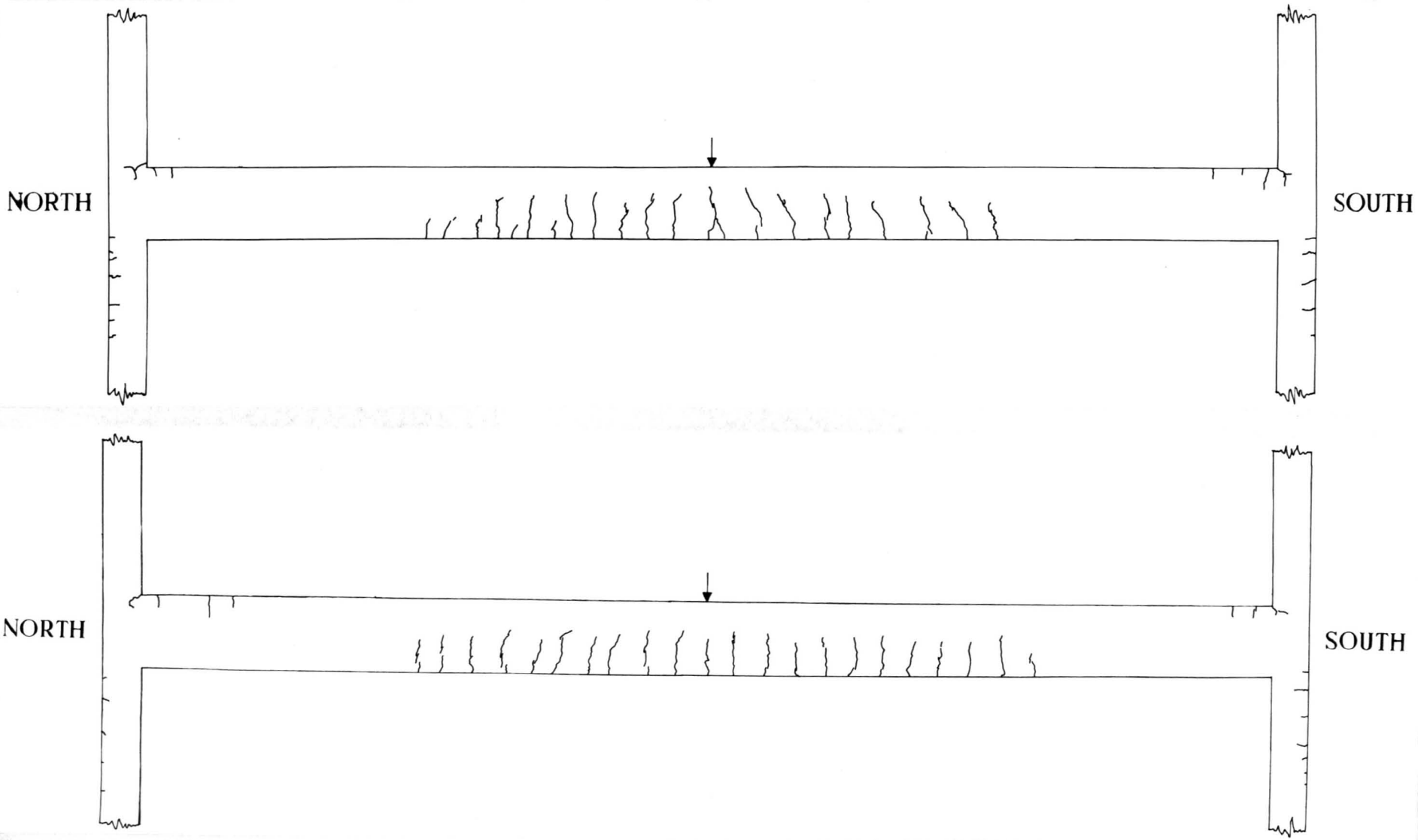

TABLE 12: Experimental Results, Frame 1.

Deflections under sustained load, mm

Location*	Time in days measured from loading												
	0	2	5	12	26	40	61	133	218	299	382	467	550
1	5.21	5.59	5.79	6.05	6.35	6.68	7.06	7.65	8.41	9.04	9.22	9.47	9.65
2	9.19	10.03	10.36	10.87	11.46	12.12	12.88	14.12	15.54	16.76	17.15	17.73	18.06
3	12.50	13.72	14.17	14.91	15.67	16.54	17.60	19.25	21.23	22.89	23.39	24.16	24.61
4	13.72	15.06	15.54	16.36	17.20	18.19	19.30	21.16	23.24	25.04	25.53	26.37	26.85
5	12.24	13.54	14.02	14.71	15.52	16.38	17.40	19.08	21.01	22.71	23.16	23.93	24.33
6	8.61	9.60	9.96	10.44	11.02	11.71	12.42	13.69	15.14	16.41	16.71	17.30	17.60
7	4.14	4.65	4.80	5.08	5.38	5.72	5.99	6.58	7.37	8.03	8.20	8.43	8.63
8	- 0.36	- 0.46	- 0.51	- 0.41	- 0.53	- 0.58	- 0.46	- 0.23	- 0.18	- 0.05	0.05	0.03	0.03
9	0.38	0.38	0.36	0.51	0.43	0.41	0.53	0.89	0.94	1.09	1.22	1.22	1.22
10	1.12	1.24	1.22	1.42	1.42	1.45	1.57	2.01	2.13	2.34	2.46	2.46	2.50
11	- 1.78	- 1.80	- 1.83	- 1.91	- 1.75	- 1.75	- 1.93	- 1.93	- 1.93	- 2.06	- 2.06	- 2.26	- 2.28
12	- 1.42	- 1.42	- 1.42	- 1.42	- 1.27	- 1.24	- 1.30	- 1.09	- 1.02	- 1.02	- 1.07	- 1.12	- 1.09
13	- 0.99	- 0.99	- 0.94	- 0.86	- 0.71	- 0.66	- 0.61	- 0.28	- 0.05	0.05	0.05	0.05	0.15
14	- 5.89	- 6.48	- 6.50	- 6.88	- 7.16	- 7.19	- 7.42	- 8.61	- 9.04	- 9.60	- 9.86	- 9.90	-10.19
15	-10.77	- 11.76	-11.86	-12.78	-13.13	-13.23	-13.92	-16.59	-17.32	-18.52	-19.15	-19.28	-19.81
16	-14.55	-15.84	-15.98	-17.30	-17.68	-17.86	-18.85	-22.53	-23.37	-25.32	-26.24	-26.39	-27.13
17	-15.82	-17.32	-17.45	-18.90	-19.35	-19.53	-20.57	-24.71	-25.63	-27.46	-28.40	-28.52	-29.27
18	-14.27	-15.67	-15.80	-17.07	-17.58	-17.73	-18.69	-22.30	-23.24	-24.92	-25.73	-25.86	-26.59
19	-10.06	-11.20	-11.25	-12.09	-12.52	-12.62	-13.23	-15.80	-16.54	-17.70	-18.29	-18.36	-18.92
20	- 4.70	- 5.31	- 5.28	- 5.66	- 5.89	- 5.92	- 6.17	- 7.32	- 7.70	- 8.20	- 8.46	- 8.51	- 8.74

* see diagram 13

Positive deflections are towards the inside of the frame.

TABLE 12: continued

Curvatures under sustained load, x 10^{-6} mm^{-1}

Location*	Time in days measured from loading												
	0	2	5	12	26	40	60	133	218	299	382	467	550
1	-0.457	-0.679	-0.491	-0.693	-0.743	-0.829	-0.081	-0.846	-1.017	-1.020	-1.018	-1.001	-1.097
2	0.821	0.764	1.036	0.979	0.900	0.757	1.050	1.229	1.400	1.714	1.743	1.879	1.886
3	2.331	2.463	2.583	2.726	2.929	3.157	3.457	3.679	3.900	4.136	4.229	4.279	4.429
4	3.006	3.080	3.186	3.300	3.443	3.593	3.900	4.164	4.514	4.836	4.979	4.971	5.107
5	2.414	2.464	2.650	2.693	2.921	2.993	3.221	3.671	3.943	4.136	4.250	4.293	4.471
6	0.821	0.950	0.986	0.950	0.986	1.107	1.093	1.329	1.550	1.807	1.864	1.907	1.979
7	-0.200	-0.300	-0.286	-0.414	-0.393	-0.414	-0.457	-0.664	-0.607	-0.564	-0.636	-0.593	-0.712
8	-1.407	-1.571	-1.679	-1.886	-2.071	-2.129	-2.286	-2.436	-2.643	-2.936	-2.914	-2.950	-2.921
9	-0.080	-0.077	-0.118	-0.076	-0.128	-0.101	-0.118	-0.061	-0.052	-0.052	-0.045	-0.061	-0.107
10	1.451	1.821	1.771	1.971	2.100	2.150	2.307	2.786	2.957	2.993	3.100	3.207	3.343
11	-1.293	-1.400	-1.621	-1.529	-1.671	-1.829	-1.857	-1.993	-2.293	-2.421	-2.464	-2.643	-2.743
12	-0.013	-0.013	-0.018	-0.017	-0.028	-0.073	-0.023	-0.010	-0.041	-0.058	-0.047	-0.085	-0.494
13	1.250	1.300	1.550	1.664	1.779	1.829	1.857	2.386	2.536	2.843	2.878	2.900	2.914
14	-0.800	-0.743	-0.736	-0.693	-0.736	-0.807	-0.779	-0.807	-0.864	-0.714	-0.693	-0.543	-0.436
15	1.051	1.029	1.014	1.157	1.221	1.279	1.457	1.800	1.886	2.021	2.129	2.021	2.107
16	3.040	3.480	3.177	3.457	3.617	3.800	3.926	4.697	5.371	5.657	5.721	5.650	5.864
17	3.260	3.600	3.286	3.121	3.307	3.607	3.571	4.243	4.450	4.743	4.814	4.779	5.071
18	2.920	3.120	3.166	3.480	3.463	3.686	3.577	4.500	4.621	4.850	4.943	4.850	5.121
19	0.780	0.800	0.686	0.700	1.234	1.183	1.320	1.879	2.114	2.386	2.486	1.977	1.983
20	-1.140	-0.940	-1.280	-1.300	-1.246	-1.337	-1.411	-1.646	-1.737	-1.869	-1.789	-0.640	-0.420

*see diagram 13

Positive curvatures indicate tension on the inside of the frame.

TABLE 12: continued

Depth of neutral axis of strain** under sustained load, mm

Location*	Time in days measured from loading												
	0	2	5	12	26	40	60	133	218	299	382	467	550
1	191	177	210	207	246	251	258	342	359	363	374	390	349
2	173	182	178	197	236	316	255	292	309	291	299	296	284
3	164	167	159	169	182	187	186	206	217	223	228	231	224
4	147	153	162	173	183	192	189	208	215	220	220	226	223
5	163	173	157	169	185	198	195	208	219	229	229	359	229
6	213	198	203	233	260	261	282	311	307	301	304	309	297
7	286	228	288	309	352	393	392	416	503	587	559	560	494
8	172	174	192	190	206	219	219	241	248	247	252	245	241
9	-	-	-	-	-	-	-	-	-	-	-	-	-
10	154	178	187	183	200	213	211	225	234	242	246	243	233
11	173	179	188	198	212	217	231	258	261	269	271	253	243
12	-	-	-	-	-	-	-	-	-	-	-	-	-
13	192	221	200	198	205	229	239	233	256	251	254	255	249
14	131	140	169	192	227	250	263	341	377	457	495	606	736
15	141	160	165	177	188	209	201	230	244	248	248	262	254
16	123	131	143	146	155	164	166	179	176	181	184	188	187
17	119	128	140	154	167	173	177	192	201	204	207	211	206
18	127	137	141	143	158	164	171	178	189	195	198	202	199
19	128	151	171	201	164	195	188	193	195	190	192	225	219
20	106	114	117	120	140	164	156	200	186	185	194	474	662

* see diagram 13

†* measured from the compression face

At some locations the neutral axis of strain was so far outside the section that its depth value is meaningless.

TABLE 12: continued

Deflections during recovery, mm

Location*	Time in days measured from loading									
	578	581	584	587	591	598	605	619	633	678
1	5.16	5.00	4.93	4.90	4.95	4.85	4.80	4.80	4.75	4.75
2	9.73	9.35	9.22	9.22	9.17	9.02	8.99	8.92	8.86	8.79
3	13.00	12.45	12.32	12.27	12.22	12.04	11.94	11.86	11.79	11.66
4	14.00	13.39	13.26	13.16	13.11	12.90	12.83	12.73	12.65	12.50
5	12.93	12.37	12.27	12.19	12.14	11.96	11.89	11.79	11.71	11.56
6	9.65	9.27	9.17	9.12	9.09	8.97	8.92	8.86	8.81	8.69
7	4.93	4.75	4.72	4.69	4.67	4.97	4.60	4.57	4.54	4.50
8	0.61	0.66	0.61	0.61	0.66	0.79	0.61	0.69	0.69	0.74
9	0.97	1.04	0.99	1.02	1.07	1.17	0.97	1.04	1.04	1.07
10	1.42	1.45	1.37	1.37	1.45	1.49	1.29	1.37	1.37	1.40
11	- 1.06	- 1.07	- 1.02	- 1.04	- 1.04	- 1.17	- 0.97	- 1.04	- 1.04	- 1.04
12	- 0.33	- 0.31	- 0.28	- 0.28	- 0.35	- 0.48	- 0.25	- 0.36	- 0.33	- 0.33
13	0.48	0.48	0.48	0.48	0.43	0.28	0.48	0.43	0.41	0.41
14	- 5.08	- 4.93	- 4.91	- 4.87	- 4.88	- 4.83	- 4.78	- 4.78	- 4.72	- 4.67
15	- 9.83	- 9.53	- 9.45	- 9.37	- 9.35	- 9.19	- 9.09	- 9.02	- 8.99	- 8.89
16	-13.28	-12.83	-12.73	-12.62	-12.60	-12.40	-12.24	-12.17	-12.09	-11.96
17	-14.20	-13.69	-13.56	-13.49	-13.44	-13.23	-13.06	-12.95	-12.88	-12.73
18	-13.13	-12.62	-12.55	-12.47	-12.42	-12.22	-12.04	-11.94	-11.91	-11.73
19	- 9.68	- 9.35	- 9.32	- 9.22	- 9.25	- 9.04	- 8.94	- 8.92	- 8.86	- 8.76
20	- 4.80	- 4.67	- 4.65	- 4.62	- 4.62	- 4.55	- 4.50	- 4.47	- 4.47	- 4.42

*see diagram 13

Positive deflections are towards the inside of the frame

TABLE 12: continued

Curvatures during recovery, x 10^{-6} mm^{-1}

Location*	Time in days measured from loading									
	578	581	584	587	591	598	605	619	633	678
1	-0.556	-0.522	-0.522	-0.555	-0.507	-0.553	-0.483	-0.485	-0.452	-4.749
2	1.221	1.000	1.179	1.100	1.121	1.193	1.071	1.129	1.093	1.064
3	1.907	1.821	1.800	1.757	1.786	1.743	1.714	1.679	1.743	1.621
4	2.229	2.257	2.171	2.221	2.143	2.171	2.079	2.064	2.100	1.943
5	2.171	2.057	2.071	1.986	2.021	1.943	1.964	1.871	1.871	1.807
6	1.150	1.286	1.100	0.879	1.143	1.121	1.036	1.056	1.043	1.007
7	-1.286	-0.093	-0.064	-0.100	-0.071	-0.050	-0.064	-0.071	-0.064	-0.107
8	-1.771	-1.486	-1.600	-1.507	-1.564	-1.493	-1.564	-1.450	-1.464	-1.543
9	0.049	0.042	0.027	0.114	0.062	0.075	0.051	0.020	0.046	0.034
10	1.936	1.836	1.829	1.964	1.836	1.764	1.850	1.857	1.800	1.821
11	-1.364	-0.800	-1.457	-1.264	-1.493	-1.429	-1.364	-1.329	-1.379	-1.314
12	-0.006	0.038	0.378	0.020	0.010	0.015	0.001	0.020	0.031	0.005
13	1.693	1.779	1.743	0.174	1.757	1.679	1.671	1.700	1.614	1.757
14	0.357	0.386	0.443	0.500	0.400	0.543	0.579	0.557	0.550	0.543
15	1.550	1.379	1.400	1.521	1.429	1.414	1.493	1.407	1.329	1.421
16	3.136	3.121	3.121	3.036	2.993	2.979	3.014	3.000	3.000	2.943
17	2.507	2.236	2.200	2.279	2.307	2.200	2.193	2.193	2.179	2.343
18	1.550	1.364	1.421	1.393	1.307	1.300	1.221	1.150	1.143	1.164
19	1.543	1.457	1.543	1.436	1.386	0.989	1.350	1.343	1.307	1.229
20	0.700	0.800	0.543	0.360	0.446	0.800	0.400	0.383	0.389	0.240

*see diagram 13

Positive curvatures indicate tension on the inside of the frame

TABLE 12: continued

Depth of neutral axis of strain** during recovery, mm

Location*	Time in days measured from loading									
	578	581	584	587	591	598	605	619	633	678
1	-	-	-	-	-	-	-	-	-	-
2	328	382	331	355	346	291	356	336	343	371
3	291	288	290	296	290	269	294	296	286	306
4	294	284	287	286	292	267	296	294	290	312
5	286	291	288	297	292	278	297	307	305	316
6	371	339	376	463	367	333	391	377	385	417
7	-	-	-	-	-	-	-	-	-	-
8	267	295	287	284	291	271	290	299	294	278
9	-	-	-	-	-	-	-	-	-	-
10	275	276	274	266	273	257	275	265	270	273
11	307	471	299	312	303	283	313	326	309	305
12	-	-	-	-	-	-	-	-	-	-
13	295	287	283	287	284	265	293	286	295	281
14	508	434	395	329	388	218	268	245	261	292
15	288	310	314	294	301	278	300	304	320	311
16	211	206	210	213	210	194	209	206	206	212
17	242	256	259	251	246	235	252	250	248	243
18	289	300	294	293	301	269	311	314	324	319
19	221	225	221	233	230	260	231	231	235	237
20	141	105	282	390	294	340	327	319	305	495

* see diagram 13

** measured from the compression face

At some locations the neutral axis of strain was so far outside the section that its depth value is meaningless.

(c) Continuous beams. A pair of two span continuous beams were tested under sustained load of 18 months duration. The beams were loaded "back to back" as shown in plate 6 and the results were averaged so that the effects of self weight were excluded. The principal advantage in testing a pair of beams in this way is that each will serve as the reaction frame for the other.. The geometry of the beams and the loads which were applied are shown in diagram 17. The loads were applied using tension springs of 20 KN capacity; the extension of the springs was used to measure the magnitude of the load. Each load was applied by two springs one each side of the beam and the load was transferred to the beams via a ball seating at each end of the spring assembly. Every spring was extended at one end with a length of threaded rod so that the load could be applied directly with a nut bearing against a thrust race. Loading was performed incrementally, that is a fraction of the final load was applied at one location and the same fraction at the other locations and so on until the final values were reached. By "topping up" operations the loads were maintained in the range $\pm$ 2.5% of the required values.

Strain and deflection observations were taken at the locations shown in diagram 17; readings were taken immediately after loading and at roughly equal intervals of log time up to a maximum time between observations of approximately three months. The position of the targets is shown in diagram 17; 16 gauge lengths were provided at each location. The readings were computer processed and the values of curvature, neutral axis depth and deflection at each location are shown in table 14. The extent of cracking was observed and is shown in diagram 18.

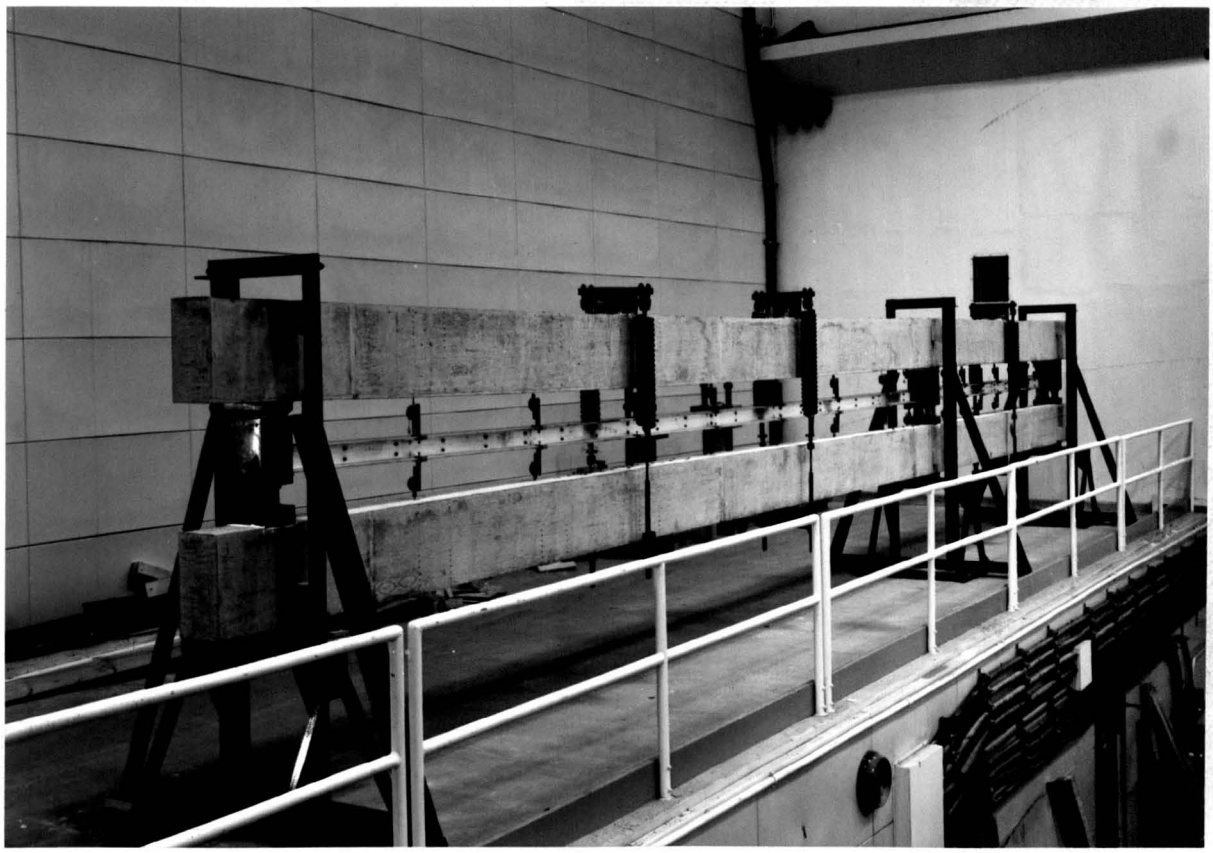

PLATE 6: Continuous Beams under Test.

DIAGRAM 17: Continuous Beam

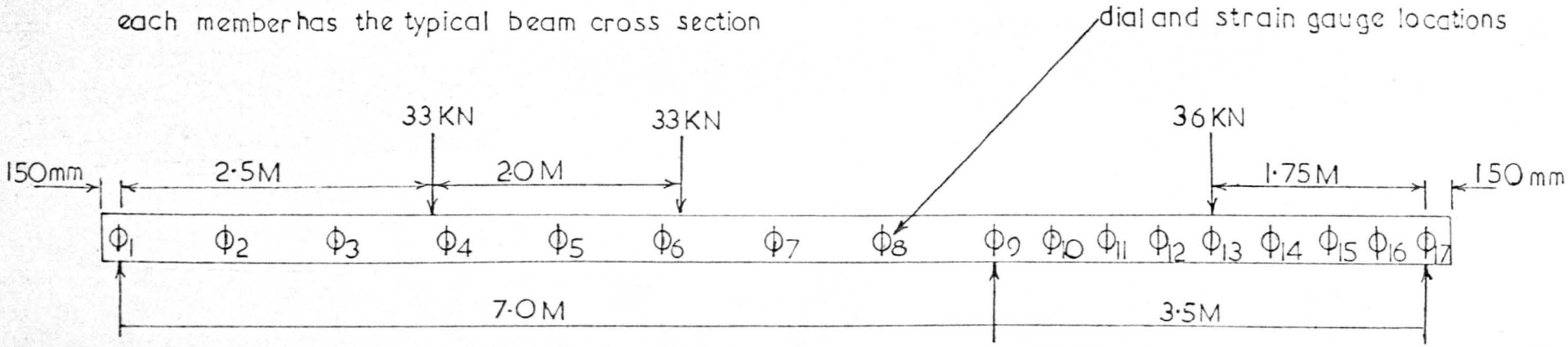

DIAGRAM 18: Cracking Patterns in Continuous Beams

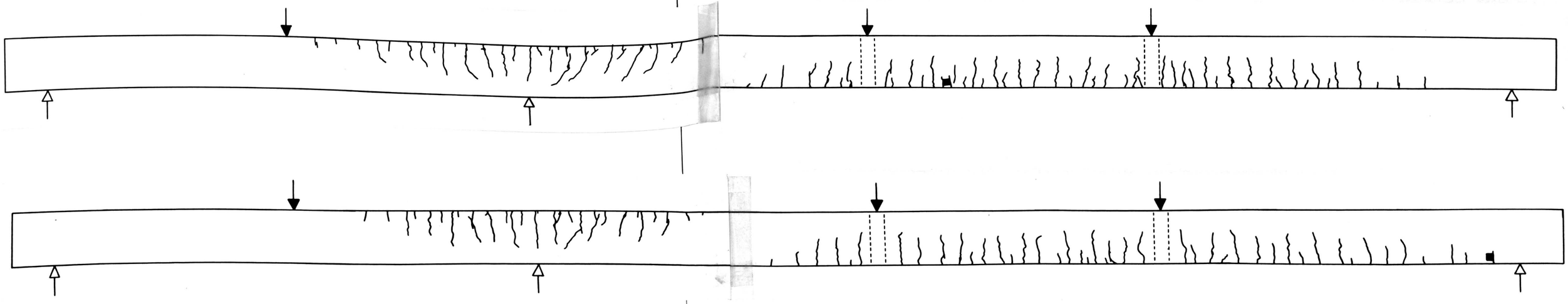

TABLE 13: Experimental Results, Frame 2

Deflections under sustained load, mm

Location*	Time in days measured from loading											
	0	1	5	12	26	60	144	218	299	382	466	551
1	- 1.85	- 1.98	- 2.18	- 2.34	- 2.46	- 2.82	- 3.07	- 3.30	- 3.45	- 3.66	- 3.71	- 3.73
2	- 2.21	- 2.39	- 2.72	- 3.00	- 3.15	- 3.73	- 4.11	- 4.45	- 4.70	- 4.98	- 5.05	- 5.03
3	- 1.96	- 2.18	- 2.54	- 2.77	- 2.95	- 3.51	- 3.86	- 4.11	- 4.39	- 4.70	- 4.55	- 4.72
4	0.99	0.99	0.98	1.07	0.97	1.09	0.81	0.84	1.12	1.22	1.42	1.37
5	1.68	1.65	1.70	1.75	1.73	1.83	1.98	1.93	2.13	2.29	2.57	2.51
6	1.98	1.88	1.80	1.85	1.75	1.68	1.75	1.68	1.80	1.88	2.29	2.10
7	4.29	4.09	4.06	4.47	5.00	5.82	6.40	6.96	7.47	7.92	8.15	8.20
8	6.12	6.50	7.11	7.65	8.00	9.25	10.13	11.02	11.84	12.55	12.88	13.00
9	8.10	8.59	9.42	10.16	10.57	12.19	13.26	14.38	15.47	16.43	16.97	17.04
10	8.51	8.99	9.91	10.74	11.15	12.90	14.07	15.24	16.46	17.50	18.08	18.16
11	8.03	8.51	9.32	10.08	10.49	12.12	15.72	14.30	15.39	16.36	16.84	16.97
12	5.89	6.27	6.91	7.47	7.80	8.99	9.86	10.69	11.53	12.24	12.62	12.70
13	4.45	4.70	5.08	5.46	5.66	6.45	7.01	7.49	8.05	8.48	8.66	8.76
14	- 1.27	- 1.27	- 1.37	- 1.30	- 1.40	- 1.55	- 1.47	- 1.55	- 1.63	- 1.65	- 1.78	- 1.80
15	- 1.75	- 1.70	- 1.75	- 1.87	- 1.80	- 1.91	- 1.88	- 1.96	- 1.96	- 2.08	- 2.26	- 2.13
16	- 1.24	- 1.14	- 1.17	- 1.24	- 1.09	- 1.09	- 0.86	- 0.97	- 0.84	- 0.86	- 1.02	- 0.94
17	1.70	1.93	2.26	2.54	2.84	3.51	4.09	4.65	4.98	5.36	5.33	5.46
18	2.36	2.62	2.95	3.25	3.56	4.29	4.98	5.54	5.94	6.32	6.27	6.40
19	2.41	2.64	2.69	2.72	3.00	3.63	4.24	4.75	5.08	5.36	5.21	5.30

* see diagram 14

At beam locations downward deflections are positive, at column locations deflections towards the inside of the frame are positive.

TABLE 13: continued

Curvatures under sustained load, x 10^{-6} mm^{-1}

Location *	Time in days measured from loading										
	0	5	12	26	61	144	218	299	382	466	551
1	-0.911	-1.028	-1.089	-1.155	-1.393	- 1.339	-1.732	-1.804	-1.887	-1.923	-1.917
2	-2.048	-2.316	-2.591	-2.673	-3.048	- 3.387	-3.679	-3.869	-3.964	-4.066	-4.214
3	-3.833	-4.167	-4.333	-4.567	-5.150	- 5.591	-5.962	-6.371	-6.700	-6.838	-6.881
4	1.869	2.226	2.530	3.577	3.226	3.560	3.833	5.214	4.494	4.554	4.589
5	1.399	1.595	1.631	1.667	2.095	2.304	2.458	2.679	2.869	2.941	2.917
6	0.619	0.667	0.070	0.816	0.988	1.101	1.208	1.381	1.488	1.530	1.500
7	-0.021	-0.089	-0.008	-0.112	00.038	0.246	0.234	0.305	3.435	0.377	0.384
8	0.836	0.929	1.057	0.957	1.329	1.529	1.757	1.850	2.000	2.093	2.157
9	2.700	2.740	2.940	2.920	3.583	3.650	3.971	4.100	4.286	4.464	4.493
10	-	-	-	-	-	-	-	-	-	-	-
11	2.240	2.480	2.697	2.766	3.223	3.529	3.779	3.936	4.150	4.236	4.236
12	0.907	1.182	1.164	1.207	1.450	1.686	2.000	2.121	2.271	2.307	2.371
13	0.095	1.060	0.122	0.055	0.184	0.219	0.262	0.291	0.322	0.314	0.353
14	-0.875	-1.804	-1.119	-1.173	-1.363	-1.506	-1.667	-1.810	-1.875	-2.000	-1.952
15	-1.643	-1.804	-1.952	-2.036	-2.316	-2.482	-2.601	-2.833	-2.976	-2.994	-3.054
16	-2.829	-3.233	-3.481	-3.619	-4.167	-4.060	-4.286	-4.548	-4.756	-4.899	-4.899
17	1.919	2.124	2.300	2.400	2.957	3.262	3.661	3.970	4.363	4.482	4.566
18	1.316	1.512	1.720	1.720	2.107	2.351	2.625	2.863	3.018	3.179	3.155
19	0.839	0.958	0.994	1.060	1.244	1.524	1.607	1.833	1.893	1.953	2.030

* see diagram 14

At beam locations positive curvatures indicate tension at the underside, at column locations positive curvatures indicate tension at the inside face.

Strain readings were not taken at location 10 as the loading arrangement restricted access.

TABLE 13: continued

Depth of neutral axis of strain** under sustained load

Location*	Time in days measured from loading										
	0	5	12	26	61	144	218	299	382	466	551
1	-	-	-	-	-	-	-	-	-	-	-
2	188	193	185	200	204	231	236	240	248	243	248
3	141	142	145	152	154	174	177	180	182	182	186
4	189	187	182	185	200	221	221	219	221	223	227
5	-	-	-	-	-	-	-	-	-	-	-
6	-	-	-	-	-	-	-	-	-	-	-
7	-	-	-	-	-	-	-	-	-	-	-
8	185	170	180	186	201	229	235	239	252	248	257
9	132	141	143	149	151	169	177	183	190	188	194
10	-	-	-	-	-	-	-	-	-	-	-
11	154	150	152	151	163	176	184	188	195	196	203
12	168	172	165	172	194	222	226	230	238	238	251
13	148	127	189	384	370	-	-	-	-	-	-
14	-	-	-	-	-	-	-	-	-	-	-
15	-	-	-	-	-	-	-	-	-	-	-
16	161	154	159	166	166	200	200	208	210	209	215
17	172	168	169	164	177	197	193	198	196	194	199
18	-	-	-	-	-	-	-	-	-	-	-
19	-	-	-	-	-	-	-	-	-	-	-

* see diagram 14

** measured from the compression face

At some locations the neutral axis of strain was so far outside the section that its depth value is meaningless.

Strain readings were not taken at location 10 as the loading arrangement restricted access.

TABLE 13: continued

Mean strain over cross section under sustained load, x 10^{-6}

Location*	Time in days measured from loading										
	0	5	12	26	61	144	218	299	382	466	551
1	185	225	219	267	308	441	460	501	544	539	572
2	180	214	219	266	318	445	501	544	586	581	624
3	154	177	193	238	277	416	459	509	548	559	592
4	167	194	207	219	322	429	464	501	545	558	584
5	163	184	194	209	323	431	465	511	556	561	597
6	142	181	196	213	309	392	424	461	503	513	545
14	181	195	223	262	293	421	445	528	545	533	569
15	184	201	238	265	311	434	470	534	562	564	594
16	171	175	210	241	279	408	429	493	524	533	564
17	141	148	162	160	231	316	342	389	421	422	463
18	149	156	173	176	245	348	375	424	465	469	504
19	152	172	201	193	273	396	431	495	531	534	571

*see diagram 14

Compression strain positive

TABLE 13: continued

Deflections during recovery, mm

Location*	Time in days measured from loading									
	586	587	588	593	601	607	615	628	642	686
1	-1.55	-1.47	-1.45	-1.45	-1.42	-1.42	-1.40	-1.42	-1.35	-1.32
2	-2.24	-2.13	-2.11	-2.11	-2.01	-1.98	-2.01	-2.01	-1.96	-1.85
3	-1.98	1.90	1.85	1.83	1.78	1.78	1.83	1.83	1.70	1.47
4	0.46	0.46	0.38	0.36	0.33	0.31	0.20	0.18	0.25	0.15
5	1.09	1.04	1.04	0.99	0.94	0.91	0.74	0.71	0.76	0.66
6	0.76	0.76	0.79	0.74	0.69	0.66	0.43	0.41	0.46	0.38
7	3.35	3.26	3.20	3.05	3.00	3.00	2.92	2.92	2.87	2.67
8	5.64	5.41	5.33	5.16	5.08	5.03	4.95	4.90	4.85	4.52
9	7.19	6.93	6.83	6.58	6.48	6.40	6.27	6.20	6.12	5.69
10	7.26	6.98	6.86	6.60	6.45	6.38	6.27	6.15	6.07	5.61
11	7.21	6.93	6.80	6.58	6.48	6.40	6.27	6.20	6.12	5.72
12	5.66	5.46	5.41	5.21	5.13	5.11	5.00	5.00	4.90	5.33
13	4.50	4.37	4.42	4.22	4.19	4.17	4.09	4.06	4.06	3.86
14	-0.43	-0.28	-0.36	-0.30	-0.25	-0.28	-0.18	-0.18	-0.22	-0.13
15	-0.56	-0.56	-0.56	-0.46	-0.43	-0.43	-0.28	-0.28	-0.30	-0.18
16	0.18	0.20	0.25	0.30	0.56	0.33	0.51	0.48	0.79	0.61
17	2.92	2.87	2.82	2.74	2.72	2.74	2.85	2.85	2.77	2.72
18	3.25	3.18	3.12	3.07	3.05	3.05	3.18	3.18	3.07	3.00
19	2.41	2.34	2.31	2.29	2.41	2.41	2.59	2.54	2.34	2.31

* see diagram 14

At beam locations downward deflections are positive, at column locations deflections towards the inside of the frame are positive.

TABLE 13: continued

Curvatures during recovery, x 10^{-6} mm^{-1}

Location*	Time in days measured from loading									
	586	587	588	593	601	607	615	628	642	686
1	-1.012	-0.946	-0.869	-0.881	-0.869	-0.887	-0.821	-0.923	-0.899	-0.839
2	-2.476	-2.369	-2.411	-2.286	-2.256	-2.250	-2.214	-2.173	-2.149	-1.994
3	-3.625	-3.441	-3.411	-3.357	-3.286	-3.262	-3.232	-3.202	-3.238	-3.042
4	1.970	1.881	1.929	1.768	1.702	1.780	1.816	1.661	1.441	1.762
5	1.821	1.744	1.714	1.619	1.744	1.685	1.649	1.679	1.589	1.393
6	0.833	0.833	0.774	0.845	0.875	0.815	0.786	0.780	0.804	0.708
7	0.379	0.353	0.334	0.319	0.339	0.336	0.348	0.328	0.373	0.343
8	1.343	1.336	1.307	1.279	1.257	1.271	1.271	0.130	1.243	1.250
9	2.350	2.200	2.193	2.179	2.186	2.093	2.100	2.136	2.057	2.007
10	-	-	-	-	-	-	-	-	-	-
11	2.207	2.093	2.093	2.079	2.029	2.021	2.000	1.993	1.986	1.843
12	1.571	1.521	1.486	1.486	1.536	1.457	1.500	1.450	1.443	1.407
13	0.367	0.385	0.391	0.363	0.391	0.352	0.380	0.373	0.363	0.407
14	-1.036	-1.030	-0.935	-0.976	-0.917	-0.964	-0.881	-0.827	-1.208	-0.696
15	-1.601	-1.536	-1.446	-1.363	-1.417	-1.375	-1.262	-1.351	-1.321	-1.179
16	-2.292	-2.274	-2.161	-2.107	-2.101	-2.060	-1.976	-1.899	-1.893	-1.738
17	2.167	2.095	2.066	1.941	1.929	1.911	1.923	1.893	1.881	1.726
18	1.673	1.631	1.619	1.518	1.571	1.512	1.476	1.435	1.482	1.411
19	1.169	1.060	1.024	0.976	1.536	0.863	0.750	0.714	0.774	6.726

* see diagram 14

At beam locations, positive curvatures indicate tension at the underside, at column locations positive curvatures indicate tension at the inside face.

Strain readings were not taken at location 10 as the loading arrangement restricted access.

TABLE 13: continued

Depth of neutral axis of strain** during recovery

Location*	Time in days measured from loading									
	586	587	588	593	601	607	615	628	642	686
1	-	-	-	-	-	-	-	-	-	-
2	-	-	-	-	-	-	-	-	-	-
3	203	202	198	198	197	200	205	212	200	206
4	-	-	-	-	-	-	-	-	-	-
5	-	-	-	-	-	-	-	-	-	-
6	-	-	-	-	-	-	-	-	-	-
7	-	-	-	-	-	-	-	-	-	-
8	303	302	295	303	307	308	323	338	319	331
9	230	235	228	229	228	237	245	254	243	254
10	-	-	-	-	-	-	-	-	-	-
11	243	247	238	239	241	244	255	270	252	273
12	285	290	282	283	274	286	297	321	303	322
13	-	-	-	-	-	-	-	-	-	-
14	-	-	-	-	-	-	-	-	-	-
15	-	-	-	-	-	-	-	-	-	-
16	-	-	-	-	-	-	-	-	-	-
17	-	-	-	-	-	-	-	-	-	-
18	-	-	-	-	-	-	-	-	-	-
19	-	-	-	-	-	-	-	-	-	-

* see diagram 14

** measured from the compression face

At some locations the neutral axis of strain was so far outside the section that its depth value is meaningless.

Strain readings were not taken at location 10 as the loading arrangement restricted access.

TABLE 13: continued

Mean strain over cross section during recovery, x 10^{-6}

Location*	Time in days measured from loading									
	586	587	588	593	601	607	615	628	642	686
1	386	377	351	365	346	347	364	383	350	341
2	441	431	405	419	406	403	430	446	406	404
3	374	350	333	329	319	326	339	359	325	323
4	341	313	289	288	296	284	305	319	301	265
5	424	408	388	384	389	394	412	429	391	363
6	386	368	349	344	349	351	366	388	353	326
14	401	385	361	372	353	353	369	394	341	359
15	408	402	371	379	369	364	383	402	371	369
16	370	341	325	324	312	315	332	354	315	314
17	309	294	276	276	261	274	295	313	274	276
18	354	341	323	323	324	329	344	370	325	324
19	404	385	364	379	331	366	374	394	361	339

*see diagram 14

Compression strain positive.

TABLE 14: Experimental Results, Continuous Beams

Deflections under sustained load, mm

Location*	Time in days measured from loading							
	0	2	6	13	27	59	136	217
1	0.09	0.10	0.10	0.10	0.11	0.13	0.02	0.12
2	5.89	6.40	6.71	6.99	7.35	8.01	8.89	9.30
3	10.92	11.89	12.46	12.95	13.58	14.77	16.31	17.01
4	13.96	15.18	15.86	16.51	17.30	18.62	20.55	21.44
5	14.34	15.57	16.29	16.93	17.74	19.20	21.19	22.06
6	12.23	13.30	13.92	14.49	15.19	16.41	18.24	18.98
7	8.18	8.89	9.31	9.69	10.16	11.03	12.17	12.73
8	3.66	3.98	4.18	4.33	4.52	4.89	5.39	5.63
9	0.06	0.07	0.07	0.07	0.07	0.08	0.08	0.07
10	- 0.59	- 0.64	- 0.66	- 0.69	- 0.73	- 0.78	- 0.89	- 0.94
11	- 0.79	- 0.84	- 0.89	- 0.94	- 0.98	- 1.08	- 1.21	- 1.25
12	- 0.71	- 0.76	- 0.80	- 0.84	- 0.86	- 0.96	- 1.06	- 1.10
13	- 0.56	- 0.62	- 0.62	- 0.65	- 0.68	- 0.74	- 0.78	- 0.80
14	- 0.43	- 0.46	- 0.48	- 0.50	- 0.50	- 0.52	- 0.56	- 0.56
15	- 0.30	- 0.31	- 0.32	- 0.32	- 0.32	- 0.33	- 0.33	- 0.33
16	- 0.13	- 0.14	- 0.14	- 0.14	- 0.14	- 0.14	- 0.13	- 0.11
17	- 0.10	- 0.10	- 0.11	- 0.11	- 0.10	- 0.12	- 0.11	- 0.13

Location*	Time continued								
	258	300	345	391	424	461	547		547
1	0.16	0.17	0.17	0.16	0.22	0.16	0.18		0.16
2	9.46	9.62	9.88	9.95	10.06	10.14	10.30		3.04
3	17.29	17.55	18.07	18.18	18.41	18.56	18.80		5.17
4	21.79	22.13	22.76	22.90	23.14	23.33	23.67		6.16
5	22.43	22.79	23.41	23.58	23.83	24.00	24.34		6.63
6	19.29	19.60	20.17	20.32	20.56	20.74	21.02		6.03
7	12.91	13.08	13.56	13.67	13.83	13.96	14.17	load	4.28
8	5.73	5.82	6.00	6.05	6.11	6.15	6.30	removed	1.85
9	0.18	0.16	0.13	0.08	0.12	0.58	0.59		- 0.03
10	- 0.97	- 0.97	- 0.99	- 0.99	- 1.02	- 1.02	- 1.03		- 0.20
11	- 1.27	- 1.28	- 1.31	- 1.32	- 1.33	- 1.35	- 1.37		- 0.30
12	- 1.12	- 1.13	- 1.16	- 1.16	- 1.16	- 1.16	- 1.17		- 0.19
13	- 0.80	- 0.80	- 0.82	- 0.80	- 0.80	- 0.80	- 0.80		- 0.02
14	- 0.56	- 0.58	- 0.56	- 0.55	- 0.54	- 0.54	- 0.48		0.05
15	- 0.33	- 0.32	- 0.33	- 0.33	- 0.32	- 0.32	- 0.32		0.05
16	- 0.14	- 0.14	- 0.12	- 0.10	- 0.12	- 0.12	- 0.10		0.05
17	- 0.19	- 0.19	- 0.18	- 0.18	- 0.18	- 0.18	- 0.18		- 0.14

* see diagram 15

Downward deflections are positive.

TABLE 14:, continued

Curvatures under sustained load, x 10^{-6} mm^{-1}

Location*	Time in days measured from loading								
	0	2	6	13	27	54	136	215	258
2	0.911	1.057	1.136	1.250	1.325	1.539	1.771	1.864	1.921
3	2.619	2.854	2.911	2.974	3.116	3.409	3.907	4.104	4.125
4	4.120	4.340	4.533	4.683	4.682	5.514	5.671	5.836	5.940
5	3.400	3.593	3.729	3.900	4.120	4.423	4.821	4.968	5.025
6	3.260	3.420	3.760	3.780	4.001	4.207	4.816	4.914	5.035
7	0.461	0.568	0.614	0.657	0.750	0.940	1.007	1.126	1.149
8	-1.011	-1.079	-1.125	-1.246	-1.407	-1.543	-1.821	-1.921	-1.979
10	-4.420	-4.750	-4.811	-4.980	-4.809	-5.146	-5.066	-5.836	-5.964
11	-2.648	-2.791	-2.974	-3.007	-3.507	-3.282	-3.654	-3.864	-3.932
12	-1.359	-1.524	-1.593	-1.664	-1.782	-1.957	-2.250	-2.368	-2.404
13	-0.537	-0.507	-0.525	-0.589	-0.639	-0.743	-0.884	-0.931	-0.974
14	0.083	0.952	0.076	0.088	0.113	0.163	0.232	0.256	0.283
15	0.054	0.046	0.070	0.064	0.102	0.140	0.197	0.234	0.254
16	0.010	0.070	0.067	0.049	0.097	0.149	0.228	0.250	0.275

Location*	Time continued							
	300	347	391	424	461	547		547
2	2.004	2.104	2.086	2.086	2.125	2.164		1.149
3	4.196	4.339	4.346	4.364	4.432	4.539		0.788
4	6.036	6.232	6.168	6.286	6.339	6.419		1.561
5	5.021	5.211	5.236	5.243	5.325	5.393	load	0.359
6	5.114	5.257	5.311	5.386	5.293	5.461	removed	2.265
7	1.164	1.256	1.289	1.272	1.305	1.397		0.956
8	-1.982	-2.108	-2.104	-2.179	-2.143	-2.264		-0.518
10	-6.162	-6.340	-6.426	-6.573	-6.543	-6.646		-2.548
11	-3.982	-4.086	-4.150	-4.197	-4.175	-4.254		-1.572
12	-2.411	-2.479	-2.507	-2.523	-2.571	-2.611		-0.662
13	-0.977	-1.054	-1.071	-1.065	-1.104	-1.131		-0.567
14	0.272	0.280	0.338	0.313	0.320	0.310		0.341
15	0.286	0.318	0.332	0.328	0.341	0.327		0.347
16	0.292	0.331	0.319	0.338	0.373	0.385		0.449

* see diagram 15

Positive curvatures indicate tension at the underside.

TABLE 14: continued

Depth of neutral axis of strain** under sustained load

Location*	Time in days measured from loading								
	0	2	6	13	27	59	136	217	258
2	165	166	187	184	193	203	245	251	259
3	137	144	154	157	164	174	192	196	200
4	129	132	139	141	152	150	175	180	185
5	132	138	146	148	153	160	178	183	188
6	120	126	131	137	141	151	166	172	177
7	172	186	217	223	232	243	325	330	346
8	172	179	199	196	199	218	248	254	264
10	111	114	123	124	137	144	163	162	166
11	135	142	153	156	167	180	200	203	209
12	150	158	174	177	188	207	236	241	250
13	163	186	234	224	246	288	356	368	382
14	-	-	-	-	-	-	-	-	-
15	-	-	-	-	-	-	-	-	-
16	-	-	-	-	-	-	-	-	-

Location*	Time continued							
	300	347	381	424	461	547		547
2	257	254	246	255	260	255		305
3	203	203	198	204	205	203		284
4	185	186	186	189	189	198		203
5	192	191	189	194	195	194	load removed	-
6	176	179	175	178	184	181		203
7	347	336	311	334	334	323		-
8	263	259	253	257	262	255		361
10	165	165	163	165	168	167		169
11	209	211	206	211	213	214		262
12	253	251	247	254	253	254		330
13	387	366	346	366	362	361		-
14	-	-	-	-	-	-		-
15	-	-	-	-	-	-		-
16	-	-	-	-	-	-		-

* see diagram 15

** measured from the compression face

PART 3: THEORETICAL STUDIES

A. Creep in Plain Concrete

Creep in the broadest sense, namely the time-dependent deformation of a material under constant externally applied stress, is a phenomenon exhibited by a great many materials (40).

For example, bitumen, asphalt, perspex, glass, many resins and plastics, all of which have a predominantly disordered or amorphous structure, are well known to exhibit creep under quite low stresses at room temperatures. Indeed, the results of tests on plastic, perspex and resin models have been used in an effort to understand the behaviour of concrete and reinforced concrete structures under sustained load. The creep of many amorphous materials is generally accepted as being predominantly visco-elastic in nature, that is it is due to viscous flow, accompanied by the gradual transfer of load to an elastic internal structure. The term "viscous flow" implies movement of particles one over the other in an essentially laminar manner without significant cracking or fragmentation of particles. Amorphous materials generally exhibit creep at all stresses; there appears to be no stress below which creep does not occur and the rate of creep at any time after loading generally increases with the magnitude of the sustained stress. The visco-elastic nature of the deformation may be destroyed at high stresses. Creep of amorphous materials has been extensively investigated using rheological techniques (39). The time-dependent deformation of the material is compared to that of models composed of spring elements (stress proportional to strain) and dashpot elements (stress proportional to rate of strain) connected in series and/or parallel. The models provide differential equations which may be integrated and compared with the behaviour of the material. Rheology provides what is essentially a "mathematician's eye view" of creep.

Metals, which have a predominantly ordered or crystalline structure, exhibit creep generally resulting from a combined effect of the mainly viscous deformation within the inter crystalline boundaries and the complex deformation by slip and fragmentation of the ordered crystalline domains. The nature of the interaction between the crystalline and intercrystalline phases depends on the relative stiffnesses of the two zones. As long as the deformation is concentrated within the crystal boundaries the metal responds essentially like a visco-elastic material. Such conditions are present in metals subject to moderate stresses at all temperatures; at high temperatures, however, deformation of the crystalline domains usually predominates. Creep of metals is particularly important at high temperatures and considerable research has been performed in this area; the deformation is recognised as a thermally activated process and has been investigated using the techniques of statistical physics (41).

Concrete has a predominantly disordered or amorphous structure and consists of pieces of aggregate, which are crystalline, in a highly viscous cement paste. It has been mentioned earlier how concrete can be seen to be divided into fluid and solid phases at several levels. For example, at a high level concrete consists of rigid pieces of coarse aggregate in a more fluid mortar, at a lower level the mortar itself can be divided into the rigid pieces of fine aggregate and the more fluid cement paste. At all levels, the rigid pieces of aggregate tend to form a solid structure in a more fluid cementing material. It must be emphasised that the terms "solid" and "fluid" are here used only in a relative sense; "solid" implies "more stiff" and "fluid" implies "less stiff".

There is one important feature which distinguishes creep in concrete from creep in most other amorphous materials and that is the large part played by various forms of water. ~~A large part of creep in concrete is due to the~~

~~passage of water from the concrete into the environment, hence the marked influence of ambient relative humidity on creep in concrete.~~ A further part of creep in concrete is due to the internal rearrangement of water. Viscous flow of mortar and crystalline flow of aggregate also contribute. The study of creep in concrete is further complicated by free shrinkage, strength development due to ageing and the low tensile strength of the material. In addition, the term "concrete" embraces materials made from a wide range of cement types, aggregate types and mix proportions. This has led to a tendency to study creep of concrete in isolation from other amorphous materials. There has been a corresponding tendency to study creep of amorphous materials separately from creep of crystalline materials. Consequently a certain complexity in the approach to the theory of creep has been introduced which has meant that the isolation of the few essential factors governing the phenomenon has been frequently neglected in favour of procedures of devising empirical relations based on rather unco-ordinated experiments.

Despite the basic differences in the mechanisms of creep in crystalline materials, most amorphous materials and concrete there is one fundamental aspect which is common to all forms of creep. This is that all forms of time-dependent deformation must be vibrationaly activated. Thermal energy exists in a material as vibrational waves travelling in all directions. Other types of energy such as chemical energy may also be significant. The energy density at any point at any moment is a random summation of these various forms of energy. These random fluctuations activate the deformation process whether it be slip in the ordered structure of a crystal, viscous flow in an amorphous material, or water movement in concrete. This is clearly recognised in the study of creep of metals at high temperatures where activation by thermal vibrations predominates. The influence of temperature

on the creep of visco-elastic materials such as bitumen, glass and many plastics is well known.

Vibrations, however, can lead to "spontaneous" changes in the structural pattern only when the existing pattern is not perfectly stable; such changes would therefore not be possible either with the ideal crystal lattice or with materials with a statistically isotropic arrangement of particles. The possibility of time-dependent deformation therefore depends on the existence of a certain amount of disorder within the essentially ordered structure or a certain amount of order within the essentially disordered pattern. Concrete, for example, has an essentially disordered structure and the application of external stress affects the stability of the structural pattern, a tendency of "spontaneous" change towards a more stable arrangement of lower energy establishes itself.

The problem of evaluating the frequency (or the probability) of any particle in the group attaining a state of energy in which it is free to migrate from its current equilibrium position is a problem of classical statistical physics. The amount of energy required to enable a particle to overcome the energy barrier preventing its movement is called its activation energy. The probability p of finding an individual particle with an amount of energy ϵ is given by the Maxwell-Boltzmann equation as $p = Ce^{\frac{-\epsilon}{RT}}$ where C and R are constants for a given material and T is the absolute temperature.

In the absence of external forces the activation energy will be the same in all directions; let its value be Q. However, if an external force is applied in one direction the activation energy in the direction of the force is reduced by an amount (ϵ_s) called the potential energy of the force and increased by the same amount with respect to the possible movement in the opposite direction. Hence the rate of deformation in the direction

of the applied force is given by

$$\frac{du}{dt} = Ce^{\frac{-(Q-\epsilon_s)}{RT}} - Ce^{\frac{-(Q+\epsilon_s)}{RT}}$$

$$\therefore \quad \frac{du}{dt} = Ce^{-\frac{Q}{RT}}\left(e^{\frac{\epsilon_s}{RT}} - e^{-\frac{\epsilon_s}{RT}}\right)$$

$$\therefore \quad \frac{du}{dt} = C \sinh\left(\frac{\epsilon_s}{RT}\right) e^{-\frac{Q}{RT}}$$

Consequently, the time t for a barrier of magnitude Q to be overcome is given by the inverse of the rate as,

$$t = C^{-1} \operatorname{cosech}\left(\frac{\epsilon_s}{RT}\right) e^{\frac{Q}{RT}} \qquad (a)$$

This equation implies a constant rate of strain for a given material under constant load at constant temperature provided the mean activation energy Q can be considered constant throughout the process. However it will now be explained that for creep in concrete the value of Q is a function of time.

If we imagine a large number of particles within a random material such as concrete, they will be faced with a random distribution of energy barriers; this total number of particles will be referred to as the total population. In a relatively short time those particles faced with a low energy barrier will overcome that barrier and deformation will result. These particles will then be faced with a random distribution of barriers similar to the distribution originally faced by the total population. In the next small increase in time, then, a second group of particles from the parent population will overcome their energy barriers along with a part of the group which moved during the preceding time increment. If we make the assumption that the number of particles which move during creep is small relative to the total number of particles then the deformation due to the second movement of particles is small relative to the deformation due to first movement of the parent population. Precisely what this entails may also be explained

more rigidly as follows. If the total number of particles is represented by N and the number which move successfully during t_1 is denoted by N_1, then the number which move successfully for the second occasion during t_2 (where $t_2 = t_1$) is $\left(\frac{N_1}{N}\right).N_1$. The number of particles which move successfully for the first occasion during t_2 is denoted by N_2. N_2 may be less than, equal to, or greater than N_1, depending on the form of the frequency distribution of energy barriers but it will be of the same order as N_1. Now $\left(\frac{N_1}{N}\right).N_1$, is small relative to N_1 provided N_1 is small relative to N. The number of particles which move during creep of concrete in the service stress range is small relative to the total number of particles and consequently deformation due to second movement may be neglected. It should be remembered, however, that this assumption may not be valid at higher stresses (say when the stress/strength ratio exceeds 0.5). Now, since the particles faced by small energy barriers quickly perform successful vibrations and then (by the above argument) play little further part in the proceedings the effective mean magnitude of the energy barriers faced by the particles increases with time and consequently the rate of creep decreases with time. Thus the form of the frequency distributionof energy barriers becomes of great importance. The concept that during creep energy barriers of greater and greater magnitude are overcome is entirely consistent with the concept of load being gradually transferred to a stiffer phase. This approach to the problem is therefore fully compatible with the ideas of classical visco-elasticity but is based on a model which is a more realistic representation of the behaviour of materials. In short, it provides rather more of an "engineer's eye view" of creep.

In a disordered material such as concrete it seems reasonable to assume that the distribution of energy barriers is normal and governed by,

$$f = \frac{1}{\sigma\sqrt{2\pi}} e^{-\frac{(Q-Q_m)}{2\sigma^2}}$$

where f is the frequency of barriers of magnitude Q, σ is the standard deviation of the distribution and Q_m is the mean magnitude of the energy barriers.

$$\therefore f = \frac{1}{\sigma\sqrt{2\pi}} e^{-\frac{1}{2\sigma^2}[Q^2 - 2QQ_m + Q_m^2]}$$

Now, since the number of particles involved in creep in concrete under service stresses is small relative to the total number of particles, it follows that the magnitude of the energy barriers overcome during creep is small relative to the mean value,

$$\therefore f \simeq \frac{1}{\sigma\sqrt{2\pi}} e^{-\frac{1}{2\sigma^2}[Q_m^2 - 2QQ_m]} = \frac{1}{\sigma\sqrt{2\pi}} e^{-\frac{Q_m^2}{2\sigma^2}} \cdot e^{\frac{Q_m}{\sigma^2}\cdot Q}$$

and the cumulative frequency

$$F = \frac{\sigma}{Q_m\sqrt{2\pi}} e^{-\frac{Q_m^2}{2\sigma^2}} \cdot e^{\frac{Q_m}{\sigma^2}\cdot Q} + \text{const} \quad \text{(b)}$$

If the amount of deformation produced when an energy barrier is overcome is independent of the magnitude of the energy barrier, and there is no reason to think otherwise, then the rate at which energy barriers are overcome is directly proportional to the rate of creep.

Now, denoting creep strain by ϵ_c

$$\frac{d\epsilon_c}{dt} = K\frac{dF}{dt} = K\frac{dF}{dQ}\cdot\frac{dQ}{dt} = K\cdot\frac{dF}{dQ}\Big/\frac{dt}{dQ}$$

From equations (a) and (b)

$$\frac{dF}{dQ} = \frac{1}{\sigma\sqrt{2\pi}} e^{-\frac{Q_m^2}{2\sigma^2}} \cdot e^{\frac{Q_m\cdot Q}{\sigma^2}} = \frac{1}{\sigma\sqrt{2\pi}} e^{-\frac{Q_m^2}{2\sigma^2}\left[C\sinh\left(\frac{\epsilon_s}{kT}\right).t\right]^{\frac{kTQ_m}{\sigma^2}}}$$

and from equation (a)

$$\frac{dt}{dQ} = \frac{C^{-1}}{kT}\,\text{cosech}\left(\frac{\epsilon_s}{kT}\right)e^{\frac{Q}{kT}} = \frac{t}{kT}$$

Substituting and rearranging,

$$\frac{d\epsilon_c}{dt} = \frac{KkTC}{\sigma\sqrt{2\pi}}\cdot\sinh\left(\frac{\epsilon_s}{kT}\right).e^{-\frac{Q_m^2}{2\sigma^2}\left[C\sinh\left(\frac{\epsilon_s}{kT}\right).t\right]^{kT\left(\frac{Q_m}{\sigma^2}-\frac{1}{kT}\right)}}$$

integrating,

$$\epsilon_c = \frac{K\sigma}{Q_m\sqrt{2\pi}} \cdot e^{-\frac{Q_m^2}{2\sigma^2}} \left[C \sinh\left(\frac{\epsilon_s}{RT}\right)\right]^{\frac{RT Q_m}{\sigma^2}} \cdot t^{\frac{RT Q_m}{\sigma^2}}$$

Now, for a particular concrete under constant stress at uniform temperature, this can be written as, $\epsilon_c = A\, t^{n}$

or, $\log \epsilon_c = \log A + n \log t$ (c)

It is not suggested that for a material such as concrete it is possible to deduce the constants defining this relationship by theoretical considerations based on the above arguments. However, the linear relationship between log deformation and log time will hold for a vibrationally activated process in concrete under service loads.

It is generally recognised that creep in concrete involves deformation at various levels; for example, movement of free, adsorbed and zeolithic water, ~~slip of sand grains over each other and slip of pieces of coarse aggregate over each other.~~ However equation (c) will hold for the total deformation provided the component deformations have the same origin in time and for as long as they all continue. The particles at each level, whether they are sand grains or molecules of water will be faced with a normal distribution of energy barriers. When a number of independent quantities, each of which is normally distributed about its mean, are combined, the total population will be normally distributed (with a variance equal to the sum of the component variances). The distribution of energy barriers referred to during deduction of the deformation-time relationship is the parent distribution, formed by combination of the lower level normal distributions. However, if for any reason, one level of deformation ceases, or a new level commences, then a discontinuity in the relationship will occur. In other words, if after a period of creep, deformation at one

level blocks or unblocks deformation at another level, then a discontinuity may be expected. This type of situation frequently occurs in creep of metals at high temperatures (40). In concrete, a high level mechanism which would result in a discontinuity would be, for example, if creep of mortar gradually brought pieces of coarse aggregate into contact. When a rigid structure of aggregate was obtained (and this would occur fairly suddenly as the last pieces slotted into place) creep in the mortar would cease and creep by slip in the coarse aggregate structure would continue. There is also a possibility of discontinuities associated with the drying process, for example when all free water is removed. This would suggest that the likelihood of discontinuities is much greater when small pieces of concrete are tested.

Some general conclusions regarding the influence of stress on creep can also be drawn from equation (c). The potential energy (ϵ_s) of the force is proportional to the magnitude of the applied force and consequently the value of A will be stress dependent. Also, the form of the distribution of energy barriers (defined by σ) and their mean value (defined by Q_m) effective during creep are likely to be functions of the applied stress level; consequently the value of Π is likely to be stress dependent.

B. Analysis of Reinforced Concrete Continuous Beams under Sustained Service Loads

A computer program was developed to calculate the force and deformation fields in a continuous beam immediately after loading and after periods of sustained load. It was required that the program should be able to take account of the variations in flexural rigidity along the length of a member which may exist due to variations in geometry or reinforcement or due to the influence of cracking during loading. The program is based on a finite difference treatment of the basic equations of bending which is outlined below. A flow chart explaining briefly the main steps in the program is shown in diagram 19. Using the node pattern shown in diagram 20

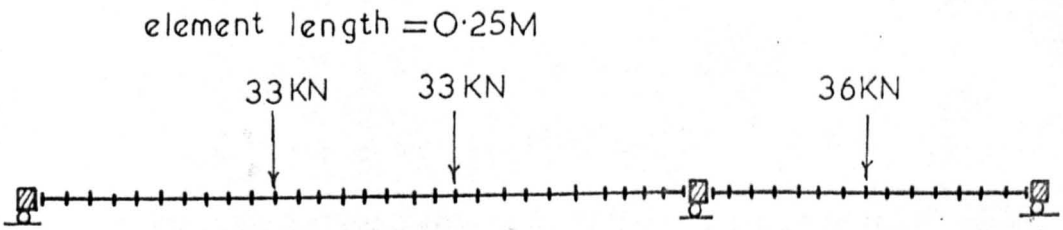

DIAGRAM 20: Node Pattern for Continuous Beam

and the experimental data given in table 8 the continuous beam tested in the laboratory was analysed. The computer prints out solutions for immediately after loading and for all the times under sustained load defined in table 8. Two typical print-outs are shown in diagram 21.

The co-ordinate system is defined in diagram 22. The internal force system

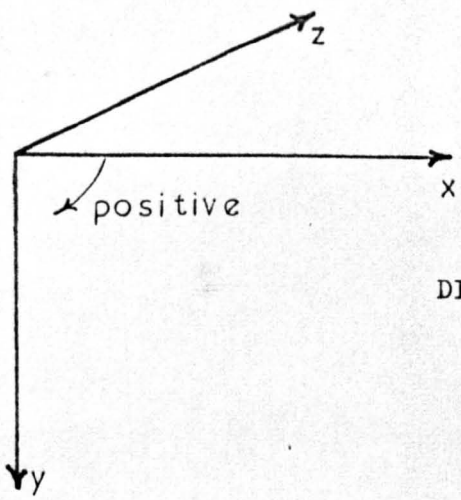

DIAGRAM 22: Co-ordinate System for Horizontal Members

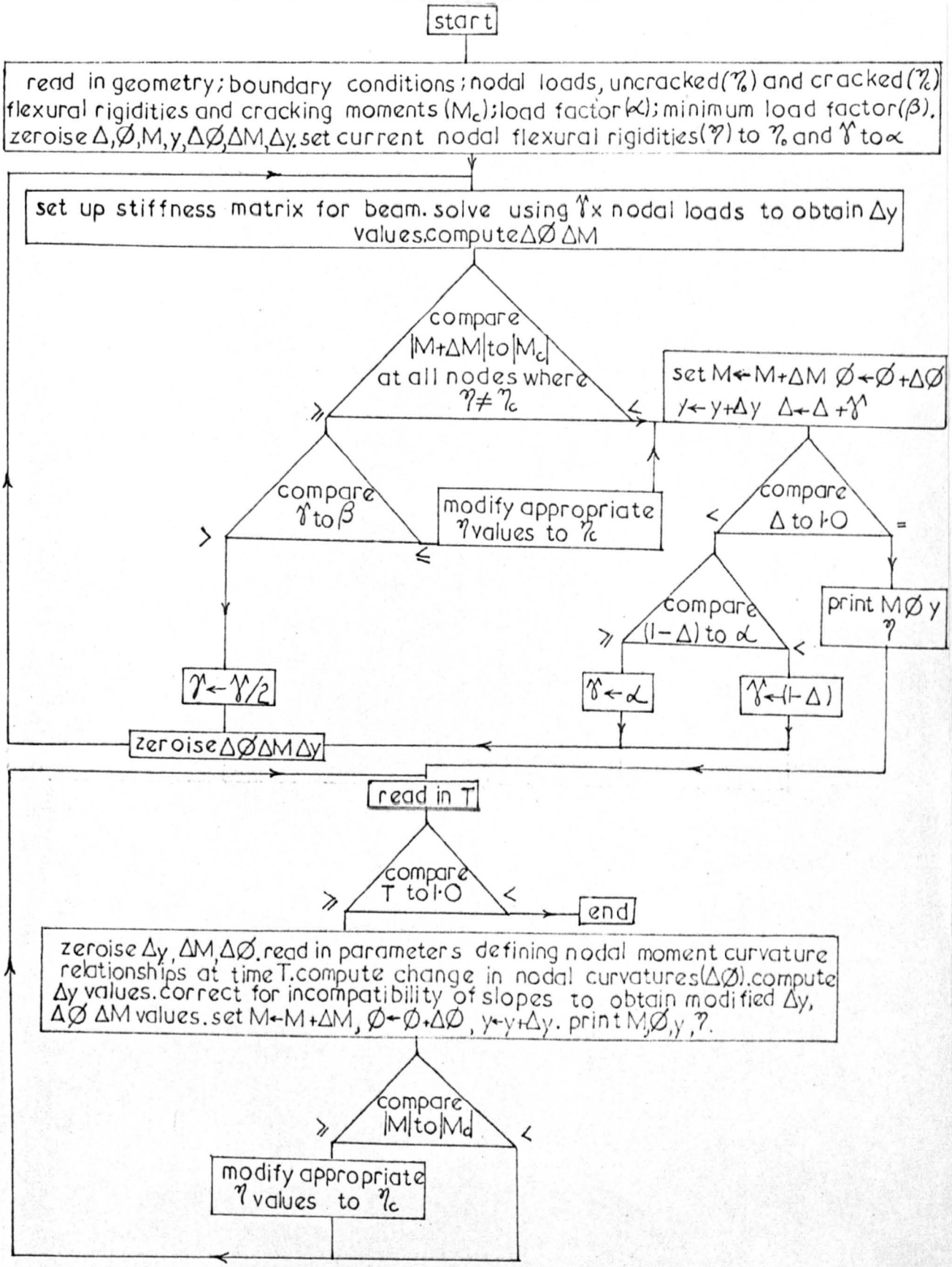

DIAGRAM 19: Simplified Flow Chart for the Computer Program for the Analysis of Continuous Beams

DIAGRAM 21: Typical Computer Print Outs from Continuous Beam Analysis

BEAM ANALYSIS

IMMEDIATELY AFTER LOADING

DEFLNS		BENDING MOMENTS	SHEAR FORCE	FLEXURAL RIGIDITY	CURVATURE
METRES		NEWTON-METRES	NEWTONS	NEWTON (METRE)↑2	PER METRE
0.00000		0.0	-24183.5	31800000.0	0.0000000000
0.00154		6045.9	-24183.5	31800000.0	-0.0001901221
0.00307		12091.8	-24042.1	31800000.0	-0.0003802443
0.00458		18066.9	-23984.2	13800000.0	-0.0005852854
0.00605		24083.9	-24218.3	13800000.0	-0.0010212947
0.00745		30176.1	-24237.7	13800000.0	-0.0014627582
0.00877		36202.7	-24102.6	13800000.0	-0.0018994738
0.00996		42227.4	-23822.5	13800000.0	-0.0023360424
0.01101		48114.0	-24360.7	13800000.0	-0.0027626074
0.01189		54407.7	-24201.5	13800000.0	-0.0032186758
0.01257		60214.7	-7089.9	13800000.0	-0.0036394744
0.01302		57952.7	8978.2	13800000.0	-0.0034755579
0.01325		55725.7	8825.5	13800000.0	-0.0033141784
0.01327		53539.9	8665.3	13800000.0	-0.0031557924
0.01310		51393.0	8537.1	13800000.0	-0.0030002166
0.01274	long span	49271.4	8436.0	13800000.0	-0.0028464789
0.01220		47175.0	8794.9	13800000.0	-0.0026945644
0.01149		44873.9	9196.6	13800000.0	-0.0025278216
0.01063		42576.7	25150.0	13800000.0	-0.0023613545
0.00961		32298.9	41407.7	13800000.0	-0.0016165905
0.00850		21872.8	41670.8	13800000.0	-0.0008610739
0.00733		11463.6	41726.8	31800000.0	-0.0003604891
0.00614		1009.4	41816.5	31800000.0	-0.0000317432
0.00495		-9444.7	41636.2	31800000.0	0.0002970026
0.00378		-19808.7	41515.4	13800000.0	0.0007114984
0.00265		-30202.4	41614.7	13800000.0	0.0014646660
0.00161		-40616.0	41503.7	13800000.0	0.0022192784
0.00071		-50954.2	41690.3	13800000.0	0.0029684227
0.00000		-61461.2	42027.9	13800000.0	0.0037297975
0.00000		-61461.2	-35600.0	13800000.0	0.0037297975
-0.00048		-52561.2	-35223.8	13800000.0	0.0030848709
-0.00077		-43849.3	-35489.1	13800000.0	0.0024535740
-0.00090		-34816.7	-35577.3	13800000.0	0.0017990339
-0.00092		-26060.7	-35285.1	13800000.0	0.0011645408
-0.00087	short span	-17174.1	-35589.6	31800000.0	0.0005400662
-0.00079		-8265.9	-35632.9	31800000.0	0.0002599331
-0.00068		642.4	-17632.9	31800000.0	-0.0000202001
-0.00058		550.6	367.1	31800000.0	-0.0000173143
-0.00049		458.8	367.1	31800000.0	-0.0000144286
-0.00039		367.1	367.1	31800000.0	-0.0000115429
-0.00029		275.3	367.1	31800000.0	-0.0000086572
-0.00019		183.5	367.1	31800000.0	-0.0000057714
-0.00010		91.8	367.1	31800000.0	-0.0000028857
0.00000		0.0	367.1	31800000.0	0.0000000000

SUPPORT REACTIONS

NEWTONS

24183.5
77627.8
367.1

DIAGRAM 21: Continued

BEAM ANALYSIS

547 DAYS AFTER LOADING

DEFLNS		BENDING MOMENTS	SHEAR FORCE	FLEXURAL RIGIDITY	CURVATURE
METRES		NEWTON-METRES	NEWTONS	NEWTON (METRE)↑2	PER METRE
0.00000		0.0	-24202.2	31800000.0	-0.0003646441
0.00285		6050.6	-24202.2	31800000.0	-0.0007176511
0.00566		12101.1	-24060.8	31800000.0	-0.0010706581
0.00840		18081.0	-24002.9	13800000.0	-0.0019015353
0.01103		24102.6	-24237.0	13800000.0	-0.0024863140
0.01349		30199.4	-24256.4	13800000.0	-0.0030784002
0.01577		36230.8	-24121.4	13800000.0	-0.0036641251
0.01782		42260.1	-23841.2	13800000.0	-0.0042496532
0.01960		48151.4	-24379.4	13800000.0	-0.0048217784
0.02108		54449.8	-24220.2	13800000.0	-0.0054334323
0.02221		60261.5	-7108.7	13800000.0	-0.0059978315
0.02298		58004.1	8959.5	13800000.0	-0.0057788261
0.02338		55781.8	8806.8	13800000.0	-0.0055632197
0.02344		53600.7	8646.6	13800000.0	-0.0053516241
0.02316		51458.5	8518.3	13800000.0	-0.0051437937
0.02256	long span	49341.6	8417.3	13800000.0	-0.0049384259
0.02165		47249.8	8776.2	13800000.0	-0.0047355007
0.02045		44953.4	9177.9	13800000.0	-0.0045127086
0.01896		42660.9	25131.3	13800000.0	-0.0042902859
0.01720		32387.8	41389.0	13800000.0	-0.0032930576
0.01524		21966.4	41652.1	13800000.0	-0.0022814229
0.01314		11561.8	41708.1	31800000.0	-0.0010391668
0.01097		1112.3	41797.8	31800000.0	-0.0004295132
0.00878		-9337.1	41617.5	31800000.0	0.0009094286
0.00664		-19696.4	41496.7	13800000.0	0.0020541431
0.00463		-30085.5	41596.0	13800000.0	0.0030626306
0.00281		-40494.4	41485.0	13800000.0	0.0040730538
0.00125		-50828.0	41671.6	13800000.0	0.0050761510
0.00000		-61330.2	42009.2	13800000.0	0.0060956345
0.00000		-61330.2	-35562.5	13800000.0	0.0060956345
-0.00087		-52439.6	-35186.4	13800000.0	0.0052327797
-0.00140		-43737.1	-35451.7	13800000.0	0.0043881861
-0.00167		-34713.8	-35539.9	13800000.0	0.0035124512
-0.00171		-25967.1	-35247.7	13800000.0	0.0026635754
-0.00159		-17089.9	-35552.2	31800000.0	0.0013617448
-0.00139		-8191.0	-35595.5	31800000.0	0.0008425544
-0.00113		707.8	-17595.5	31800000.0	-0.0004059242
-0.00089		606.7	404.5	31800000.0	-0.0004000270
-0.00068		505.6	404.5	31800000.0	-0.0003941299
-0.00050	short span	404.5	404.5	31800000.0	-0.0003882327
-0.00034		303.4	404.5	31800000.0	-0.0003823356
-0.00020		202.2	404.5	31800000.0	-0.0003764384
-0.00009		101.1	404.5	31800000.0	-0.0003705413
0.00000		0.0	404.5	31800000.0	-0.0003646441

SUPPORT REACTIONS

NEWTONS

24202.2
77571.7
404.5

set up at a cross-section reduces to a vertical shear force Q and a bending moment M. Q is defined by the action of the left portion of the beam on the right portion; that is, it is that shear force which must be exerted on the right hand portion of a member to maintain equilibrium should the left hand portion be removed. Q is taken as positive when it is in the direction of the y co-ordinate. In the regions where M is positive the beam deflects so that its concavity is upwards; that is, the curve of deflection is convex with respect to the axes of co-ordinates. Thus the two well known equations of bending are, according to the elastic theory:-

$$\frac{d^2M}{dx^2} = -q \qquad (1)$$

$$\eta \frac{d^2y}{dx^2} = -M \qquad (2)$$

where q is the load per unit length of beam at the section considered and η is the flexural rigidity at the section considered.

Immediate Response to Load Application

Equation (2) implies a linear relationship between moment and curvature. For reinforced concrete beams the moment curvature relationship is linear but contains a discontinuity. This difficulty can be overcome if the load is applied incrementally by the computer and when the cracking moment is reached at any section the flexural rigidity (ie the gradient of the moment curvature diagram) there is modified for future increments. The two values of flexural rigidity relevant to each node are termed the "before cracking" and "after cracking" values.

Equations (1) and (2) can be combined to give the bi-harmonic form,

$$\frac{d^2}{dx^2}\left(\eta \frac{d^2y}{dx^2}\right) = q \qquad (3)$$

For the nodal system defined in diagram 23 this can be expressed in finite

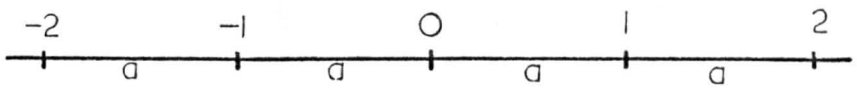

DIAGRAM 23: General Node Pattern

difference terms as follows:-

$$q_0 = \frac{1}{a^2}\left[\left(\eta\frac{d^2y}{dx^2}\right)_{-1} - 2\left(\eta\frac{d^2y}{dx^2}\right)_0 + \eta\left(\frac{d^2y}{dx^2}\right)_1\right]$$

$$\therefore \quad q_0 = \frac{1}{a^2}\left[\frac{1}{a^2}\eta_{-1}(y_{-2}-2y_{-1}+y_0) - \frac{2}{a^2}\eta_0(y_{-1}-2y_0+y_1) + \frac{1}{a^2}\eta_1(y_0-2y_1+y_2)\right]$$

Rearranging in matrix form,

$$[q_0] = \frac{1}{a^4}\left[\eta_{-1}, -2(\eta_{-1}+\eta_0), \eta_{-1}+4\eta_0+\eta_1, -2(\eta_0+\eta_1), \eta_1\right]\begin{bmatrix} y_{-2} \\ y_{-1} \\ y_0 \\ y_1 \\ y_2 \end{bmatrix} \qquad (4)$$

Consider the beam to be covered by a nodal pattern as shown in diagram 20. Excluding the possibility of settlement of supports, if equation (4) could be written at every node at which the deflection is unknown then a matrix equation could be written for the whole structure and solved to give deflections at every node. The difficulty lies in writing the equation for the nodes adjacent to internal supports and for the nodes adjacent to and at Boundaries. These situations are now considered separately.

(i) Nodes adjacent to a simple support (diagram 24)

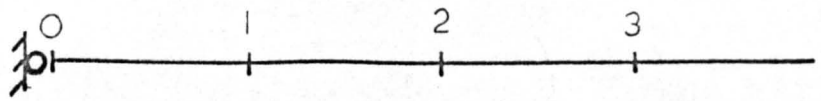

DIAGRAM 24: Node Pattern at Simple Supports

Now, $$q_1 = \frac{-1}{a^2}(M_0 - 2M_1 + M_2)$$

but $$M_0 = 0$$

$$\therefore q_1 = \frac{1}{a^2}\left(-2\eta_1\left(\frac{d^2y}{dx^2}\right)_1 + \eta_2\left(\frac{d^2y}{dx^2}\right)_2\right)$$

Substituting and rearranging in matrix form,

$$[q_1] = \frac{1}{a^4}\left[4\eta_1+\eta_2, -2(\eta_1+\eta_2), \eta_2\right]\begin{bmatrix} y_1 \\ y_2 \\ y_3 \end{bmatrix}$$

(ii) Nodes adjacent to fully fixed supports (diagram 25)

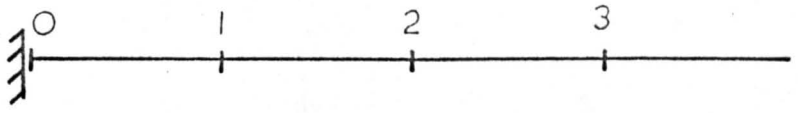

DIAGRAM 25: Node Pattern at Fully Fixed Supports

Approximately by Taylor's theorem,

$$y_1 = y_0 + a\left(\frac{dy}{dx}\right)_0 + \frac{a^2}{2}\left(\frac{d^2y}{dx^2}\right)_0$$

but

$$y_0 = \left(\frac{dy}{dx}\right)_0 = 0 \quad , \quad \therefore \left(\frac{d^2y}{dx^2}\right)_0 = \frac{2y_1}{a^2}$$

Now $$[q_1] = -\frac{1}{a^2}(M_0 - 2M_1 + M_2) = \frac{1}{a^2}\left(\eta_0\left(\frac{d^2y}{dx^2}\right)_0 - 2\eta_1\left(\frac{d^2y}{dx^2}\right)_1 + \eta_2\left(\frac{d^2y}{dx^2}\right)_2\right)$$

Substituting and rearranging in matrix form,

$$[q_1] = \frac{1}{a^4}\left[2\eta_0+4\eta_1+\eta_2, -2(\eta_1+\eta_2), \eta_2\right]\begin{bmatrix} y_1 \\ y_2 \\ y_3 \end{bmatrix}$$

(iii) Cantilever free end (diagram 26)

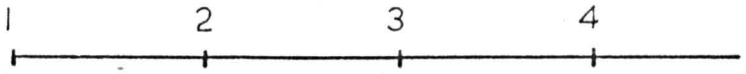

DIAGRAM 26: Node Pattern at Tip of Cantilever

Approximately, by Taylor's theorem,

$$M_2 = M_1 + a\left(\frac{dM}{dx}\right)_1 + \frac{a^2}{2}\left(\frac{d^2M}{dx^2}\right)_1$$

but $$M_1 = Q_1 = 0 \qquad \therefore \left(\frac{dM}{dx}\right)_1 = 0$$

$$\therefore \left(\frac{d^2M}{dx^2}\right)_1 = \frac{2M_2}{a^2} \qquad \therefore q_1 = \frac{2\eta_2}{a^2}\left(\frac{d^2y}{dx^2}\right)_2$$

Substituting and rearranging in matrix form,

$$[q_1] = \frac{2}{a^4}\left[\eta_2, -2\eta_2, \eta_2\right]\begin{bmatrix} y_1 \\ y_2 \\ y_3 \end{bmatrix}$$

also,

$$q_2 = -\frac{1}{a^2}\left[M_1 - 2M_2 + M_3\right]$$

$$\therefore q_2 = \frac{1}{a^2}\left[-2\eta_2\left(\frac{d^2y}{dx^2}\right)_2 + \eta_3\left(\frac{d^2y}{dx^2}\right)_3\right]$$

Substituting and rearranging in matrix form,

$$[q_2] = \frac{1}{a^4}\left[-2\eta_2, 4\eta_2 + \eta_3, -2\eta_2 + \eta_3, \eta_3\right]\begin{bmatrix} y_1 \\ y_2 \\ y_3 \\ y_4 \end{bmatrix}$$

(iv) Line of symmetry (diagram 27) Beams which are symmetric about a

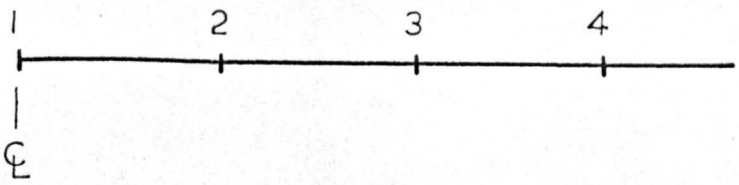

DIAGRAM 27: Node Pattern at Line of Symmetry

support can be treated as fully fixed at that support. When the line of symmetry is at a midspan the following treatment may be used.

Approximately, by Taylor's theorem,

$$M_2 = M_1 + a\left(\frac{dM}{dx}\right)_1 + \frac{a^2}{2}\left(\frac{d^2M}{dx^2}\right)_1$$

but $Q = \left(\frac{dM}{dx}\right)_1 = 0$ $\quad\therefore \frac{2}{a^2}(M_2 - M_1) = \left(\frac{d^2M}{dx^2}\right)_1 = -q_1$

Also, approximately,

$$y_2 = y_1 + a\left(\frac{dy}{dx}\right)_1 + \frac{a^2}{2}\left(\frac{d^2y}{dx^2}\right)_1$$

but

$$\left(\frac{dy}{dx}\right)_1 = 0 \qquad \therefore \frac{2}{a^2}(y_2 - y_1) = \left(\frac{d^2y}{dx^2}\right)_1$$

$$\therefore q_1 = \frac{2}{a^2}\left(\eta_2\left(\frac{d^2y}{dx^2}\right)_2 - \eta_1\left(\frac{d^2y}{dx^2}\right)_1\right)$$

Substituting and rearranging in matrix form,

$$[q_1] = \frac{2}{a^4}\left[2\eta_1 + \eta_2,\ -2(\eta_1 + \eta_2),\ \eta_2\right]\begin{bmatrix} y_1 \\ y_2 \\ y_3 \end{bmatrix}$$

Also,

$$q_2 = -\frac{1}{a^2}\left[M_1 - 2M_2 + M_3\right]$$

$$\therefore q_2 = \frac{1}{a^2}\left[\eta_1\left(\frac{d^2y}{dx^2}\right)_1 - 2\eta_2\left(\frac{d^2y}{dx^2}\right)_2 + \eta_3\left(\frac{d^2y}{dx^2}\right)_3\right]$$

Substituting and rearranging in matrix form,

$$[q_2] = \frac{1}{a^4}\left[-2(\eta_1 + \eta_2),\ 2\eta_1 + 4\eta_2 + \eta_3,\ -2(\eta_2 + \eta_3),\ \eta_3\right]\begin{bmatrix} y_1 \\ y_2 \\ y_3 \\ y_4 \end{bmatrix}$$

(v) Nodes adjacent to internal supports (diagram 28)

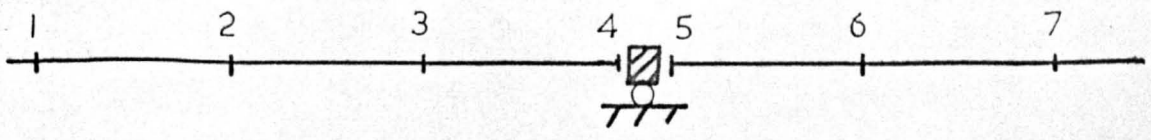

DIAGRAM 28: Node Pattern at Internal Support

By Taylor's theorem,

$$y_3 = y_4 - a\left(\frac{dy}{dx}\right)_4 + \frac{a^2}{2}\left(\frac{d^2y}{dx^2}\right)_4$$

and

$$y_6 = y_5 + a\left(\frac{dy}{dx}\right)_5 + \frac{a^2}{2}\left(\frac{d^2y}{dx^2}\right)_5$$

Compatibility of slopes at the support is satisfied if $\left(\frac{dy}{dx}\right)_4 = \left(\frac{dy}{dx}\right)_5$ and

thus by adding the above equations and applying compatibility of slopes:-

$$y_3 + y_6 = y_4 + y_5 + \frac{a^2}{2}\left[\left(\frac{d^2y}{dx^2}\right)_4 + \left(\frac{d^2y}{dx^2}\right)_5\right]$$

Equilibrium of moments is satisfied if $M_4 - M_5 = 0$

$$\therefore \eta_4\left(\frac{d^2y}{dx^2}\right)_4 = \eta_5\left(\frac{d^2y}{dx^2}\right)_5 \qquad \text{also} \qquad y_4 = y_5$$

by substitution,

$$\left(\frac{d^2y}{dx^2}\right)_4 = \frac{2}{a^2}\frac{\eta_5}{\eta_4+\eta_5}(y_3+y_6)$$

Now,

$$q_3 = -\frac{1}{a^2}\left[M_2 - 2M_3 + M_4\right] = \frac{1}{a^2}\left[\eta_2\left(\frac{d^2y}{dx^2}\right)_2 - 2\eta_3\left(\frac{d^2y}{dx^2}\right)_3 + \eta_4\left(\frac{d^2y}{dx^2}\right)_4\right]$$

Substituting and rearranging in matrix form

$$\left[q_3\right] = \frac{1}{a^4}\left[\eta_1,\ -2(\eta_2+\eta_3),\ \eta_2+4\eta_3+\frac{2\eta_4\eta_5}{\eta_4+\eta_5},\ \frac{2\eta_4\eta_5}{\eta_4+\eta_5}\right]\begin{bmatrix} y_1 \\ y_2 \\ y_3 \\ y_6 \end{bmatrix}$$

Using the above equations, a matrix equation can be set up for a continuous beam in terms of the nodal flexural rigidities, nodal load values and nodal deflections. A simple example is shown in diagram 29.

The force and deformation field in a continuous beam immediately after loading is obtained by computer in the following way. The geometry of the beam, nodal flexural rigidities (both before and after cracking values), nodal load values and element length are first read in. The matrix equation for the beam is set up and solved in the computer using a fraction (specified

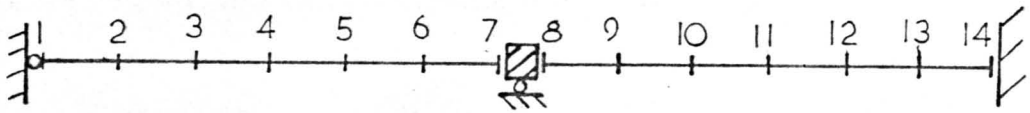

$$
\begin{bmatrix}
4\eta_2+\eta_3 & -2(\eta_2+\eta_3) & \eta_3 & 0 & 0 & 0 & 0 & 0 & 0 & 0 \\
-2(\eta_2+\eta_3) & \eta_2+4\eta_3+\eta_4 & -2(\eta_3+\eta_4) & \eta_4 & 0 & 0 & 0 & 0 & 0 & 0 \\
\eta_3 & -2(\eta_3+\eta_4) & \eta_3+4\eta_4+\eta_5 & -2(\eta_4+\eta_5) & \eta_5 & 0 & 0 & 0 & 0 & 0 \\
0 & \eta_4 & -2(\eta_4+\eta_5) & \eta_4+4\eta_5+\eta_6 & -2(\eta_5+\eta_6) & 0 & 0 & 0 & 0 & 0 \\
0 & 0 & \eta_5 & -2(\eta_5+\eta_6) & \eta_5+4\eta_6+\frac{2\eta_7\eta_8}{\eta_7+\eta_8} & \frac{2\eta_7\eta_8}{\eta_7+\eta_8} & 0 & 0 & 0 & 0 \\
0 & 0 & 0 & 0 & \frac{2\eta_7\eta_8}{\eta_7+\eta_8} & \frac{2\eta_7\eta_8}{\eta_7+\eta_8}+4\eta_9+\eta_{10} & -2(\eta_9+\eta_{10}) & \eta_{10} & 0 & 0 \\
0 & 0 & 0 & 0 & 0 & -2(\eta_9+\eta_{10}) & \eta_9+4\eta_{10}+\eta_{11} & -2(\eta_{10}+\eta_{11}) & \eta_{11} & 0 \\
0 & 0 & 0 & 0 & 0 & \eta_{10} & -2(\eta_{10}+\eta_{11}) & \eta_{10}+4\eta_{11}+\eta_{12} & -2(\eta_{11}+\eta_{12}) & \eta_{12} \\
0 & 0 & 0 & 0 & 0 & 0 & \eta_{11} & -2(\eta_{11}+\eta_{12}) & \eta_{11}+4\eta_{12}+\eta_{13} & -2(\eta_{12}+\eta_{13}) \\
0 & 0 & 0 & 0 & 0 & 0 & 0 & \eta_{12} & -2(\eta_{12}+\eta_{13}) & \eta_{12}+4\eta_{13}+2\eta_{14}
\end{bmatrix}
\begin{bmatrix} \Delta y_2 \\ \Delta y_3 \\ \Delta y_4 \\ \Delta y_5 \\ \Delta y_6 \\ \Delta y_9 \\ \Delta y_{10} \\ \Delta y_{11} \\ \Delta y_{12} \\ \Delta y_{13} \end{bmatrix}
=
\begin{bmatrix} \Delta q_2 \\ \Delta q_3 \\ \Delta q_4 \\ \Delta q_5 \\ \Delta q_6 \\ \Delta q_9 \\ \Delta q_{10} \\ \Delta q_{11} \\ \Delta q_{12} \\ \Delta q_{13} \end{bmatrix}
\cdot a^4
$$

DIAGRAM 29: The Matrix Equation for a Two Span Beam

in the input) of the total load. It should be noted that using the mathematics outlined earlier a stiffness matrix is obtained which is symmetric about the leading diagonal and has a band width of five provided that each beam is divided into not less than five element lengths. The computer program was written in such a way that only the leading diagonal and the two diagonals on one side of it need be stored. Having found the deflection field under this fraction of the total load the computer calculates the curvature and bending moment at each node. The moment at each node is then compared to the cracking moment for that node (defined in the input). If the cracking moment is not exceeded at any node the next load increment is performed in a similar way. If the cracking moment is exceeded at one or more nodes then part of the load is removed until the load at which cracking occurs is established to a degree of accuracy specified during input. The flexural rigidity at the nodes where the moment exceeds the cracking moment is changed to the after cracking value. Loading is then continued and any new cracking is identified and dealt with in a similar way. Thus the complete force and deformation fields after application of the total load are evaluated. The computer program produces non-linear load-deflection behaviour but is essentially "disguised linear" in format.

Deformation under Sustained Load

Time effects are now included; this involves allowing each member of the beam to deform for a small increment of time on the assumption that the force field is unchanged. Then the conditions of compatibility of slopes are checked at internal supports and boundaries. If slopes are found to be incompatible at any location changes in bending moment are introduced which correct for this without violating equilibrium conditions. The process is now discussed in more detail.

The sustained moment curvature diagram (in the form of η_o, ρ_o and η_c, ρ_c values) at various times after loading is read in. The time intervals

chosen may be selected for each situation but it is advisable to use roughly equal intervals of log time. A typical moment curvature diagram (time = t_o) and a typical diagram at a later time (time = $t_o + \Delta t$) are shown in diagram 30. Using this information the computer calculates the change

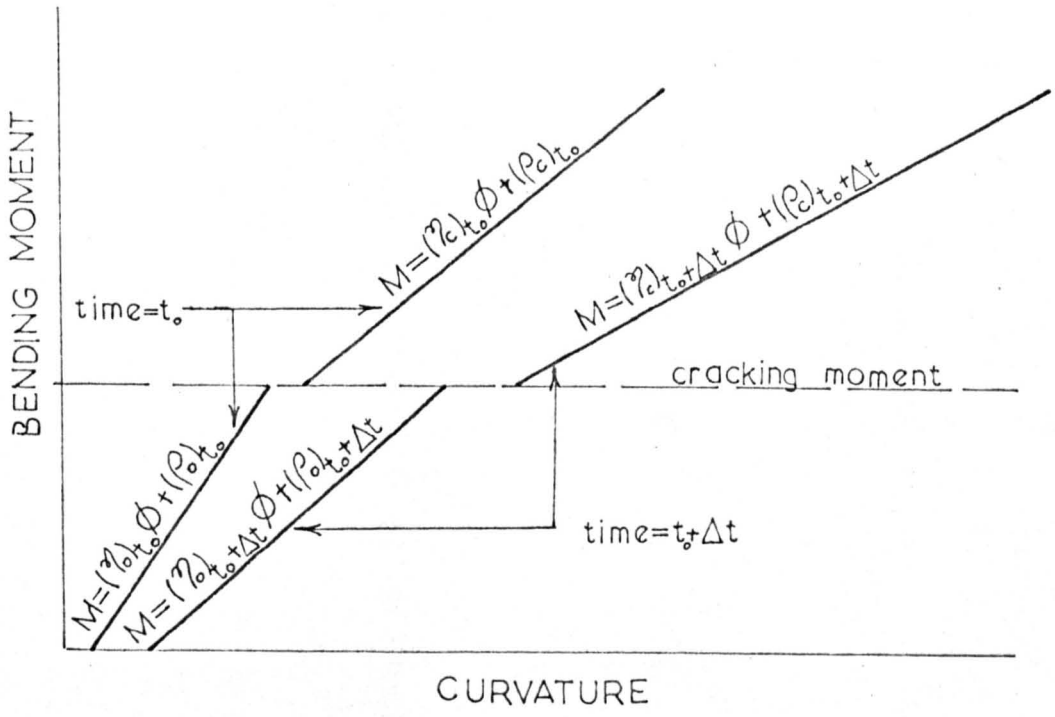

DIAGRAM 30: General Sustained Moment Curvature Diagrams

in curvature at each node during the time Δt on the assumption that the change in curvature is a function of only the moment at the beginning of that interval and the moment curvature diagram. This is a similar approach to the rate of creep method for stress-strain; it neglects moment history and under gradually reducing moments will over estimate the change in curvature. Similarly under gradually increasing moments it will under estimate the curvature change but these errors will be minimised if small time increments are selected. The calculation of the curvature changes in this way can be justified on three grounds.

(i) to do it any more accurate way would require considerably more experimental data, computer time and store space.

(ii) although time dependent moment redistribution has a considerable effect on deflection the moment changes under sustained service loads are unlikely to exceed 25% of the values immediately after loading.

(iii) Ross (21) investigated the rate of creep method for stress strain in plain concrete and concluded "... these tests have shown that from a single creep curve and a single value of the elastic modulus the strain can be predicted with reasonable success by the rate of creep method for widely varying regimes of stress."

With reference to diagram 30 the equations by which the curvature change at every node is calculated are:-

when $M \leq M_c$, $$\Delta^\circ\phi = \left[\frac{M-(P_o)_{t_o+\Delta t}}{(\eta_o)_{t_o+\Delta t}}\right] - \left[\frac{M-(P_o)_{t_o}}{(\eta_o)_{t_o}}\right]$$

when $M > M_c$, $$\Delta^\circ\phi = \left[\frac{M-(P_c)_{t_o+\Delta t}}{(\eta_c)_{t_o+\Delta t}}\right] - \left[\frac{M-(P_c)_{t_o}}{(\eta_c)_{t_o}}\right]$$

The prefix Δ° is used to denote the change in a small increment of time Δt during which the force field is assumed constant.

When the curvature changes at each node are known the corresponding deflection changes can be computed using the equation:-

$$\Delta^\circ\left(\frac{d^2y}{dx^2}\right)_o = \frac{1}{a^2}\left(\Delta^\circ y_{-1} - 2\Delta^\circ y_o + \Delta^\circ y_1\right)$$

This is done by setting up and solving a matrix equation for each member of the beam, see diagram 31.

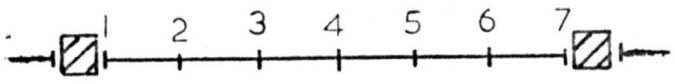

$$\begin{bmatrix} -2 & 1 & 0 & 0 & 0 \\ 1 & -2 & 1 & 0 & 0 \\ 0 & 1 & -2 & 1 & 0 \\ 0 & 0 & 1 & -2 & 1 \\ 0 & 0 & 0 & 1 & -2 \end{bmatrix} \begin{bmatrix} \Delta^{\circ}\gamma_2 \\ \Delta^{\circ}\gamma_3 \\ \Delta^{\circ}\gamma_4 \\ \Delta^{\circ}\gamma_5 \\ \Delta^{\circ}\gamma_6 \end{bmatrix} = a^2 \cdot \begin{bmatrix} \Delta^{\circ}\phi_2 \\ \Delta^{\circ}\phi_3 \\ \Delta^{\circ}\phi_4 \\ \Delta^{\circ}\phi_5 \\ \Delta^{\circ}\phi_6 \end{bmatrix}$$

DIAGRAM 31: Matrix Equation Relating Deflection and Curvature Changes

Next a moment redistribution procedure is used which corrects for any incompatibility of slopes; this is now outlined with reference to diagram 23. The prefix Δ^r is used to denote changes resulting from moment redistribution.

Since the applied load is constant we know,

$$\Delta^r M_{-1} - 2\Delta^r M_o + \Delta^r M_1 = 0$$

also, the immediate response of the beam to moment change, at for example node O, is defined by

$$-\eta_o \Delta^r \left(\frac{d^2y}{dx^2}\right)_o = \Delta^r M_o$$

η here is the value defining the moment curvature response during loading, either the cracked or uncracked value as appropriate. Thus it is assumed that the immediate response of the beam to changes in bending moment is

independent of time; this is justified on the grounds that provided the age at loading is 28 days or more the errors introduced by this assumption are small and to do it any more accurate way would require considerably more experimental data, computer store and computer time.

These equations can be combined to give in matrix form,

$$[0] = \frac{1}{a^4}\left[\eta_{-1}, -2(\eta_{-1}+\eta_0), \eta_{-1}+4\eta_0+\eta_1, -2(\eta_0+\eta_1), \eta_1\right]\begin{bmatrix}\Delta^r y_{-2}\\ \Delta^r y_{-1}\\ \Delta^r y_0\\ \Delta^r y_1\\ \Delta^r y_2\end{bmatrix} \qquad (5)$$

The difficulty lies in writing equation (5) for the nodes adjacent to internal supports and for the nodes adjacent to and at boundaries. These situations are now considered separately.

(i) Nodes adjacent to a simple support (diagram 24)

Now, $$0 = \Delta^r M_0 - 2\Delta^r M_1 + \Delta^r M_2$$

but $$\Delta^r M_0 = 0 \qquad \therefore 0 = 2\eta_1 \Delta^r\left(\frac{d^2y}{dx^2}\right)_1 + \eta_2 \Delta^r\left(\frac{d^2y}{dx^2}\right)_2$$

Substituting and rearranging in matrix form.

$$[0] = \frac{1}{a^4}\left[4\eta_1+\eta_2, -2(\eta_1+\eta_2), \eta_2\right]\begin{bmatrix}\Delta^r y_1\\ \Delta^r y_2\\ \Delta^r y_3\end{bmatrix}$$

(ii) Nodes adjacent to fully fixed supports (diagram 25)

Approximately, by Taylor's theorem,

$$\Delta^r y_1 = \Delta^r y_0 + a\,\Delta^r\left(\frac{dy}{dx}\right)_0 + \frac{a^2}{2}\Delta^r\left(\frac{d^2y}{dx^2}\right)_0$$

To re-establish compatibility (destroyed during the deformation under constant moment) we require $$\Delta^r\left(\frac{dy}{dx}\right)_0 + \Delta^0\left(\frac{dy}{dx}\right)_0 = 0\,, \quad \Delta^r y_0 = 0$$

$$\therefore \Delta^r\left(\frac{d^2y}{dx^2}\right)_0 = \frac{2}{a^2}\left[\Delta^r y_1 + a\Delta^0\left(\frac{dy}{dx}\right)_0\right]$$

Now

$$0 = \Delta^r M_0 - 2\Delta^r M_1 + \Delta^r M_2$$

Substituting and rearranging in matrix form,

$$\left[-2a\,\eta_0\,\Delta^{\circ}\left(\frac{dy}{dx}\right)_0\right] = \left[2\eta_0+4\eta_1+\eta_2,\ -2(\eta_1+\eta_2),\ \eta_2\right]\begin{bmatrix}\Delta^{r}y_1\\ \Delta^{r}y_2\\ \Delta^{r}y_3\end{bmatrix}$$

(iii) Cantilever free end (diagram 26)

Approximately by Taylor's theorem,

$$\Delta^{r}M_2 = \Delta^{r}M_1 + a\,\Delta^{r}\left(\frac{dM}{dx}\right)_1 + \frac{a^2}{2}\Delta^{r}\left(\frac{d^2M}{dx^2}\right)_1$$

but we require

$$\Delta^{r}M_1 = \Delta^{r}\left(\frac{dM}{dx}\right)_1 = 0$$

$$\therefore \Delta^{r}\left(\frac{d^2M}{dx^2}\right)_1 = \frac{2M_2}{a^2} \qquad \therefore 0 = \frac{2\eta_2}{a^2}\,\Delta^{r}\left(\frac{d^2y}{dx^2}\right)_2$$

Substituting and rearranging in matrix form,

$$[0] = [\eta_2,\ -2\eta_2,\ \eta_2]\begin{bmatrix}\Delta^{r}y_1\\ \Delta^{r}y_2\\ \Delta^{r}y_3\end{bmatrix}$$

Also,

$$0 = -\frac{1}{a^2}\left[\Delta^{r}M_1 - 2\Delta^{r}M_2 + \Delta^{r}M_3\right]$$

$$\therefore\ 0 = -\frac{1}{a^2}\left[-2\eta_2\,\Delta^{r}\left(\frac{d^2y}{dx^2}\right)_2 + \eta_3\Delta^{r}\left(\frac{d^2y}{dx^2}\right)_3\right]$$

Substituting and rearranging in matrix form,

$$[0] = [-2\eta_2,\ 4\eta_2+\eta_3,\ -2\eta_2+\eta_3,\ \eta_3]\begin{bmatrix}\Delta^{r}y_1\\ \Delta^{r}y_2\\ \Delta^{r}y_3\\ \Delta^{r}y_4\end{bmatrix}$$

(iv) Line of symmetry (diagram 27). Beams which are symmetric about a support can be treated as fully fixed at that support. When the line of symmetry is at midspan the following treatment may be used.

Approximately, by Taylor's theorem,

$$\Delta^{r}M_2 = \Delta^{r}M_1 + a\,\Delta^{r}\left(\frac{dM}{dx}\right)_1 + \frac{a^2}{2}\Delta^{r}\left(\frac{d^2M}{dx^2}\right)_1$$

but we require

$$\Delta^r\left(\frac{dM}{dx}\right)_1 = 0 \qquad \therefore \frac{2}{a^2}\left(\Delta^r M_2 - \Delta^r M_1\right) = \Delta^r\left(\frac{d^2M}{dx^2}\right)_1$$

Also, approximately,

$$\Delta^r y_2 = \Delta^r y_1 + a\,\Delta^r\left(\frac{dy}{dx}\right)_1 + \frac{a^2}{2}\Delta^r\left(\frac{d^2y}{dx^2}\right)_1$$

but we require

$$\Delta^r\left(\frac{dy}{dx}\right)_1 = 0 \qquad \therefore \frac{2}{a^2}\left(\Delta^r y_2 - \Delta^r y_1\right) = \Delta^r\left(\frac{d^2y}{dx^2}\right)_1$$

$$\therefore\ 0 = \eta_2 \cdot \Delta^r\left(\frac{d^2y}{dx^2}\right)_2 - \eta_1\,\Delta^r\left(\frac{d^2y}{dx^2}\right)_1$$

Substituting and rearranging in matrix form,

$$[0] = \left[2\eta_1 + \eta_2,\ -2(\eta_1+\eta_2),\ \eta_2\right]\begin{bmatrix}\Delta^r y_1\\ \Delta^r y_2\\ \Delta^r y_3\end{bmatrix}$$

Also,

$$0 = \Delta^r M_1 - 2\Delta^r M_2 + \Delta^r M_3$$

$$0 = \eta_1\,\Delta^r\left(\frac{d^2y}{dx^2}\right)_1 - 2\eta_2\Delta^r\left(\frac{d^2y}{dx^2}\right)_2 + \eta_3\,\Delta^r\left(\frac{d^2y}{dx^2}\right)_3$$

Substituting and rearranging in matrix form,

$$[0] = \left[-2(\eta_1+\eta_2),\ 2\eta_1+4\eta_2+\eta_3,\ -2(\eta_2+\eta_3),\ \eta_3\right]\begin{bmatrix}\Delta^r y_1\\ \Delta^r y_2\\ \Delta^r y_3\\ \Delta^r y_4\end{bmatrix}$$

(v) Nodes adjacent to internal supports (diagram 28)

Approximately by Taylor's theorem,

$$\Delta^r y_3 = \Delta^r y_4 - a\,\Delta^r\left(\frac{dy}{dx}\right)_4 + \frac{a^2}{2}\Delta^r\left(\frac{d^2y}{dx^2}\right)_4$$

and

$$\Delta^r y_2 = \Delta^r y_5 + a\,\Delta^r\left(\frac{dy}{dx}\right)_5 + \frac{a^2}{2}\Delta^r\left(\frac{d^2y}{dx^2}\right)_5$$

For compatibility of slopes we require

$$\Delta^o\left(\frac{dy}{dx}\right)_4 + \Delta^r\left(\frac{dy}{dx}\right)_4 = \Delta^o\left(\frac{dy}{dx}\right)_5 + \Delta^r\left(\frac{dy}{dx}\right)_5$$

In order that equilibrium should be preserved we require,

$$\Delta' M_4 - \Delta' M_5 = 0 \qquad \therefore \eta_4 \Delta'\left(\frac{d^2y}{dx^2}\right)_4 = \eta_5 \Delta'\left(\frac{d^2y}{dx^2}\right)_5$$

and

$$\Delta' y_4 = \Delta' y_5 = 0$$

By combining the above equations,

$$\Delta'\left(\frac{d^2y}{dx^2}\right)_4 = \frac{2}{a^2} \cdot \frac{\eta_5}{\eta_4+\eta_5}\left[\Delta' y_3 + \Delta' y_6 + a\Delta^\circ\left(\frac{dy}{dx}\right)_5 - a\Delta^\circ\left(\frac{dy}{dx}\right)_4\right]$$

Also, we require for equilibrium,

$$\Delta' M_2 - \Delta' M_3 + \Delta' M_4 = 0$$

$$\eta_2 \Delta'\left(\frac{d^2y}{dx^2}\right)_2 - 2\eta_3 \Delta'\left(\frac{d^2y}{dx^2}\right)_3 + \eta_4 \Delta'\left(\frac{d^2y}{dx^2}\right)_4 = 0$$

Substituting and rearranging in matrix form,

$$2a\frac{\eta_4\eta_5}{\eta_4+\eta_5}\left(\Delta^\circ\left(\frac{dy}{dx}\right)_4 - \Delta^\circ\left(\frac{dy}{dx}\right)_5\right) = \left[\eta_2, -2(\eta_2+\eta_3), \eta_2+4\eta_3+\frac{2\eta_4\eta_5}{\eta_4+\eta_5}, \frac{2\eta_4\eta_5}{\eta_4+\eta_5}\right]\begin{bmatrix}\Delta' y_1\\ \Delta' y_2\\ \Delta' y_3\\ \Delta' y_6\end{bmatrix}$$

Using the above equations, a matrix equation can be set up for a continuous beam in terms of the nodal flexural rigidities, the slope errors produced during deformation under constant moment and the deflection changes required to re-establish compatibility of slopes without destroying equilibrium. A simple example is shown in diagram 32. The similarity between this equation and that shown in diagram 29 should be noted. Thus by setting up and solving the matrix equation shown in diagram 32 the computer obtains the deflection changes required to re-establish compatibility of slopes, then the corresponding curvature and moment changes are calculated. The beam in then examined to determine whether the moment changes have caused the moment at any previously uncracked nodes to exceed the cracking moment; if so, the flexural rigidity at these nodes is modified to the "after cracking" value.

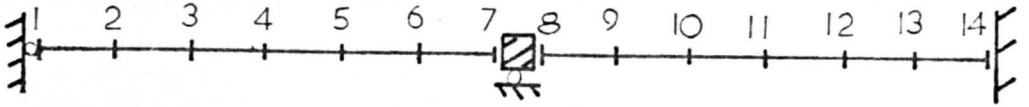

$$
\begin{bmatrix}
4\eta_2+\eta_3 & -2(\eta_2+\eta_3) & \eta_3 & 0 & 0 & 0 & 0 & 0 & 0 & 0 \\
-2(\eta_2+\eta_3) & \eta_2+4\eta_3+\eta_4 & -2(\eta_3+\eta_4) & \eta_4 & 0 & 0 & 0 & 0 & 0 & 0 \\
\eta_3 & -2(\eta_3+\eta_4) & \eta_3+4\eta_4+\eta_5 & -2(\eta_4+\eta_5) & \eta_5 & 0 & 0 & 0 & 0 & 0 \\
0 & \eta_4 & -2(\eta_4+\eta_5) & \eta_4+4\eta_5+\eta_6 & -2(\eta_5+\eta_6) & 0 & 0 & 0 & 0 & 0 \\
0 & 0 & \eta_5 & -2(\eta_5+\eta_6) & \eta_5+4\eta_6+\frac{2\eta_7\eta_8}{\eta_7+\eta_8} & \frac{2\eta_7\eta_8}{\eta_7+\eta_8} & 0 & 0 & 0 & 0 \\
0 & 0 & 0 & 0 & \frac{2\eta_7\eta_8}{\eta_7+\eta_8} & \frac{2\eta_7\eta_8}{\eta_7+\eta_8}+4\eta_9+\eta_{10} & -2(\eta_9+\eta_{10}) & \eta_{10} & 0 & 0 \\
0 & 0 & 0 & 0 & 0 & -2(\eta_9+\eta_{10}) & \eta_9+4\eta_{10}+\eta_{11} & -2(\eta_{10}+\eta_{11}) & \eta_{11} & 0 \\
0 & 0 & 0 & 0 & 0 & \eta_{10} & -2(\eta_{10}+\eta_{11}) & \eta_{10}+4\eta_{11}+\eta_{12} & -2(\eta_{11}+\eta_{12}) & \eta_{12} \\
0 & 0 & 0 & 0 & 0 & 0 & \eta_{11} & -2(\eta_{11}+\eta_{12}) & \eta_{11}+4\eta_{12}+\eta_{13} & -2(\eta_{12}+\eta_{13}) \\
0 & 0 & 0 & 0 & 0 & 0 & 0 & \eta_{12} & -2(\eta_{12}+\eta_{13}) & \eta_{12}+4\eta_{13}+2\eta_{14}
\end{bmatrix}
\begin{bmatrix}
\Delta y_2 \\ \Delta y_3 \\ \Delta y_4 \\ \Delta y_5 \\ \Delta y_6 \\ \Delta y_9 \\ \Delta y_{10} \\ \Delta y_{11} \\ \Delta y_{12} \\ \Delta y_{13}
\end{bmatrix}
=
\begin{bmatrix}
0 \\ 0 \\ 0 \\ 0 \\ \left(\Delta^\circ\left(\frac{dy}{dx}\right)_7-\Delta^\circ\left(\frac{dy}{dx}\right)_8\right)\cdot\frac{2a\eta_7\eta_8}{\eta_7+\eta_8} \\ \left(\Delta^\circ\left(\frac{dy}{dx}\right)_7-\Delta^\circ\left(\frac{dy}{dx}\right)_8\right)\cdot\frac{2a\eta_7\eta_8}{\eta_7+\eta_8} \\ 0 \\ 0 \\ 0 \\ 2a\eta_{14}\,\Delta^\circ\left(\frac{dy}{dx}\right)_{14}
\end{bmatrix}
$$

DIAGRAM 32: Moment Redistribution Equation for a Two Span Beam

There is an assumption implicit in this redistribution procedure which must be mentioned. It had been assumed in this thesis that in zones where the moment is reducing the immediate response is still governed by the moment-curvature diagram for increasing moment. It is well known that this is not strictly true for reinforced concrete; the real and assumed moment curvature diagrams for reinforced concrete under one loading cycle of service load are compared in diagram 33. Again, provided moment changes are less than 25% of the immediately after loading values, the errors introduced by this assumption are small and, to deal with this problem more accurately would require considerably more experimental data, computer store and computer time.

Now that the complete force and deformation fields are known the next time increment is performed in an identical manner.

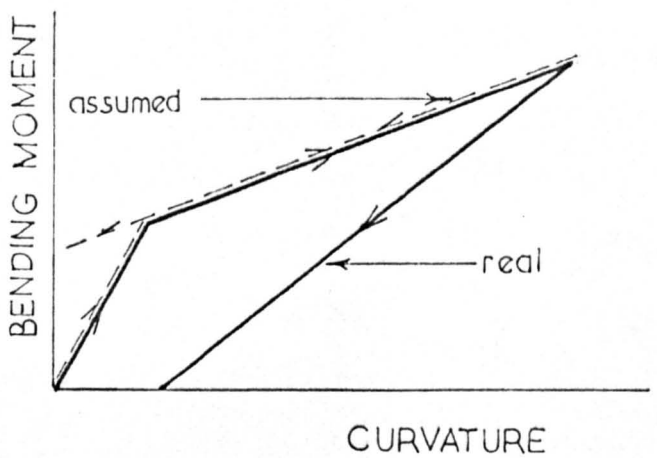

DIAGRAM 33: Real and Assumed Moment Curvature Diagrams

C. Analysis of Reinforced Concrete Plane Frames under Sustained Service Loads

A computer program was developed to calculate the force and deformation fields immediately after loading and after periods of sustained load in a one bay plane frame of one or two storeys. It was required that the program should be able to take account of the variations in flexural rigidity along the length of a member which may exist due to variations in geometry or reinforcement or due to the influence of cracking during loading. A flow chart explaining briefly the main steps in the program is shown in diagram 34. Using the node patterns shown in diagram 35, and the experimental data given in tables 8 and 11, the two plane frames tested in the laboratory were analysed. In the case of frame 1, no experimental data regarding axial strains had been obtained, consequently this data was "manufactured" for the computer analysis. However in this frame, member axial forces are very small relative to bending effects and the influence of the particular data chosen on the computer solutions is negligible. The computer prints out solutions for immediately after loading and for all the times under sustained load defined in tables 8 and 11. Typical print-outs are shown in diagram 36. The program is based on mathematics which are extensions of the finite difference techniques used in the continuous beam analysis. These extensions are now outlined. The co-ordinate system for horizontal members, sign conventions and notations used earlier are retained. The co-ordinate system for vertical members is shown in diagram 37.

Immediate Response to Load Application

As for continuous beam analysis a matrix equation based on equation (4) is set up and solved. In order to facilitate this, the modified form of equation 4 for nodes adjacent to joints was developed for the four member

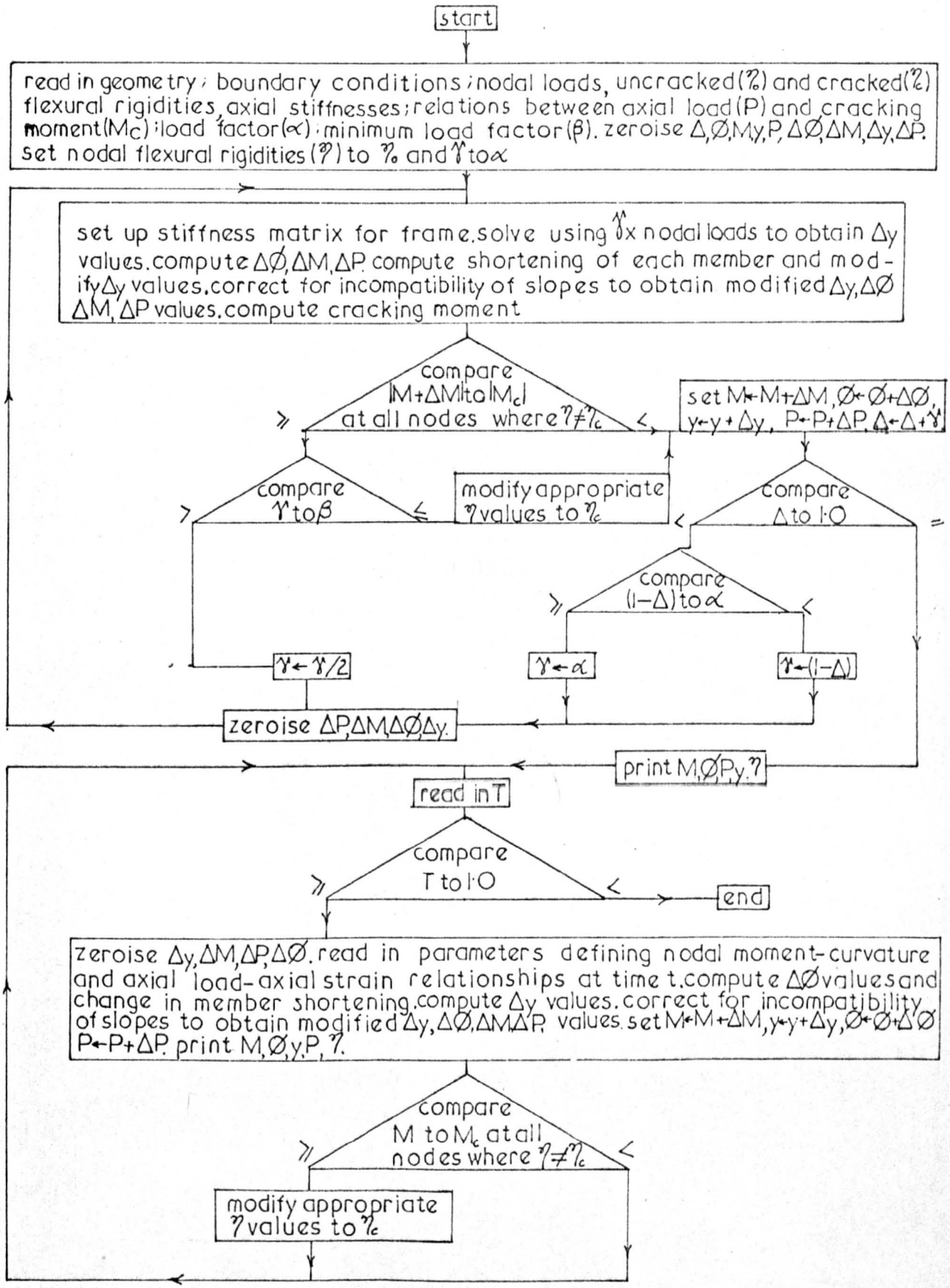

DIAGRAM 34: Simplified Flow Chart for the Computer Program for the Analysis of Plane Frames

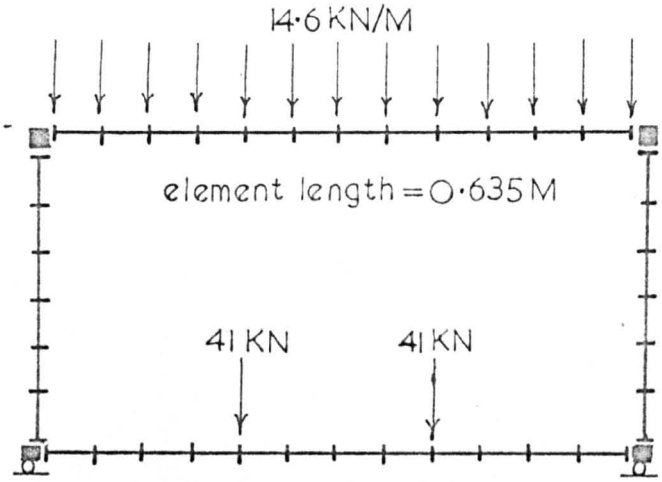

Frame 1

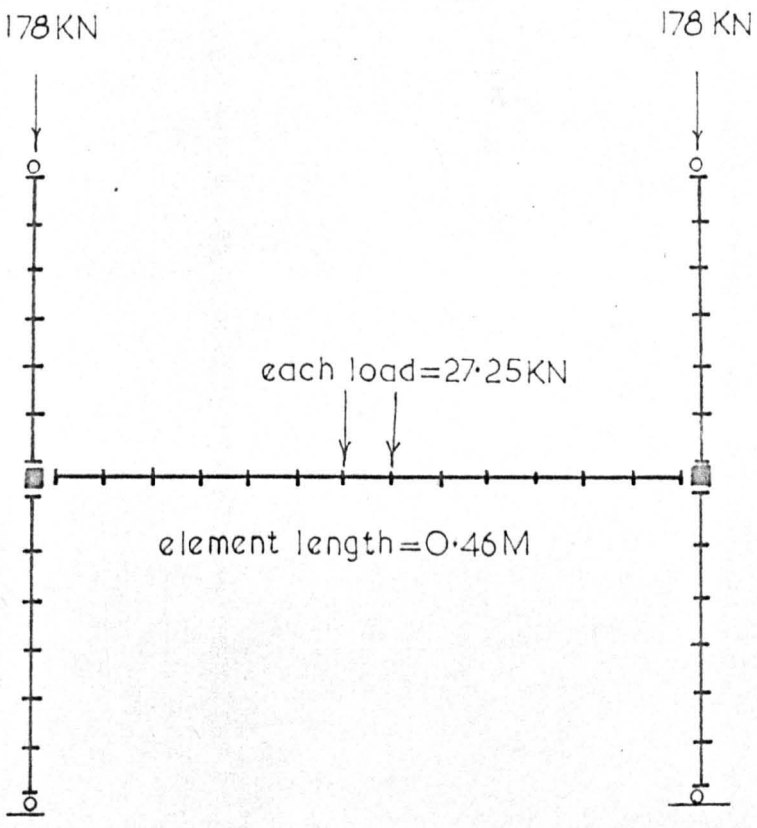

Frame 2

DIAGRAM 35: Node Patterns for Plane Frames

DIAGRAM 36: Typical Computer Print Out from Analysis of Frame 1

FRAME ANALYSIS

IMMEDIATELY AFTER LOADING

DEFLNS	BENDING MOMENTS		FLEXURAL RIGIDITY	CURVATURE
METRES	NEWTON-METRES		NEWTON (METRE)↑2	PER METRE
-0.00003	59298.7	l.h. col.	13800000.0	-0.0034937467
0.00063	39604.1		13800000.0	-0.0020448491
0.00046	19909.5		31800000.0	-0.0006260850
0.00004	214.9		31800000.0	-0.0000067580
-0.00039	-19479.7		31800000.0	0.0006125689
-0.00056	-39174.3		13800000.0	0.0020193213
0.00007	-58868.9		13800000.0	0.0034829182
0.00003	-59298.7	r.h. col.	13800000.0	0.0034937468
-0.00063	-39604.1		13800000.0	0.0020448491
-0.00046	-19909.5		31800000.0	0.0006260850
-0.00004	-214.9		31800000.0	0.0000067581
0.00039	19479.7		31800000.0	-0.0006125689
0.00056	39174.3		13800000.0	-0.0020193212
-0.00007	58868.9		13800000.0	-0.0034829182
0.00000	-59298.7	lower beam	13800000.0	0.0035768931
0.00208	-33210.0		13800000.0	0.0017160693
0.00486	-7121.4		31800000.0	0.0002239430
0.00772	18967.3		13800000.0	-0.0007265308
0.01029	45055.9		13800000.0	-0.0025503986
0.01183	45055.9		13800000.0	-0.0025503986
0.01235	45055.9		13800000.0	-0.0025503986
0.01183	45055.9		13800000.0	-0.0025503986
0.01029	45055.9		13800000.0	-0.0025503986
0.00772	18967.3		13800000.0	-0.0007265308
0.00486	-7121.4		31800000.0	0.0002239430
0.00208	-33210.0		13800000.0	0.0017160693
0.00000	-59298.7		13800000.0	0.0035768931
0.00010	-58868.9	upper beam	13800000.0	0.0035108080
0.00215	-26489.9		13800000.0	0.0011158986
0.00464	2.0		31800000.0	-0.0000000617
0.00714	20606.8		13800000.0	-0.0006697256
0.00937	35324.5		13800000.0	-0.0017768577
0.01088	44155.1		13800000.0	-0.0024214860
0.01141	47098.6		13800000.0	-0.0026520479
0.01088	44155.1		13800000.0	-0.0024214860
0.00937	35324.5		13800000.0	-0.0017768576
0.00714	20606.8		13800000.0	-0.0006697255
0.00464	2.0		31800000.0	-0.0000000616
0.00215	-26489.9		13800000.0	0.0011158988
0.00010	-58868.9		13800000.0	0.0035108079

MEMBER AXIAL FORCES

NEWTONS

96710.5
55626.0
96710.5

55626.0
-31015.1
31015.1

SUPPORT REACTIONS

NEWTONS

96710.5
96710.5

0.0
-0.0

DIAGRAM 36: Typical Computer Print Out from Analysis of Frame 1

FRAME ANALYSIS

547 DAYS AFTER LOADING

DEFLNS	BENDING MOMENTS		FLEXURAL RIGIDITY	CURVATURE
METRES	NEWTON-METRES		NEWTON (METRE)↑2	PER METRE
-0.00010	59196.5	l.h. col.	13800000.0	-0.0059767062
0.00118	39477.6		13800000.0	-0.0040428805
0.00084	19758.6		31800000.0	-0.0015099007
-0.00011	39.7		31800000.0	0.0003016236
-0.00094	-19679.3		31800000.0	0.0015132097
-0.00116	-39398.3		13800000.0	0.0040483572
0.00025	-59117.2		13800000.0	0.0059968822
0.00010	-59196.6	r.h. col.	13800000.0	0.0059767062
-0.00118	-39477.6		13800000.0	0.0040428806
-0.00084	-19758.6		31800000.0	0.0015099008
0.00011	-39.7		31800000.0	-0.0003016235
0.00094	19679.3		31800000.0	-0.0015132097
0.00116	39398.3		13800000.0	-0.0040483571
-0.00025	59117.2		13800000.0	-0.0059968821
0.00000	-59196.6	lower beam	13800000.0	0.0057886283
0.00366	-33107.9		13800000.0	0.0032854076
0.00864	-7019.2		31800000.0	0.0007595391
0.01393	19069.4		13800000.0	-0.0019868930
0.01842	45158.1		13800000.0	-0.0044531577
0.02112	45158.1		13800000.0	-0.0044531577
0.02201	45158.1		13800000.0	-0.0044531577
0.02112	45158.1		13800000.0	-0.0044531577
0.01842	45158.1		13800000.0	-0.0044531577
0.01393	19069.4		13800000.0	-0.0019868930
0.00864	-7019.2		31800000.0	0.0007595391
0.00366	-33107.9		13800000.0	0.0032854076
0.00000	-59196.6		13800000.0	0.0057886284
0.00033	-59117.2	upper beam	13800000.0	0.0059477292
0.00415	-26738.3		13800000.0	0.0027555328
0.00908	-246.4		31800000.0	0.0003187238
0.01414	20358.4		13800000.0	-0.0021230515
0.01834	35076.1		13800000.0	-0.0035925868
0.02110	43906.7		13800000.0	-0.0044546570
0.02206	46850.3		13800000.0	-0.0047576996
0.02110	43906.7		13800000.0	-0.0044546570
0.01834	35076.1		13800000.0	-0.0035925866
0.01414	20358.4		13800000.0	-0.0021230513
0.00908	-246.4		31800000.0	0.0003187240
0.00415	-26738.3		13800000.0	0.0027555331
0.00033	-59117.2		13800000.0	0.0059477294

MEMBER AXIAL FORCES

NEWTONS

96710.5
55626.0
96710.5

55526.0
-51053.5
51053.5

SUPPORT REACTIONS

NEWTONS

96710.5
96710.5

0.0
-0.0

DIAGRAM 36: Typical Computer Print Out from Analysis of Frame 2

FRAME ANALYSIS

IMMEDIATELY AFTER LOADING

DEFLNS	BENDING MOMENTS		FLEXURAL RIGIDITY	CURVATURE
METRES	NEWTON-METRES		NEWTON (METRE)↑2	PER METRE
0.00000	0.0		4400000.0	0.0000000000
-0.00055	-1874.0		4400000.0	0.0004259148
-0.00100	-3748.1		4400000.0	0.0008518297
-0.00128	-5622.1		4400000.0	0.0012777445
-0.00128	-7496.1		4400000.0	0.0017036594
-0.00093	-9370.1		1950000.0	0.0027728720
0.00001	-11244.2		1950000.0	0.0038962098
0.00001	11068.2	l.h. col.	1950000.0	-0.0038964101
0.00095	9223.5		1950000.0	-0.0028339506
0.00129	7378.8		4400000.0	-0.0016769953
0.00128	5534.1		4400000.0	-0.0012577465
0.00100	3689.4		4400000.0	-0.0008384976
0.00055	1844.7		4400000.0	-0.0004192488
0.00000	-0.0		4400000.0	0.0000000001
0.00000	0.0		4400000.0	0.0000000000
0.00055	1874.0		4400000.0	-0.0004259149
0.00100	3748.1		4400000.0	-0.0008518297
0.00128	5622.1		4400000.0	-0.0012777446
0.00128	7496.1		4400000.0	-0.0017036594
0.00093	9370.1		1950000.0	-0.0027728720
-0.00001	11244.2		1950000.0	-0.0038962098
-0.00001	-11068.2	r.h. col.	1950000.0	0.0038964101
-0.00095	-9223.5		1950000.0	0.0028339506
-0.00129	-7378.8		4400000.0	0.0016769953
-0.00128	-5534.1		4400000.0	0.0012577465
-0.00100	-3689.4		4400000.0	0.0008384976
-0.00055	-1844.7		4400000.0	0.0004192488
0.00000	0.0		4400000.0	-0.0000000001
0.00047	-22312.3		13800000.0	0.0008901239
0.00191	-9764.4		31800000.0	0.0003070579
0.00343	2783.4		31800000.0	-0.0000875295
0.00492	15331.3		31800000.0	-0.0004821169
0.00631	27879.2		13800000.0	-0.0012884281
0.00743	40427.1		13800000.0	-0.0021963454
0.00809	52975.0		13800000.0	-0.0030949401
0.00809	52975.0	beam	13800000.0	-0.0030949401
0.00743	40427.1		13800000.0	-0.0021963454
0.00631	27879.2		13800000.0	-0.0012884281
0.00492	15331.3		31800000.0	-0.0004821169
0.00343	2783.4		31800000.0	-0.0000875295
0.00191	-9764.4		31800000.0	0.0003070579
0.00047	-22312.3		13800000.0	0.0008901239

MEMBER AXIAL FORCES

NEWTONS

205298.0

178020.0
205298.0
178020.0
63.8
4010.2

SUPPORT REACTIONS

NEWTONS

205298.0 4074.0
205298.0 -4074.0

DIAGRAM 36: Typical Computer Print Out from Analysis of Frame 2

FRAME ANALYSIS

547 DAYS AFTER LOADING

DEFLNS	BENDING MOMENTS		FLEXURAL RIGIDITY	CURVATURE
METRES	NEWTON-METRES		NEWTON (METRE)↑2	PER METRE
0.00000	0.0		4400000.0	-0.0000000000
-0.00127	-1791.4		4400000.0	0.0010536035
-0.00232	-3582.8		4400000.0	0.0021072070
-0.00292	-5374.3		4400000.0	0.0031608105
-0.00286	-7165.7		4400000.0	0.0042144140
-0.00190	-8957.1		1950000.0	0.0046294453
0.00004	-10748.5		1950000.0	0.0060888216
0.00004	10856.7	l.h. col.	1950000.0	-0.0061471267
0.00197	9047.3		1950000.0	-0.0047183812
0.00290	7237.8		1950000.0	-0.0041178039
0.00297	5428.4		4400000.0	-0.0031922796
0.00235	3618.9		4400000.0	-0.0021281862
0.00129	1809.5		4400000.0	-0.0010640929
0.00000	-0.0		4400000.0	0.0000000004
0.00000	0.0		4400000.0	-0.0000000000
0.00127	1791.4		4400000.0	-0.0010536035
0.00232	3582.8		4400000.0	-0.0021072070
0.00292	5374.3		4400000.0	-0.0031608105
0.00286	7165.7		4400000.0	-0.0042144140
0.00190	8957.1		1950000.0	-0.0046294453
-0.00004	10748.5		1950000.0	-0.0060888216
-0.00004	-10856.7	r.h. col.	1950000.0	0.0061471267
-0.00197	-9047.3		1950000.0	0.0047183811
-0.00290	-7237.8		1950000.0	0.0041178039
-0.00297	-5428.4		4400000.0	0.0031922795
-0.00235	-3618.9		4400000.0	0.0021281862
-0.00129	-1809.5		4400000.0	0.0010640929
0.00000	0.0		4400000.0	-0.0000000004
0.00178	-21605.3		13800000.0	0.0022433601
0.00460	-9057.4		31800000.0	0.0009014178
0.00761	3490.5		31800000.0	-0.0005599521
0.01050	16038.4		31800000.0	-0.0012920338
0.01312	28586.2		13800000.0	-0.0029105758
0.01512	41134.1		13800000.0	-0.0041274671
0.01625	53682.0		13800000.0	-0.0053350360
0.01625	53682.0		13800000.0	-0.0053350360
0.01512	41134.1	beam	13800000.0	-0.0041274671
0.01312	28586.2		13800000.0	-0.0029105758
0.01050	16038.4		31800000.0	-0.0012920338
0.00761	3490.5		31800000.0	-0.0005599521
0.00460	-9057.4		31800000.0	0.0009014178
0.00178	-21605.3		13800000.0	0.0022433601

MEMBER AXIAL FORCES

NEWTONS

205298.0

178020.0
205298.0
178020.0
-39.2
3933.6

SUPPORT REACTIONS

NEWTONS

205298.0 3894.4
205298.0 -3894.4

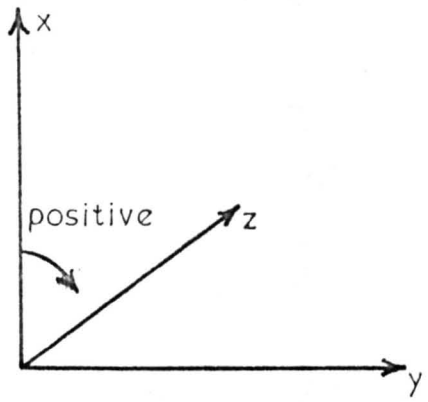

DIAGRAM 37: Co-ordinate System for Vertical Members

joint shown in diagram 38. This is a general equation which can be reduced

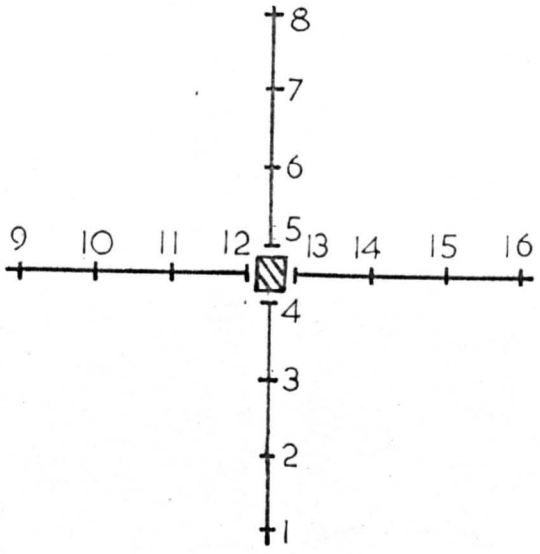

DIAGRAM 38: Node Pattern at Four Member Joint

to give the equation for any node adjacent to 3 or 2 member joints by putting the appropriate η values to zero.

Approximately by Taylor's theorem,

$$y_3 = y_4 - a\left(\frac{dy}{dx}\right)_4 + \frac{a^2}{2}\left(\frac{d^2y}{dx^2}\right)_4 \qquad \text{(i)}$$

$$y_{11} = y_{12} - a\left(\frac{dy}{dx}\right)_{12} + \frac{a^2}{2}\left(\frac{d^2y}{dx^2}\right)_{12} \qquad \text{(ii)}$$

$$y_6 = y_5 + a\left(\frac{dy}{dx}\right)_5 + \frac{a^2}{2}\left(\frac{d^2y}{dx^2}\right)_5 \qquad \text{(iii)}$$

$$y_{14} = y_{13} + a\left(\frac{dy}{dx}\right)_{13} + \frac{a^2}{2}\left(\frac{d^2y}{dx^2}\right)_{13} \qquad \text{(iv)}$$

From compatibility of slopes we have,

$$\left(\frac{dy}{dx}\right)_4 = \left(\frac{dy}{dx}\right)_{12} = \left(\frac{dy}{dx}\right)_5 = \left(\frac{dy}{dx}\right)_{13}$$

From equilibrium we have,

$$M_4 + M_{12} - M_5 - M_{13} = 0$$

Multiplying (ii) by η_{12} , (iii) by η_5 and (iv) by η_{13} , forming equation (ii) - equation (iii) - equation (iv) and substituting using equilibrium and compatibility conditions we obtain,

$$\eta_{12}y_{11} - \eta_5 y_6 - \eta_{13}y_{14} = \eta_{12}y_{12} - \eta_5 y_5 - \eta_{13}y_{13} - a(\eta_{12}+\eta_5+\eta_{13})\left(\frac{dy}{dx}\right)_4 - \frac{a^2}{2}\eta_4\left(\frac{d^2y}{dx^2}\right)_4$$

Making use of (i) to remove $\left(\frac{dy}{dx}\right)_4$ we obtain

$$\left(\frac{d^2y}{dx^2}\right)_4 = \frac{2}{a^2(\eta_{12}+\eta_5+\eta_{13}+\eta_4)}\left[\eta_{12}(y_{12}-y_{11}) + \eta_5(y_6-y_5) + \eta_{13}(y_{14}-y_{13}) - (\eta_{12}+\eta_5+\eta_{13})(y_4-y_3)\right] \qquad (6)$$

Now

$$q_3 = -\frac{1}{a^2}\left[M_2 - 2M_3 + M_4\right] = \frac{1}{a^2}\left[\eta_2\left(\frac{d^2y}{dx^2}\right)_2 - 2\eta_3\left(\frac{d^2y}{dx^2}\right)_3 + \eta_4\left(\frac{d^2y}{dx^2}\right)\right]$$

Now,

$$y_{12} = y_{13} = 0 \quad , \quad y_4 = y_3$$

Substituting and rearranging,

$$q_3 = \frac{1}{a^4}\left[\eta_2 y_1 - 2(\eta_2+\eta_3)y_2 + \left(\eta_2 + 4\eta_3 + \frac{2\eta_4(\eta_{12}+\eta_5+\eta_{13})}{\eta_4+\eta_{12}+\eta_5+\eta_{13}}\right)y_3 - 2\left(\eta_3 + \frac{\eta_4(\eta_{12}+2\eta_5+\eta_{13})}{\eta_4+\eta_{12}+\eta_5+\eta_{13}}\right)y_4\right.$$

$$\left. + \frac{2\eta_4\eta_5}{\eta_4+\eta_5+\eta_{12}+\eta_{13}}y_6 - \frac{2\eta_4\eta_{12}}{\eta_4+\eta_5+\eta_{12}+\eta_{13}}y_{11} + \frac{2\eta_4\eta_{13}}{\eta_4+\eta_{12}+\eta_5+\eta_{13}}y_{14}\right] \qquad (7)$$

In addition, a further equation is required because of the possibility of sidesway. This is equivalent to the "shear equation" used in the moment distribution method of frame analysis. This equation is now developed for the simple frame shown in diagram 39.

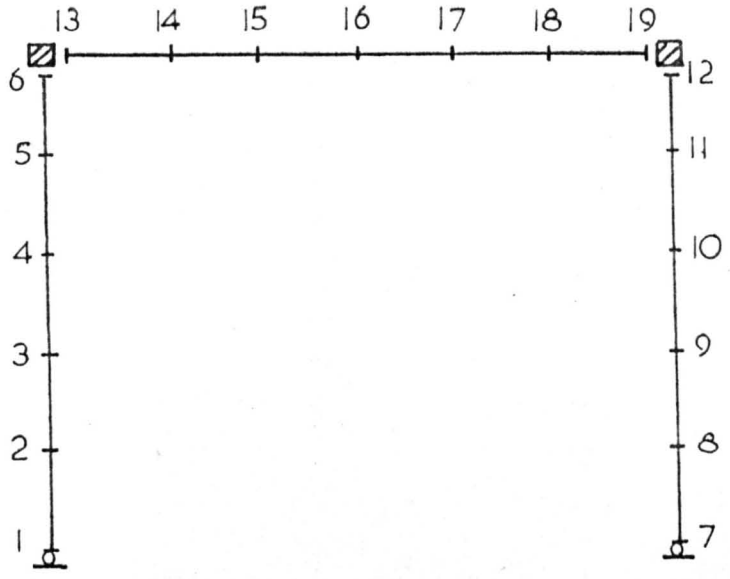

DIAGRAM 39: Typical Frame Node Pattern

Approximately, by Taylor's theorem,

$$M_5 = M_6 - a\left(\frac{dM}{dx}\right)_6 + \frac{a^2}{2}\left(\frac{d^2M}{dx^2}\right)_6$$

$$M_{11} = M_{12} - a\left(\frac{dM}{dx}\right)_{12} + \frac{a^2}{2}\left(\frac{d^2M}{dx^2}\right)_{12}$$

For the horizontal equilibrium of the beam,

$$\left(\frac{dM}{dx}\right)_6 + \left(\frac{dM}{dx}\right)_{12} = 0$$

Thus by addition and substitution,

$$M_5 + M_{11} = M_6 + M_{12} + \frac{a^2}{2}\left(-q_{12} - q_6\right)$$

Now, $y_6 = y_{12}$ and by substitution utilising equation (6),

$$\frac{a^4}{2}(q_6 + q_{12}) = \eta_5 y_4 - 2\left(\eta_5 + \frac{\eta_6\eta_{13}}{\eta_6+\eta_{13}}\right)y_5 + \eta_{11}y_{10} - 2\left(\eta_{11} + \frac{\eta_{19}\eta_{12}}{\eta_{12}+\eta_{19}}\right)y_{11}$$

$$+\left(\frac{2\eta_6\eta_{13}}{\eta_6+\eta_{13}} + \frac{2\eta_{19}\eta_{12}}{\eta_{19}+\eta_{12}} + \eta_5 + \eta_{11}\right)y_{12} - \frac{2\eta_6\eta_{13}}{\eta_6+\eta_{13}}y_{14} + \frac{2\eta_{19}\eta_{12}}{\eta_{12}+\eta_{19}}y_{18} \qquad (8)$$

Now a matrix equation for the whole frame can be set up and solved; the equation for the simple frame shown in diagram 39 is shown in diagram 40.

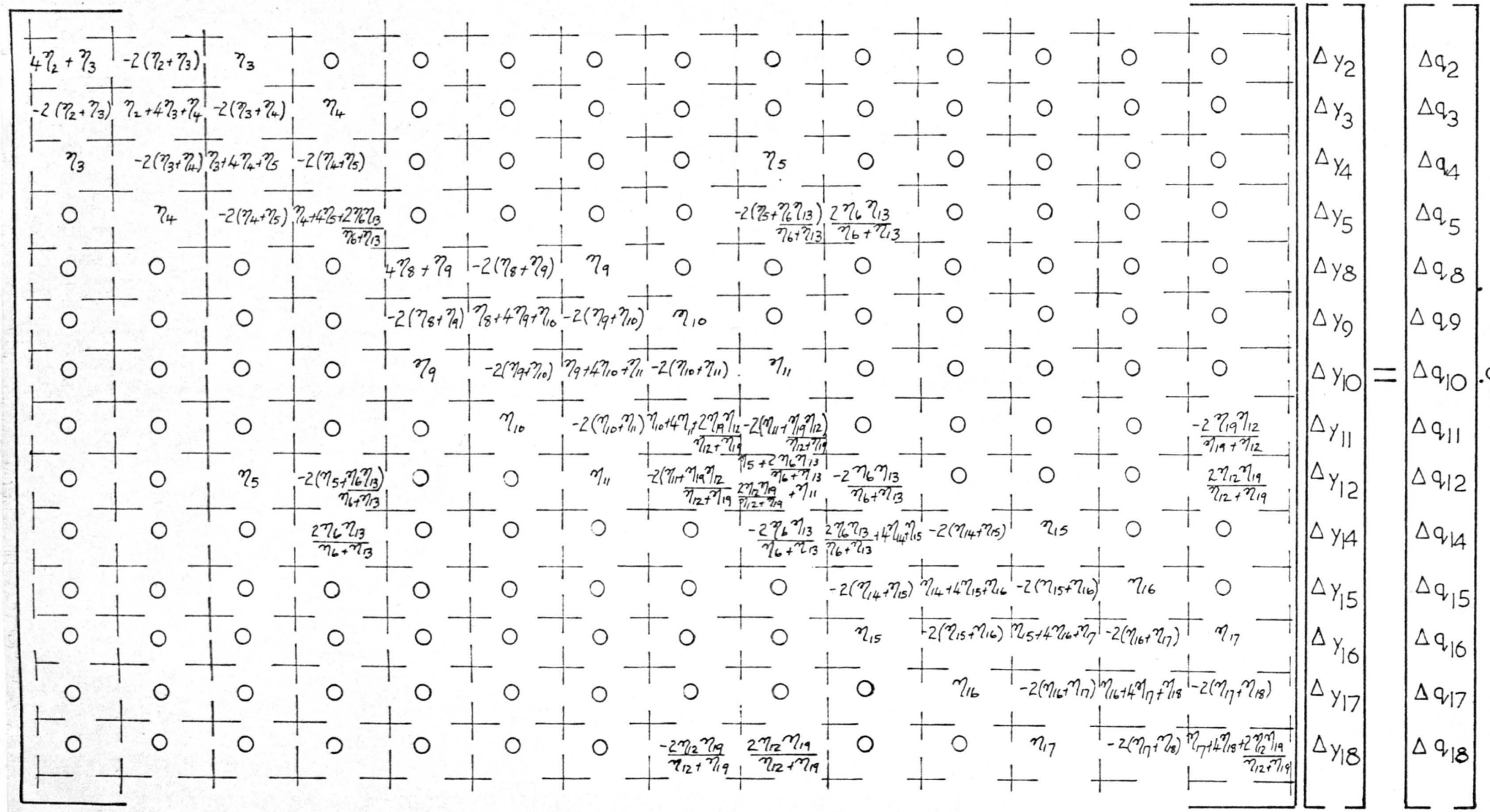

DIAGRAM 40: The Matrix Equation for a Typical Plane Frame

As during the continuous beam analysis, the load is applied incrementally by the computer to overcome the discontinuity in the moment curvature relationship. In frames, however, there is the additional complication that the cracking moment at a section is a function of the axial load at that section. During the frame analysis the assumption is made that the cracking moment for any load increment at every node is a function of the axial load present at that node after that particular load increment is applied. In other words, when the load increment has been applied and the deformation and moment fields computed, the axial load in each member is obtained using shear values calculated from the moment field. The cracking moment at every node is then computed and a search for new cracking performed. If new cracking is found then part of the load is removed using a similar procedure to that used in the continuous beam analysis until the load which produced the new cracking is located to a degree of accuracy defined during input. Consequently, it is essential during the frame analysis that the loads should be applied in small increments.

The influence of member shortening has been omitted from the discussion so far. However, it was realised that member shortening effects could be included quite accurately, by a "back door" method involving little extra work. Member axial forces must be calculated during loading owing to their influence on the cracking moments and a redistribution procedure to correct for incompatibility of slopes at joints is required for the sustained load analysis. Consequently member shortening during loading is included in the following way. After each increment of load the shortening of each member due to the increment in axial load and lateral deflection is calculated and the deformation field modified accordingly, neglecting the requirements of slope compatibility at the joints. The moment redistribution procedure is then used to remove slope incompatibilities. The consequent change in the moment field produces a change in the axial forces and a modification to the

member shortening, but this was found by trial to be negligible in practical circumstances. These effects are included before the search for cracking is performed, as shown in diagram 34.

Deformation under Sustained Load

Time effects are included in a manner similar to that used during continuous beam analysis; this involves each member of the frame deforming (including member shortening due to axial strains) for a small increment of time on the assumption that the force field is unchanged. Then the conditions of compatibility of slopes are checked at internal supports and boundaries. If slopes are found to be incompatible at any location changes in bending moment are introduced which correct for this without violating equilibrium conditions.

Using similar techniques to those used during continuous beam analysis, the deformation under constant force field is calculated using experimental moment curvature and axial load-deformation diagrams. This procedure induces errors in slope compatibility at joints and boundaries which are removed using the moment re-distribution procedure. In order to facilitate this the modified form of equation (5) for nodes adjacent to joints was developed for the four member joint shown in diagram 38. This is a general equation which can be reduced to give the equation for any node adjacent to 3 or 2 member joints by putting the appropriate η values to zero.

Approximately, by Taylor's theorem,

$$\Delta^r y_3 = \Delta^r y_4 - a\Delta^r\left(\frac{dy}{dx}\right)_4 + \frac{a^2}{2}\Delta^r\left(\frac{d^2y}{dx^2}\right)_4 \qquad \text{(i)}$$

$$\Delta^r y_{11} = \Delta^r y_{12} - a\Delta^r\left(\frac{dy}{dx}\right)_{12} + \frac{a^2}{2}\Delta^r\left(\frac{d^2y}{dx^2}\right)_{12} \qquad \text{(ii)}$$

$$\Delta^r y_6 = \Delta^r y_5 + a\Delta^r\left(\frac{dy}{dx}\right)_5 + \frac{a^2}{2}\Delta^r\left(\frac{d^2y}{dx^2}\right)_5 \qquad \text{(iii)}$$

$$\Delta^r y_{14} = \Delta^r y_{13} + a\Delta^r\left(\frac{dy}{dx}\right)_{13} + \frac{a^2}{2}\Delta^r\left(\frac{d^2y}{dx^2}\right)_{13} \qquad \text{(iv)}$$

In order to re-establish compatibility of slopes we require,

$$\Delta^{\circ}\left(\frac{dy}{dx}\right)_4 + \Delta^{r}\left(\frac{dy}{dx}\right)_4 = \Delta^{\circ}\left(\frac{dy}{dx}\right)_{12} + \Delta^{r}\left(\frac{dy}{dx}\right)_{12} = \Delta^{\circ}\left(\frac{dy}{dx}\right)_5 + \Delta^{r}\left(\frac{dy}{dx}\right)_5 = \Delta^{\circ}\left(\frac{dy}{dx}\right)_{13} + \Delta^{r}\left(\frac{dy}{dx}\right)_{13}$$

In order to preserve equilibrium we require,

$$\Delta^{r}M_4 + \Delta^{r}M_{12} - \Delta^{r}M_5 - \Delta^{r}M_{13} = 0$$

Multiplying (ii) by η_{12}, (iii) by η_5 and (iv) by η_{13}, forming equation (ii) - equation (iii) - equation (iv) and substituting using equilibrium and compatibility we obtain,

$$\eta_{12}\Delta^{r}y_{12} - \eta_5\Delta^{r}y_6 - \eta_{13}\Delta^{r}y_{14} = \eta_{12}\Delta^{r}y_{12} - \eta_5\Delta^{r}y_5 - \eta_{13}\Delta^{r}y_{13} - a\Big[\eta_{12}\left(\Delta^{\circ}\left(\frac{dy}{dx}\right)_4 - \Delta^{\circ}\left(\frac{dy}{dx}\right)_{12}\right)$$

$$+\eta_5\left(\Delta^{\circ}\left(\frac{dy}{dx}\right)_4 - \Delta^{\circ}\left(\frac{dy}{dx}\right)_5\right) + \eta_{13}\left(\Delta^{\circ}\left(\frac{dy}{dx}\right)_4 - \Delta^{\circ}\left(\frac{dy}{dx}\right)_{13}\right) - a\left(\eta_{12}+\eta_{13}+\eta_5\right)\Delta^{r}\left(\frac{dy}{dx}\right)_4\Big] - \frac{a^2}{2}\eta_4\Delta^{r}\left(\frac{d^2y}{dx^2}\right)_4$$

Making use of equation (i) to remove $\Delta^{r}\left(\frac{dy}{dx}\right)_4$ and defining

$$\psi_4 = \eta_{12}\Delta^{\circ}\left(\frac{dy}{dx}\right)_{12} + \eta_5\Delta^{\circ}\left(\frac{dy}{dx}\right)_5 + \eta_{13}\Delta^{\circ}\left(\frac{dy}{dx}\right)_{13} - \left(\eta_{12}+\eta_5+\eta_{13}\right)\Delta^{\circ}\left(\frac{dy}{dx}\right)_4$$

we obtain,

$$\Delta^{r}\left(\frac{d^2y}{dx^2}\right)_4 = \frac{2}{a^2\left(\eta_4+\eta_5+\eta_{12}+\eta_{13}\right)}\Big[a\psi_4 + \left(\eta_5+\eta_{12}+\eta_{13}\right)\left(\Delta^{r}y_3 - \Delta^{r}y_4\right) + \eta_5\left(\Delta^{r}y_6 - \Delta^{r}y_5\right)$$

$$+\eta_{12}\left(\Delta^{r}y_{12} - \Delta^{r}y_{11}\right) + \eta_{13}\left(\Delta^{r}y_{14} - \Delta^{r}y_{13}\right)\Big] \qquad (9)$$

Now $$0 = -\frac{1}{a^2}\left[\Delta^{r}M_2 - 2\Delta^{r}M_3 + \Delta^{r}M_4\right] = \frac{1}{a^2}\left[\eta_{12}\Delta^{r}\left(\frac{d^2y}{dx^2}\right)_2 - 2\eta_{13}\Delta^{r}\left(\frac{d^2y}{dx^2}\right)_3 + \eta_4\Delta^{r}\left(\frac{d^2y}{dx^2}\right)_4\right]$$

Now we require $\Delta^{r}y_8 - \Delta^{r}y_9 = 0$ and $\Delta^{r}y_4 = \Delta^{r}y_5$

Substituting and rearranging,

$$\frac{-2a\eta_4\psi_4}{\eta_4+\eta_5+\eta_{12}+\eta_{13}} = \eta_2\Delta^{r}y_1 - 2\left(\eta_2+\eta_3\right)\Delta^{r}y_2 + \left(\eta_2 + 4\eta_3 + 2\eta_4\frac{\left(\eta_5+\eta_{12}+\eta_{13}\right)}{\eta_4+\eta_5+\eta_{12}+\eta_{13}}\right)\Delta^{r}y_3$$

$$-2\left(\eta_3 + \frac{\eta_4\left(\eta_{12}+2\eta_5+\eta_{13}\right)}{\eta_4+\eta_5+\eta_{12}+\eta_{13}}\right)\Delta^{r}y_4 + \frac{2\eta_4\eta_5}{\eta_4+\eta_5+\eta_{12}+\eta_{13}}\Delta^{r}y_6 - \frac{2\eta_{12}\eta_4}{\eta_4+\eta_5+\eta_{12}+\eta_{13}}\Delta^{r}y_{11} + \frac{2\eta_{13}\eta_4}{\eta_4+\eta_5+\eta_{12}+\eta_{13}}\Delta^{r}y_{14} \qquad (10)$$

In addition, a further moment redistribution equation is required because of the possibility of sidesway. This equation is now developed for the simple frame shown in diagram 39.

Approximately by Taylor's theorem,

$$\Delta' M_5 = \Delta' M_6 - a\,\Delta'\left(\frac{dM}{dx}\right)_6 + \frac{a^2}{2}\Delta'\left(\frac{d^2M}{dx^2}\right)_6$$

$$\Delta' M_{11} = \Delta' M_{12} - a\,\Delta'\left(\frac{dM}{dx}\right)_{12} + \frac{a^2}{2}\Delta'\left(\frac{d^2M}{dx^2}\right)_{12}$$

In order that horizontal equilibrium of the beam may be preserved,

$$\Delta\left(\frac{dM}{dx}\right)_6 + \Delta\left(\frac{dM}{dx}\right)_{12} = 0 \qquad \text{and also} \qquad \Delta'\left(\frac{d^2M}{dx^2}\right)_6 = \Delta'\left(\frac{d^2M}{dx^2}\right)_{12} = 0$$

Thus $\Delta' M_5 + \Delta' M_{11} = \Delta' M_6 + \Delta' M_{12}$

Now we require $\Delta' y_6 = \Delta' y_{14}$ and by substitution utilising equation 9.

$$\frac{2a\eta_6\psi_6}{\eta_6+\eta_{13}} + \frac{2a\eta_{12}\psi_{14}}{\eta_{12}+\eta_{19}} = \eta_5\Delta' y_4 - 2\left(\eta_5 + \frac{\eta_6\eta_{13}}{\eta_6+\eta_{13}}\right)\Delta' y_5 + \eta_{11}\Delta' y_{10} - 2\left(\eta_{11} + \frac{\eta_{12}\eta_{19}}{\eta_{12}+\eta_{19}}\right)\Delta' y_{11}$$

$$+\left(\eta_5 + \frac{2\eta_6\eta_{13}}{\eta_6+\eta_{13}} + \eta_{11} + \frac{2\eta_{12}\eta_{19}}{\eta_{12}+\eta_{19}}\right)\Delta' y_{12} - \frac{2\eta_6\eta_{13}}{\eta_6+\eta_{13}}\Delta' y_{14} + \frac{2\eta_{12}\eta_{19}}{\eta_{12}+\eta_{19}}\Delta' y_{18}$$

where ψ_6 and ψ_{14} are defined analogously to ψ_4 in equation (10) namely,

$$\psi_6 = \eta_{13}\left(\Delta^\circ\left(\frac{dy}{dx}\right)_{13} - \Delta^\circ\left(\frac{dy}{dx}\right)_6\right)$$

$$\psi_{14} = \eta_9\left(\Delta^\circ\left(\frac{dy}{dx}\right)_{19} - \Delta^\circ\left(\frac{dy}{dx}\right)_{12}\right)$$

Using the above equations, a matrix equation can be set up for a plane frame in terms of the nodal flexural rigidities, the slope errors produced during deformation under constant moment and the deflection changes required to re-establish compatibility of slopes without destroying equilibrium. The equation for the simple frame shown in diagram 39 is shown in diagram 41. The similarity between this equation and that shown in diagram 40 should be noted. Thus by setting up and solving the matrix equation shown in diagram 41 the computer obtains the deflection changes required to re-establish compatibility of slopes, then the corresponding curvature and moment changes are calculated. The change in the moment field produces changes in member

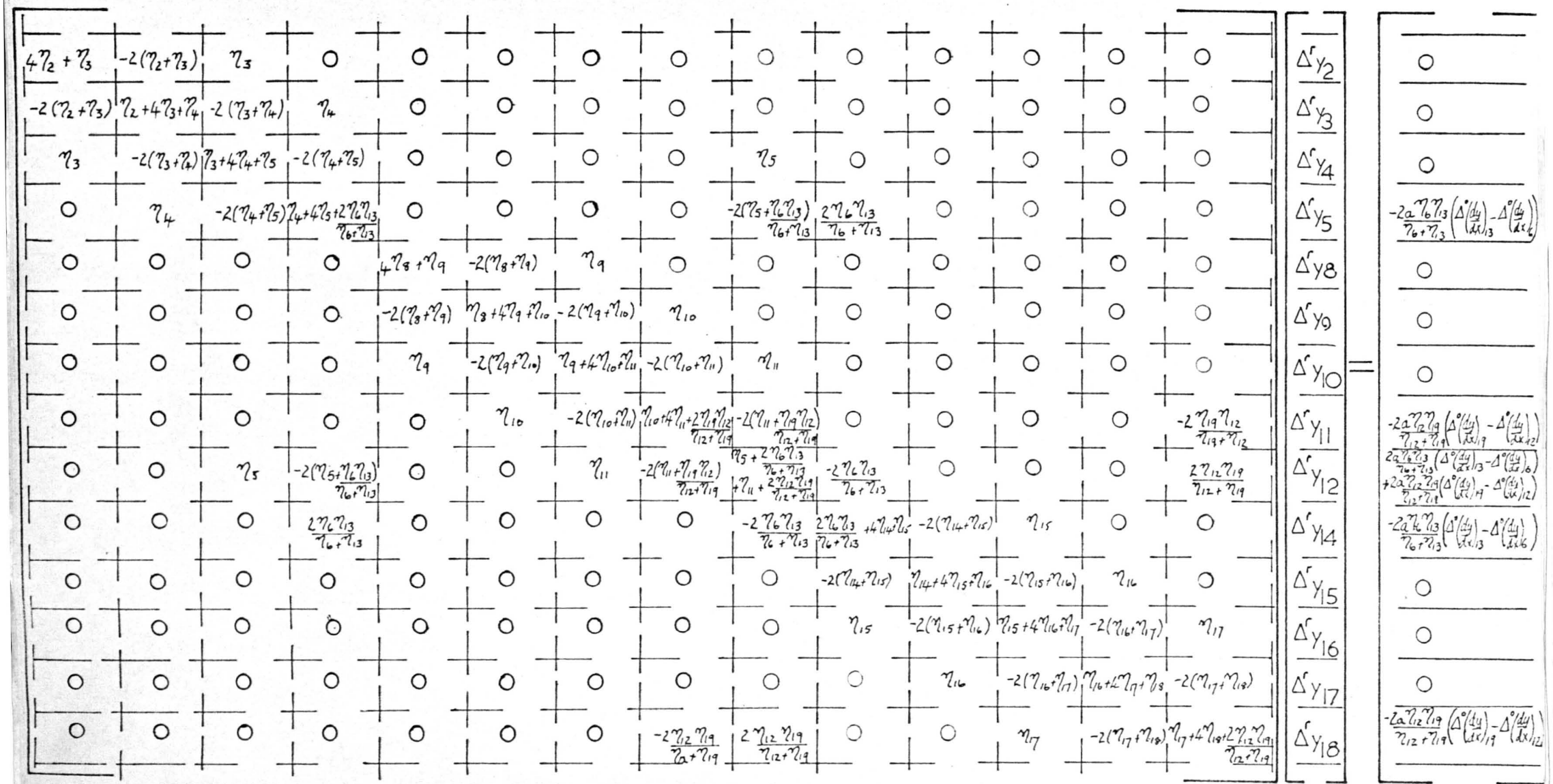

DIAGRAM 41: Moment Redistribution Equation for a Typical Frame

axial forces and, consequently, member shortening but these effects were found by trial to be small in practical circumstances. The frame is then examined to determine whether the moment changes have caused the moment at any previously uncracked nodes to exceed the cracking moment; if so, the flexural rigidity at these nodes is modified to the "after cracking" value.

Now that the complete force and deformation fields are known the next time increment is performed in an identical manner.

PART 4: DISCUSSION

A. Creep in Plain Concrete

(i) Comparison of experimental results and theory.

The experimental results obtained on the plain concrete specimens CB1, CC1, CB3, CC3 are shown in diagram 42; the log of the total time strain (creep plus shrinkage) is plotted against log of the time from loading. The data can be seen to have a bi-linear form with a discontinuity at a time between 100 and 200 days from loading. The smaller specimens (CC1 and CC3) show slightly greater strains at all times than the larger specimens under the same sustained stress. However reference to table 5 will show that the companion unloaded shrinkage specimens (CB2 and CC2) have approximately equal free shrinkage strains measured from 28 days after casting. It is well known that in general small specimens shrink more rapidly and have higher ultimate free shrinkage strains than large specimens. However, this effect occurs during the first week or two after casting and is therefore not apparent in this case. The total time strain is plotted in diagram 42 since this has much more physical meaning than the total strain minus free shrinkage. The separation of the total time strain into two components has advantages from the design point of view, however when considering the fundamental mechanisms of time dependent deformation this division is arbitary and confusing. In this investigation, since the age at loading is 28 days, the free shrinkage strains are fairly small relative to the total time strain and whether or not they are subtracted from the total strain does not greatly affect the form of the strain-time relationship.

There is one other feature of the plain concrete experimental results which requires comment. The strain on removal of load was significantly larger (on average 30%) than the strain on application of the load. This contradicts the usual argument that ageing of the concrete whilst under

DIAGRAM 42: Time Strains in specimen CB1, CC1, CB2, CC2

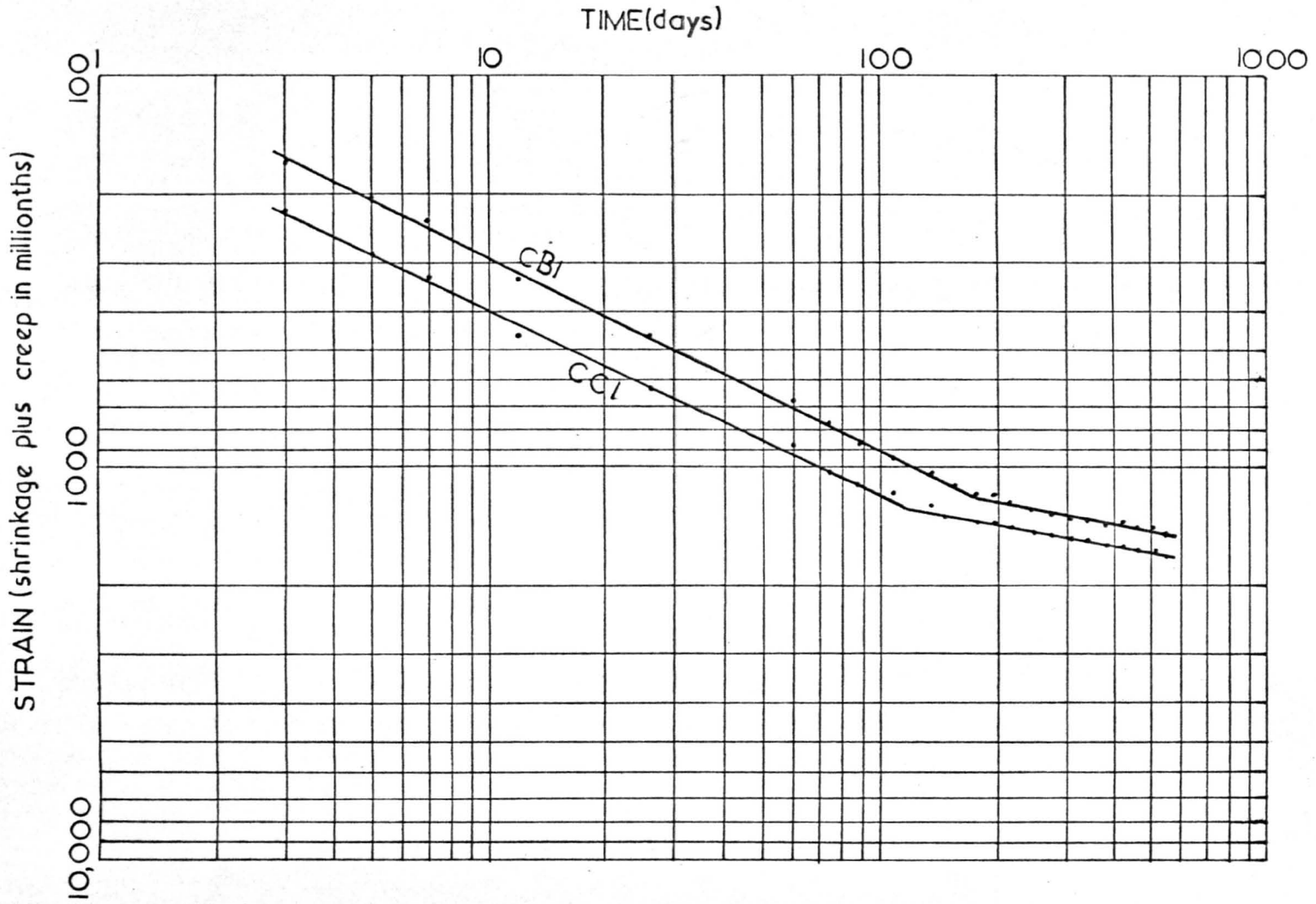

DIAGRAM 42: continued

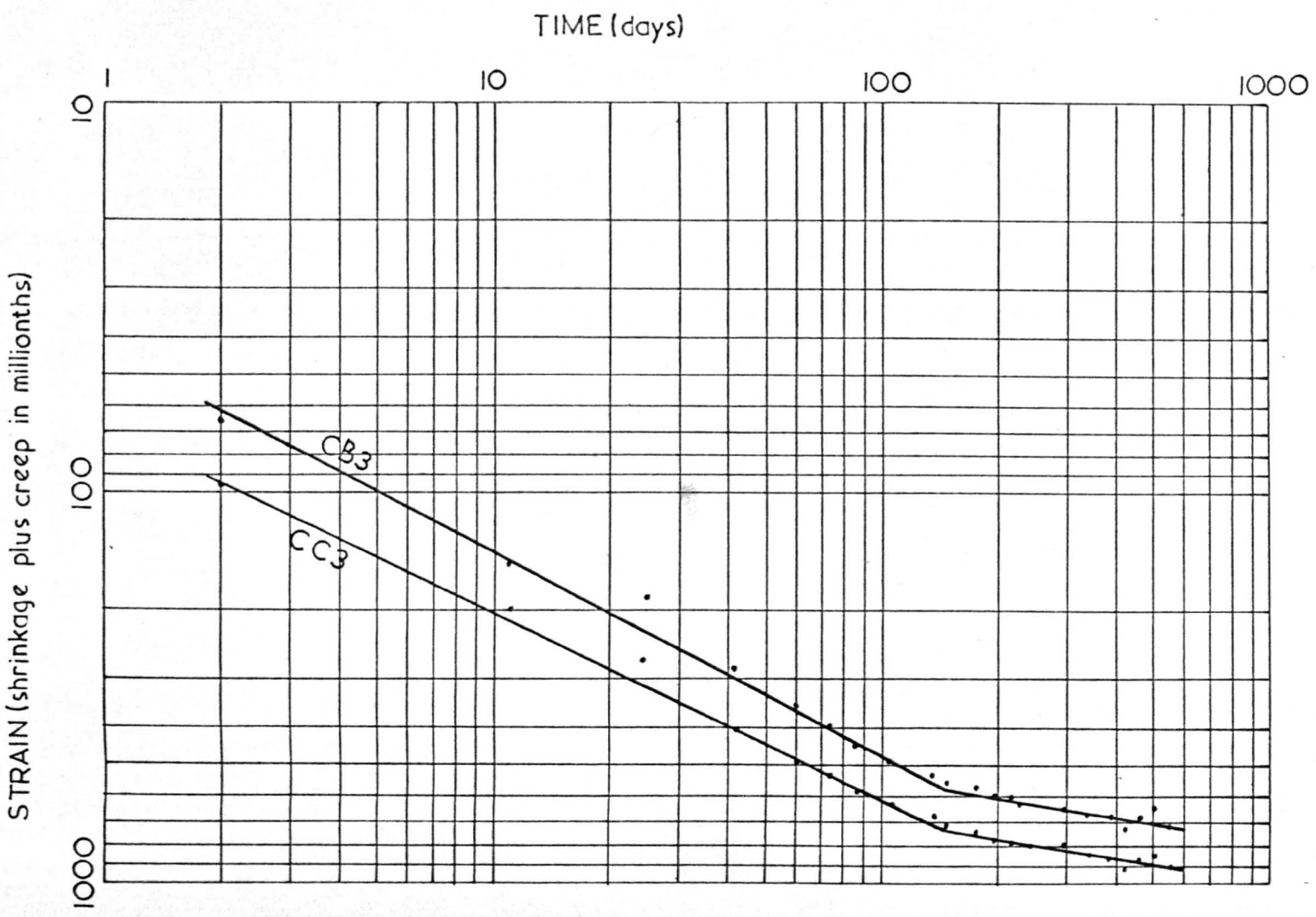

sustained load causes the instantaneous recovery to be slightly less than the strain on loading. However, this type of result was also obtained by Freudenthal and Roll (22). Their results, for 1/6 concrete under service stresses, show the modulus of elasticity of 75 x 250 mm cylinders deduced from the strain on removal of sustained load of about 200 days duration to be on average about 21% less than the modulus of elasticity at the time of loading measured on 150 x 300 mm cylinders. Freudenthal and Roll define the modulus of elasticity in the conventional manner as the slope of a secant of the stress strain curve. The results of Freudenthal and Roll show the effect to be more marked with smaller specimens and consequently they associated it with the rapid drying of small pieces of concrete. However, it is well known that the response of reinforced concrete to the removal of sustained load is frequently much greater than the response on first loading. This applies to members in bending and members in combined bending and axial load and affects both the curvature and the axial strain. The results of table 7 and table 10 confirm this. In reinforced concrete, the explanation is usually that creep of concrete in compression has led to a build-up of stress in the steel reinforcement and a decrease in stress in the concrete. On removal of load, the elastic response of the steel places the concrete in tension. Owing to the low tensile strength of the concrete cracking occurs and the reduction in stiffness causes a larger strain on removal of load than on application of load when the concrete was fully operative in compression. For members cracked in bending there is the additional factor that on removal of load the two faces of each crack will not match completely and compression is induced across the crack with a balancing tension in what was formerly the compression zone of the member. This causes a tendency for the cracks to spread across the full cross section of the member on removal of load. This behaviour was observed on specimens B4, B5 and B6. The cracking of columns on the removal of load was observed by Glanville and Thomas and the spread of cracking was also

observed during this investigation on specimens C4 and C6 following the removal of load. It is generally accepted that under sustained load on plain concrete there is a gradual transfer of stress from a viscous phase to a more elastic solid phase with consequent reduction of stress on the viscous phase and increase in stress on the solid phase. On removal of load therefore it is reasonable to expect the viscous phase to be subjected to tension. If the viscous phase can withstand this tension without significant cracking then the response to load removal will be approximately equal to the response to load application and there will be some time dependent recovery as the viscous phase creeps in tension. If, however, the viscous phase cracks in tension there will be a loss of stiffness resulting in a greater strain on removal of load than on load application; this would be followed by only a small amount of creep recovery. This mechanism is analogous to that which occurs in reinforced concrete and would explain both the high strain of the plain concrete specimens on removal of sustained load and the small amount of creep recovery.

A search was performed for data from other investigations in order to obtain further confirmation of the linear relationship between log total time strain and log time. Unfortunately, in most publications the data is presented graphically on quite small scale diagrams; this is inadequate as the small scale and distortions produced by printing make the data unreliable. However, Glanville (10) tabulated data from creep investigations on concrete under sustained stresses in the service stress range. Part of this data is shown in diagram 43, and the marked linearity is evident. Remembering that the relationship is defined by $\text{Log}\,\epsilon_c = \text{Log}\,A + n\text{Log}\,t$, diagrams 42 and 43 show that the influence of stress on the value of A is very marked and diagram 43 shows that the value of n (given by the gradient of the line) is slightly influenced by stress. Experimental data due to Stevens and Bryden-Smith (42) was also available and is shown in

DIAGRAM 43: Time Strains in Plain Concrete after Glanville (10)

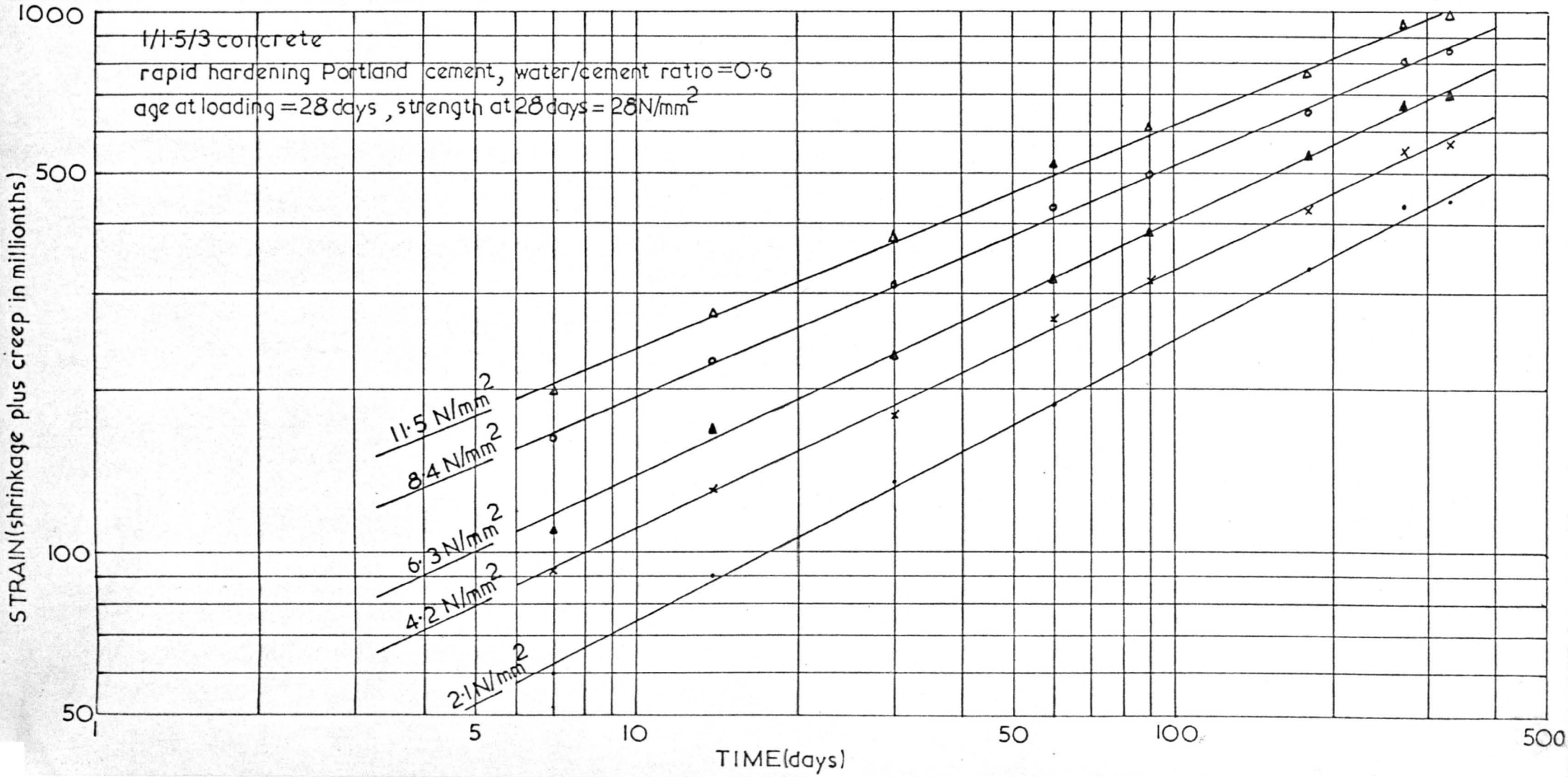

diagram 44. There is evidence of a discontinuity in this data but the investigation was not continued long enough for the data to be conclusive.

(ii) Discussion of other theories.

Creep data is normally shown on a hyperbolic plot following Ross (13). The hyperbolic relationship is purely empirical and is the result of a curve fitting exercise. Ross points out that it gives a good fit to creep data in the later stages and has the practical advantage that it gives a finite limiting value for strain at infinite time. The equation is usually shown in the form $\epsilon_c = \frac{t}{a+bt}$

where a and b are constants. This can be rearranged to give

$$a + bt = \frac{t}{\epsilon_c}$$

consequently if $\frac{t}{\epsilon_c}$ is plotted against t a straight line should result and the values of a and b can be determined from this plot. This technique was applied to the data of this investigation and the result for specimen CB1 is shown in diagram 45. The relation can be seen to be very linear from 60 days onwards and consequently a hyperbolic relation gives a good fit to the later stages of the deformation. However, it must not be overlooked that the form of hyperbolic plot proposed by Ross and shown in diagram 45 is deceptive in that it concentrates the part of the data which is a poor fit into a small area of the graph. Almost half the time strain measured over 18 months on CB1 occurs in the first 60 days as reference to table 5 will show. Consequently the hyperbolic plot gives a very poor fit over the first half of the creep process for specimen CB1. However, the practical value of the hyperbolic plot in estimating a limiting value for creep can also be seen in diagram 45. In short, the hyperbolic relation is purely empirical and gives a good fit to creep data in the later stages. Now, consider proposed power law relationship $\epsilon_c = At^n$,

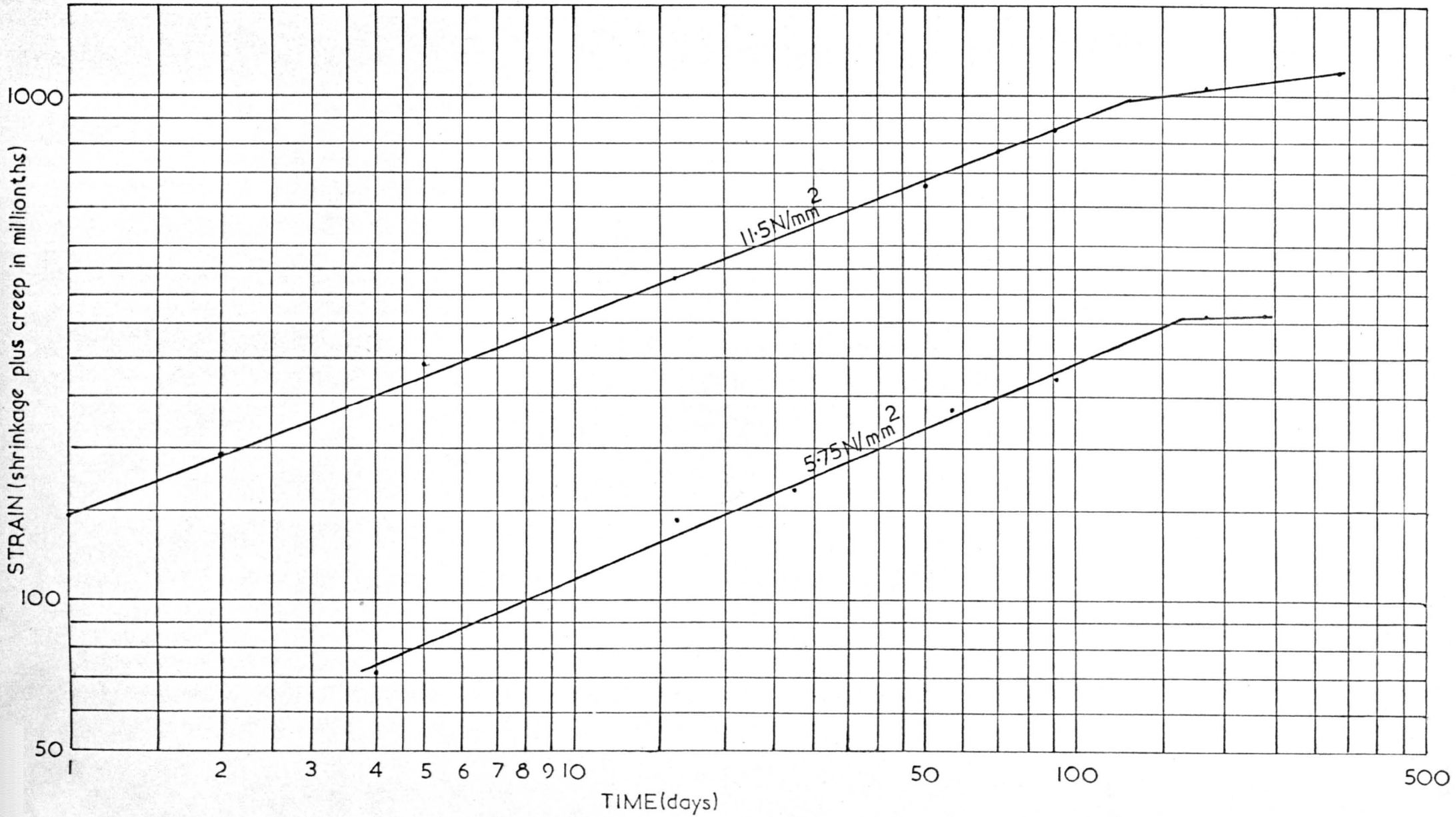

DIAGRAM 44: Time Strains in Plain Concrete after Stevens and Bryden-Smith (42)

DIAGRAM 45: Hyperbolic Plot of Data From CB1

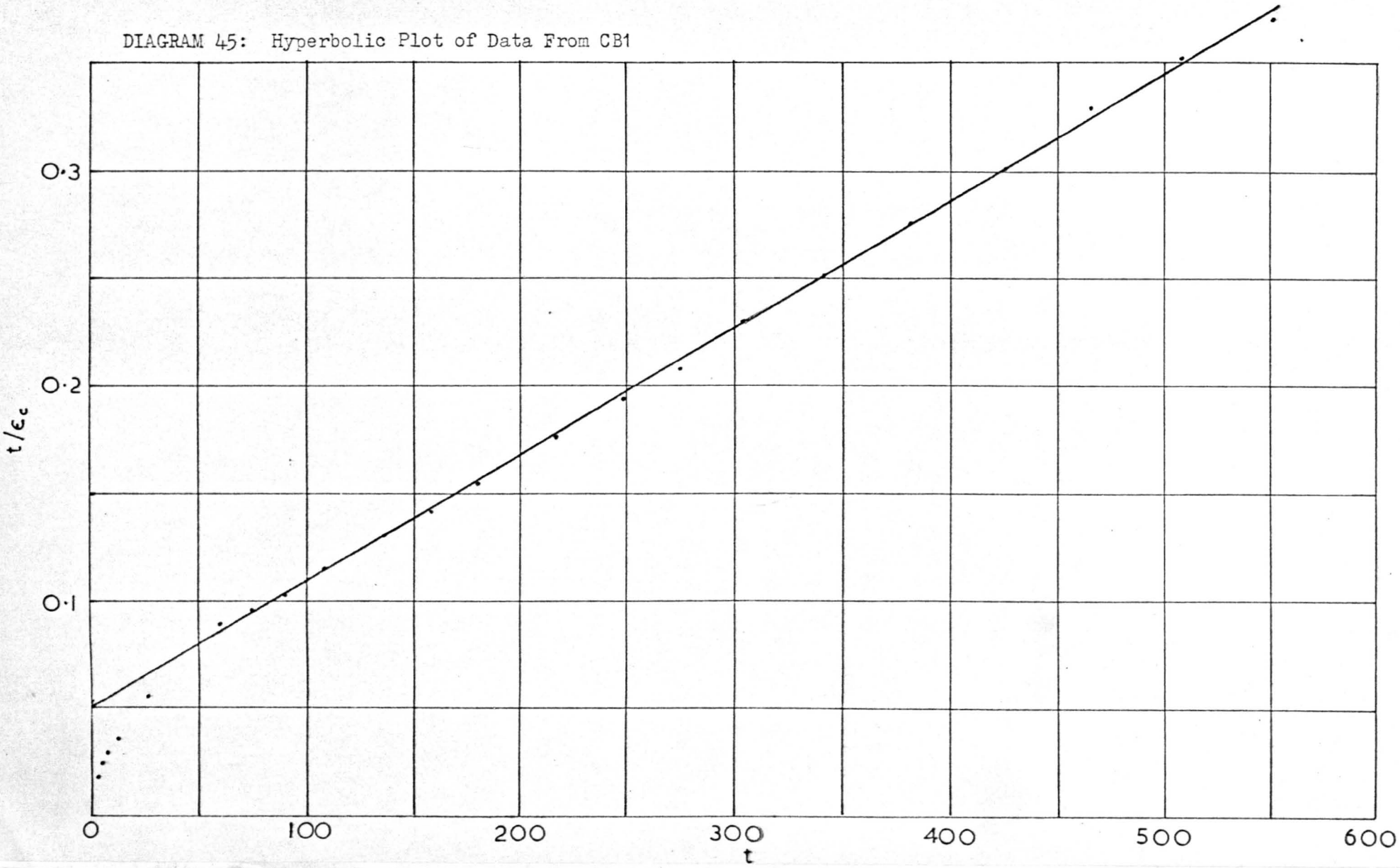

taking logs, $\text{Log}\,\epsilon_c = \text{Log}\,A + n\,\text{Log}\,t$

and rearranging, $\text{Log}\,\epsilon_c = \text{Log}\,A + \text{Log}\,t - (1-n)\,\text{Log}$

$$\therefore \text{Log}\,\epsilon_c = \text{Log}\,A + \text{Log}\,t - \text{Log}\,t^{(1-n)}$$

Now, for large values of t the function $t^{(1-n)}$ tends to become linear and can be replaced by $a'+b't$, where a' and b' are constants.

Thus $\text{Log}\,\epsilon_c = \text{Log}\,A + \text{Log}\,t - \text{Log}\,(a'+b't)$

$$= \text{Log}\,A + \log\frac{t}{a'+b't} = \text{Log}\,\frac{At}{a'+b't}$$

$$\therefore \quad \epsilon_c = \frac{At}{a'+b't} = \frac{t}{a+bt}$$

Consequently for large values of t the relationship $\epsilon_c = At^n$ tends to the hyperbolic form proposed by Ross.

The hyperbolic relationship of diagram 45 and the log-log relationship of diagram 42 were converted back to natural scales and are compared with the experimental data in diagram 46.

At first sight the hyperbolic relationship may seem more simple than the proposed power law. However this is not the case when the underlying mechanisms are considered. For example the differential form of the power law is well known to be $\frac{d\epsilon_c}{\epsilon_c} = n\frac{dt}{t}$. This implies that the rate of change at any time is a linear function of the state of affairs at that time. Now it is not so well known that the differential form of the hyperbolic relationship is $\frac{d\epsilon_c}{\epsilon_c^2} = a\frac{dt}{t^2}$. This implies that the rate of change at any time is a non linear function of the state of affairs at that time. Consequently any claim which the hyperbolic plot may make to simplicity is certainly unfounded at the fundamental level.

DIAGRAM 46: Comparison of Power Law and Hyperbolic Analysis

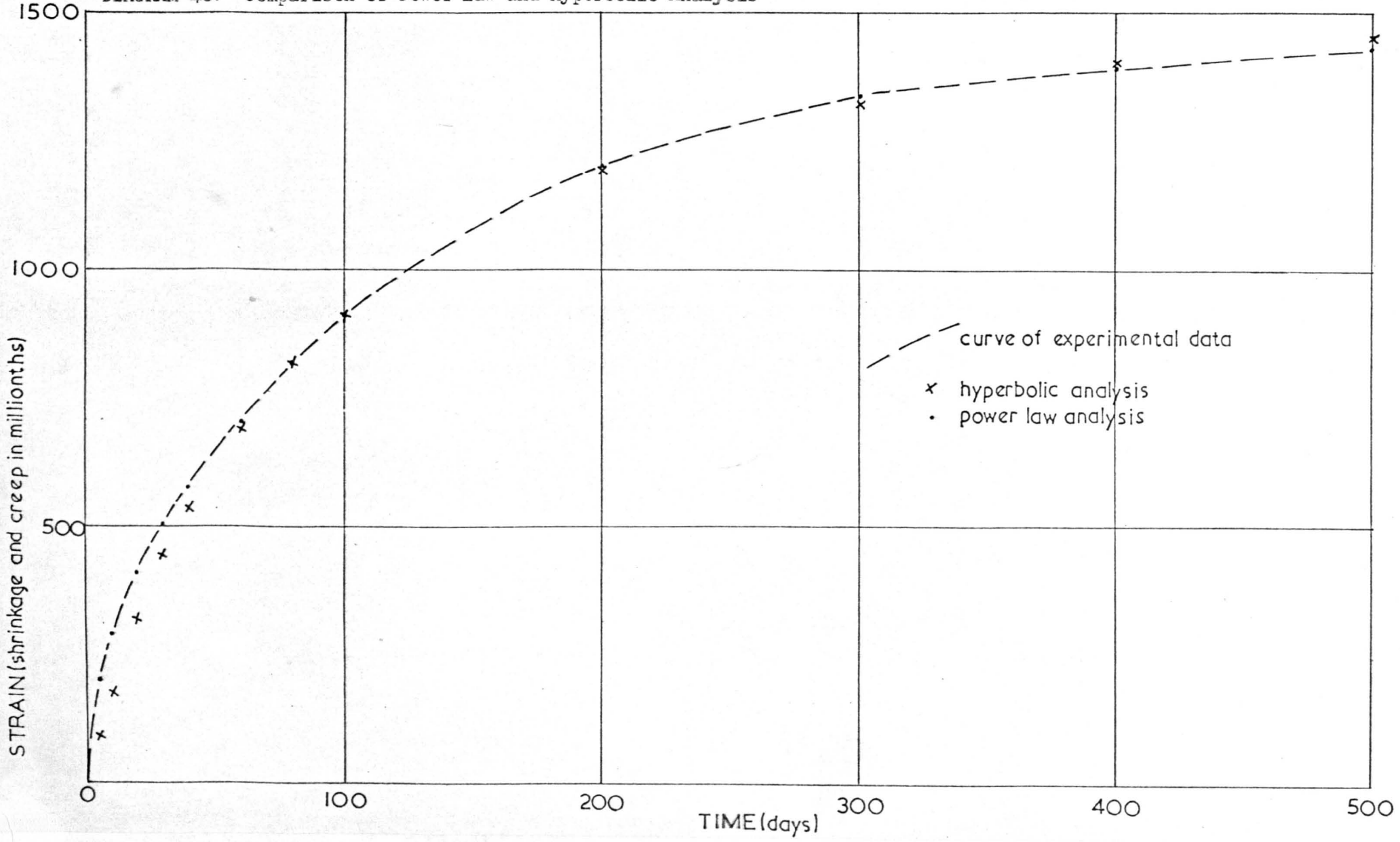

Creep data is also quite often treated by plotting ϵ_c against log t ; this is called the semi-log plot and sometimes yields a straight line. However the semi-log plot can be shown to be only a special case of the more general power law (or log-log plot). In part 3 the cumulate frequency of energy barriers (shown in diagram 47) was shown to be

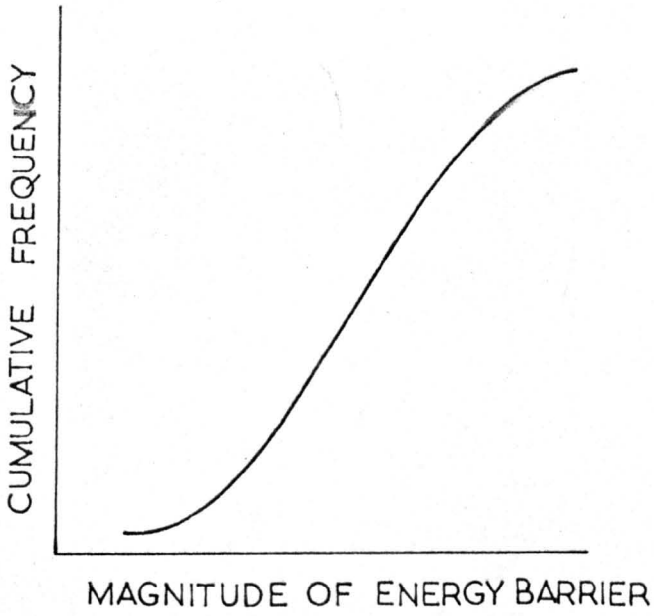

DIAGRAM 47: Cumulative Frequency Curve

exponential for low magnitudes of barrier. However, over a short range this can be approximated to a straight line and diagram 47 shows that when barriers of greater magnitude become involved this approximation holds over a much greater range. Consequently we can say that approximately $F = mQ + c$ where m and c are constants.

Thus $\frac{dF}{dQ} = m$ Now $\frac{d\epsilon_c}{dt} = K\frac{dF}{dQ}\Big/\frac{dt}{dQ} = \frac{KmkT}{t}$

Thus integrating $\epsilon_c = KmkT\log t + B$

and rearranging $\epsilon_c = A\log t + B$

where A and B are constants for a given temperature and stress.

Consequently it can be seen that the log-log relation approximates to a

semi-log relation over fairly short ranges. The experimental data from specimen CB1 is shown on a semi log plot in diagram 48.

(iii) Discussion of proposed strain-time relationship.

There are a number of assumptions made during the derivation of the strain-time relationship which merit further discussion.

The assumption of a normal distribution of energy barriers within the material was made on the basis that this appears the most likely form in a very random material such as concrete. It must be emphasised that the energy barrier distribution is not the same thing as the energy distribution. However, it should be noted that the same conclusion is reached with any assumed energy barrier distribution provided that the distribution has an exponential tail. In short, a skew energy barrier distribution would yield the same result provided it has an exponential tail.

Also, it was assumed that the deformation produced when an energy barrier is overcome is independent of the magnitude of the barrier. This assumption is reasonable because the deformation depends not on the barrier which is overcome but on the remaining structure. When a barrier is overcome load is shed to the remaining structure which deforms producing creep. Now, provided the number of particles which move during creep is small relative to the total number, the deformation characteristics of the structure will remain unaltered as the barriers break down. Consequently, on average the deformation produced when an energy barrier breaks is independent of the magnitude of that barrier.

It has been assumed that all barriers of a particular magnitude are overcome at the same time. This is clearly not strictly true as, owing to the

DIAGRAM 48: Experimental Data for Specimen CB1

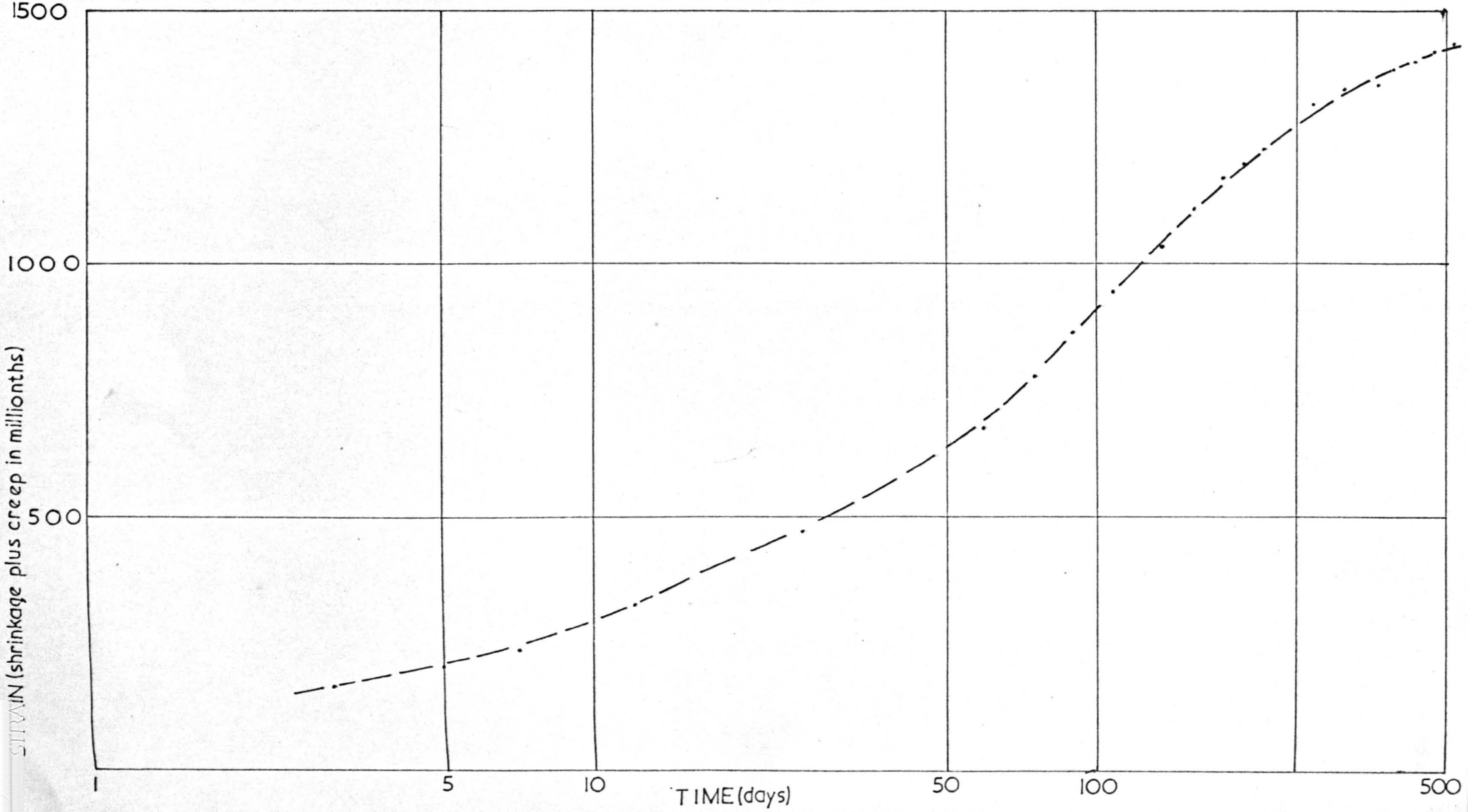

random nature of the energy fluctuations, some barriers of a particular magnitude will be overcome before the average time and some after. However it seems reasonable to assume that all barriers of a particular magnitude may be considered to be overcome at the average time and this greatly simplifies the mathematics.

There is, of course, nothing new in plotting creep data in the form shown in diagram 42. This was first proposed by Shank in the 1930's (13). However the concept of discontinuities has not been considered before and it is felt that these discontinuities have previously disguised the underlying strain-time relationship. Clearly, a lot of accurate data is required in order to show the presence of discontinuities; if the data is sparse the relationship will appear as a curve. The theoretical arguments from which the log-log relationship was derived have not previously been applied to creep in concrete, however, a similar approach was proposed, but apparently not pursued, by Best and Polivka in 1959 working under Dorn at the University of California (43).

B. Moment-Curvature Relationships

(i) Beam section.

The expected bi-linear form was obtained and the experiments confirmed that, for practical purposes, the relationship remains bi-linear under sustained moment. The discontinuity at cracking gradually become more marked under sustained load as can be seen in diagram 8. The relationship immediately after loading is clearly bi-linear and if this were approximated by any method to a single straight line, for the purpose of deflection calculations during design, appreciable error would result. However, the calculation of short term deflection on a bi-linear moment curvature diagram is a complex operation and it is often argued that it is unwise to take account of the uncracked lengths of member, since in practice restrained shrinkage, imperfect compaction of concrete or small overloads during construction may cause cracking at theoretically uncracked sections. It is the long term deflection which is usually most important and diagram 8 shows that the bi-linear form of the relationship becomes much less marked under sustained load. Clearly after only 30 days of sustained load the relationship could be approximated to a single straight line for design purposes without any serious error and this is also true after 547 days of sustained load.

It had been anticipated that there would be a greater rate of increase in curvature in an uncracked section than in a cracked section per unit moment. This was certainly true during the first few weeks of sustained load but by 547 days the cracked section curvatures had increased slightly more, per unit moment, than the uncracked values. It should be noted that the change in the relationship for uncracked sections during the first 30 days of sustained load is almost entirely a change in gradient, and therefore a creep effect. However, the change during the remaining period of sustained

load is almost independent of moment which suggests that it is a shrinkage effect. For cracked sections the change in the relationship over the entire period of sustained load is remarkable in that it is only slightly dependent on the value of the sustained moment; this again suggests that shrinkage played a large part although it is hard to imagine that such large curvature changes could be due to shrinkage. It was pointed out earlier that shrinkage effects in a cracked beam may be large as in the tension zone the concrete between cracks shrinks into itself and widens the cracks but does not tend to shorten the member whereas shrinkage in the compression zone shortens the compression face and causes warping. Another possible explanation is that cracking is equivalent to a shift of origin so that the deformation under sustained moment is proportional to moment, but moment measured from a new origin. This idea is consistent with the rather odd behaviour of reinforced concrete on unloading which can now be seen as part of a large hysteresis loop.

On removal of load, most specimens showed a significantly greater immediate response than occurred on application of load. For example, the specimen subjected to the service moment gave a curvature of 4.103×10^{-6} mm^{-1} on application of load but the response on load removal was 5.974×10^{-6} mm^{-1}.

(ii) Column section

The relationship has been taken as bi-linear (diagram 11) and in this case the rate of increase in curvature of the uncracked sections is greater than that for cracked sections (per unit moment). However it should be remembered that the cracked section specimens had been subjected to previous loading at a moment below the cracking moment and this, no doubt, reduced the amount of creep on later loading.

When a section under increasing pure moment reaches its cracking moment a stable crack pattern is established almost immediately and there is only a small amount of spread of cracking, (diagram 9). In the case of a section under axial load and bending moment diagram 12 shows that the extent of cracking is very dependent on moment. This behaviour must produce some non-linearity in the moment-curvature relationship after cracking but the experimental data is not sufficiently accurate to reflect this.

On removal of load most specimens showed a significantly greater response than occurred on application of load. For example, the specimen subjected to the service moment gave a curvature of 2.789×10^{-6} mm^{-1} on application of load but the response to load removal was 4.567×10^{-6} mm^{-1}.

C. Full Scale Structures

(i) Frame 1

The deflection of the upper beam immediately after loading was 13.72 mm (span/555) and this increased to 26.85 mm (span/284) after 18 months of sustained load. The computer analysis based on the experimental pure moment data gave a value of 11.41 mm (approximately 17% error) for immediately after loading and 22.06 mm (approximately 22% error) after 18 months of sustained load, see diagrams 49, 50 and 51.

The deflection of the lower beam immediately after loading was 15.82 mm (span/482) and this increased to 29.27 mm (span/260) after 18 months of sustained load. The computer analysis gave a value of 12.35 mm (approximately 22% error) for immediately after loading and 22.01 mm (approximately 25% error) after 18 months of sustained load (diagram 36).

For the upper beam these figures should be compared with the deflection of 5.9 mm calculated using the concrete section flexural rigidity and 13.8 mm calculated using the cracked transformed flexural rigidity. For the lower beam the deflection calculated using the concrete section flexural rigidity was 6.2 mm and the deflection calculated using the cracked transformed flexural rigidity was 14.4 mm.

The agreement between theory and experiment is poor, much worse than for the other full scale structures. The reason for this can be seen in diagram 14. The marked influence of shear on cracking in flexure is apparent together with local cracking around the joints; the theoretical analysis completely neglected the influence of shear. In frame 1 under sustained load the service moment was achieved (approximately) at both the midspan

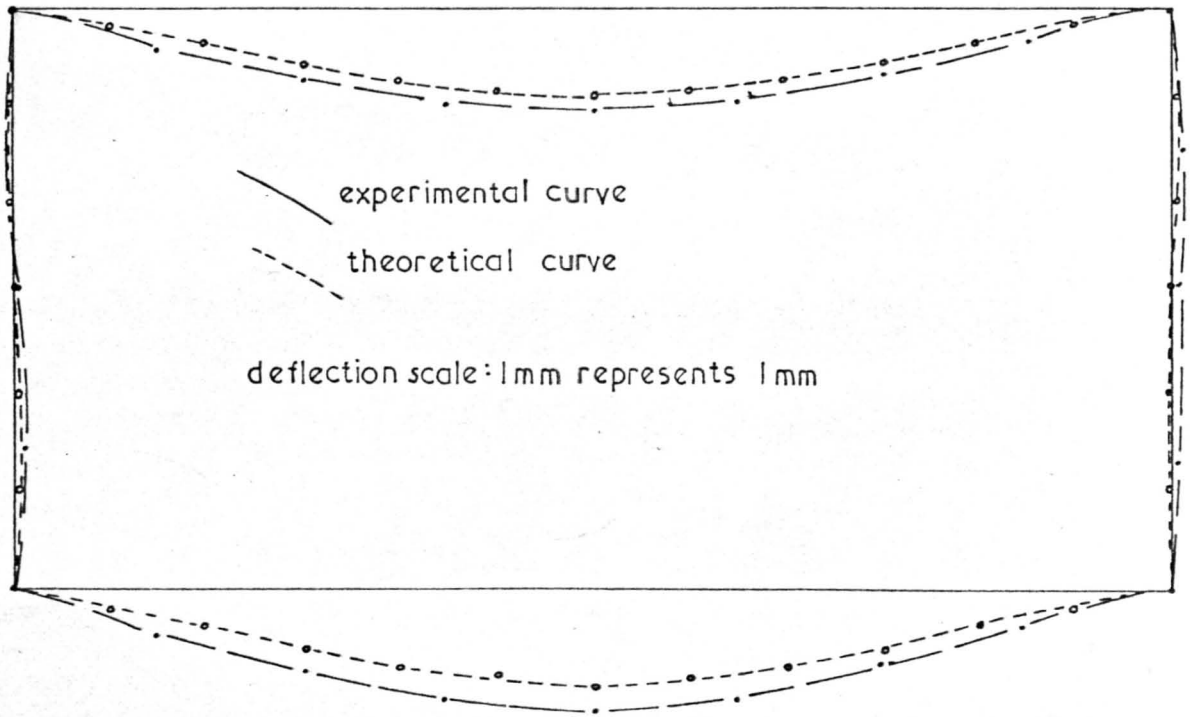

DIAGRAM 49: Deflection Profile of Frame 1 Immediately after Loading

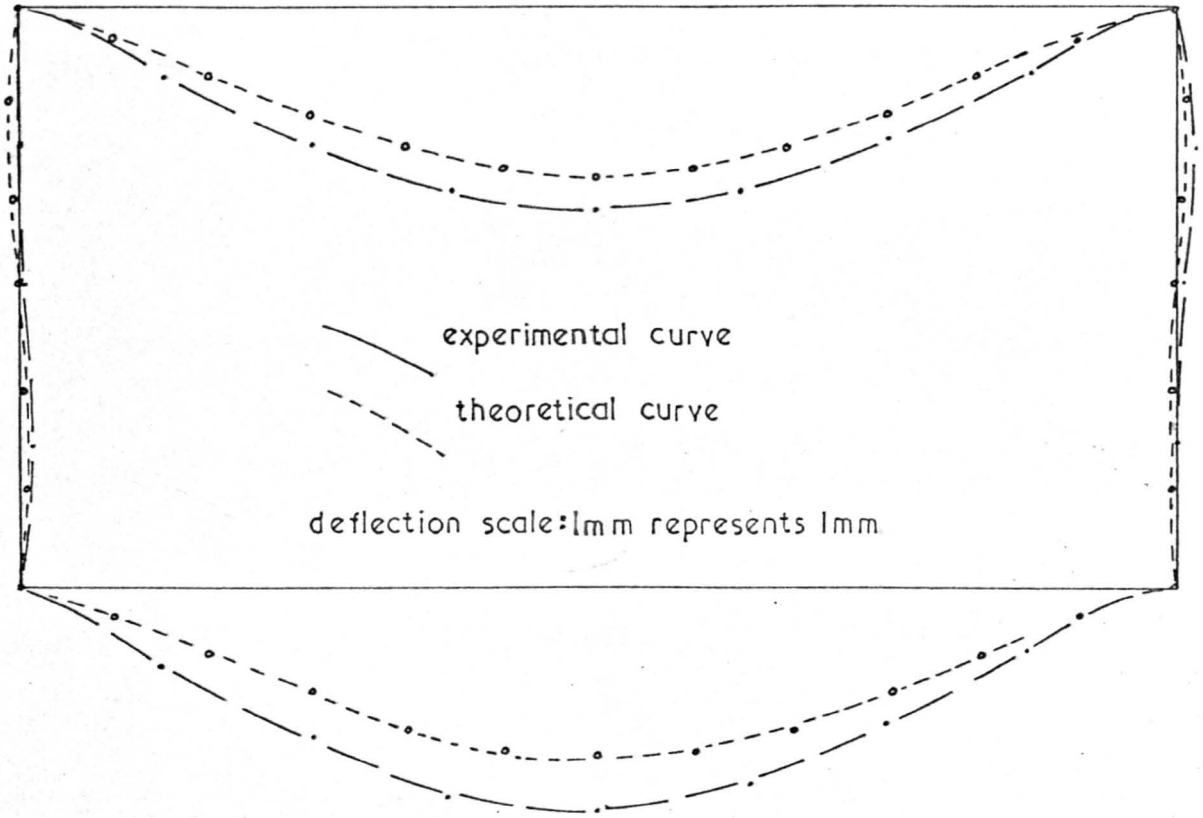

DIAGRAM 50: Deflection Profile of Frame 1 after 550 days of Sustained Load

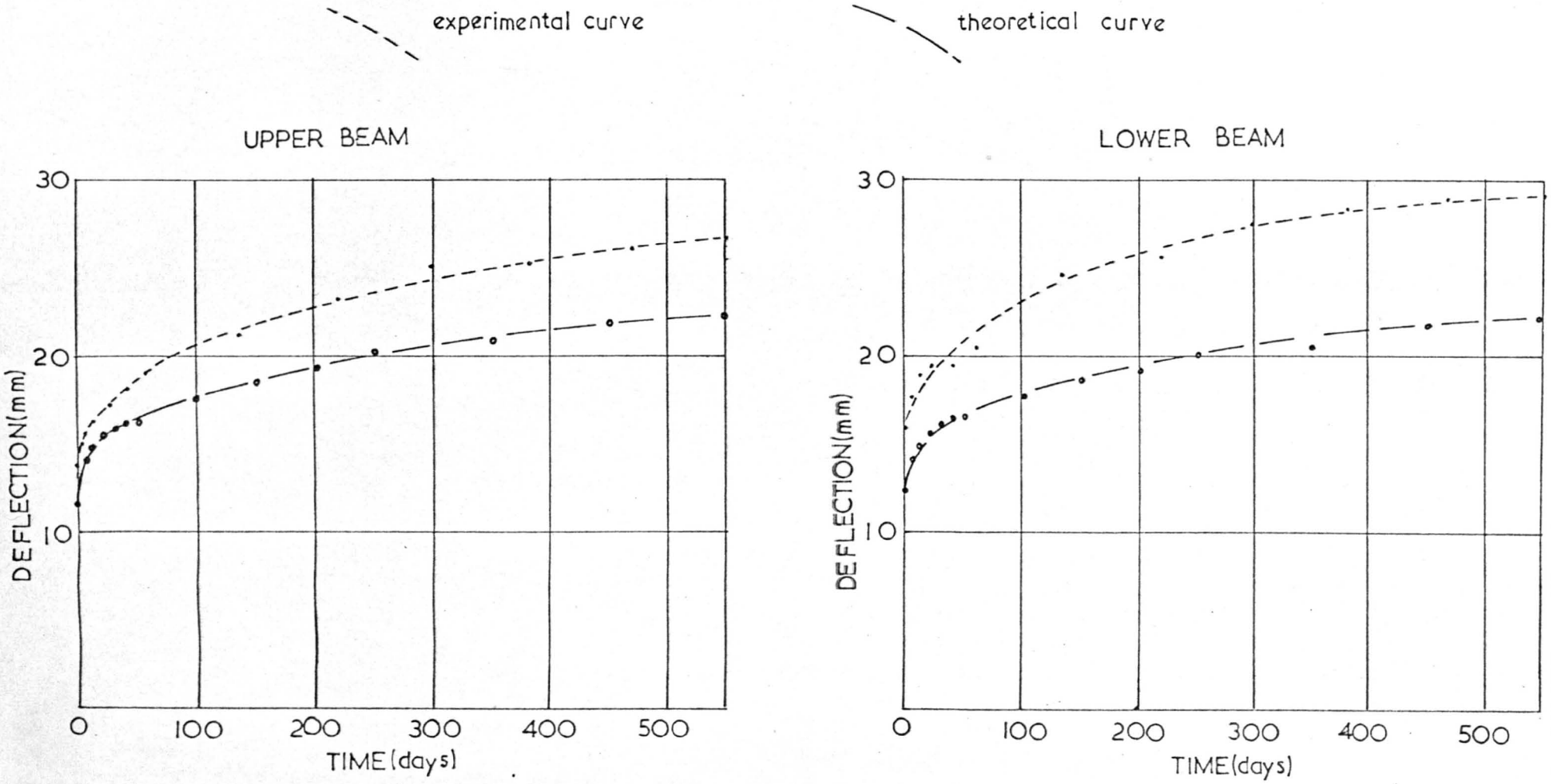

DIAGRAM 51: Centre Line Deflections of Frame 1 under Sustained Load

and the supports of the lower beam. However, diagram 14 shows that the extent of cracking is much more marked close to the supports than at midspan. The influence of shear on cracking in the lower beam can also be seen by considering the zones around the points of load application. On the support side of the point of load application shear is present whereas on the midspan side shear is zero and the effect on cracking is apparent. The influence of shear can also be seen in the top beam but, since this member is under uniformly distributed load, the length subjected to high shear is much less than in the lower beam. Extra cracking produces larger strains and consequently higher deflections; in this case, it is unknown how much of this extra deflection is due to flexural cracking and how much is due to the local cracking around the joints. Local cracking at the joints is marked in this frame as almost the full service moment was achieved in each member at each joint and the compressive axial load in the vertical members is very low.

As the members of the frame have the same cross section throughout, significant moment redistribution was not expected and this was confirmed by the computer solution shown in diagram 36.

On removal of load, the immediate recovery was approximately equal to the deformation on the application of load and the time dependent recovery over 100 days was approximately 10% of the immediate recovery.

The rather odd deflection profile of the right hand vertical member (diagrams 49 and 50) is thought to be due to a misreading of the dial gauge at the lowest location before loading.

(ii) Frame 2.

The deflection of the beam immediately after loading was 8.5 mm (span/715) and this increased to 18.16 mm (span/336) after 18 months of sustained load. The computer analysis gave a value of 8.1 mm (approximately 5% error) for immediately after loading and 16.3 mm (approximately 10% error) after 18 months of sustained load, see diagrams 52, 53 and 54.

These figures should be compared with the deflection of 6.9 mm calculated using the concrete section flexural rigidity and 16.1 mm calculated using the cracked transformed flexural rigidity. In both calculations the bending moment distribution was obtained using the concrete section throughout.

The agreement between theory and experiment is good but again the influence of local cracking at the joints is evident (see diagram 16). The computer analysis (diagram 36) shows cracking in the upper columns and the negative moment zone of the beam which has apparently been concentrated in local cracks at the joints.

The fact that the computer analysis shows slightly less time dependent deformation than was measured is probably due to the use of the moment curvature data from specimens which had been previously loaded. The effect of this previous loading would reduce creep and consequently the theoretical analysis gave rather less time dependent column deformation than in fact occurred and this is reflected in the slight under estimate of the deformation of the beam under sustained load.

The computer analysis shows redistribution of moments producing a reduction of approximately 3% in the support moment. This is due to time-dependent deformation of the column exceeding that of the beam. The computer analysis

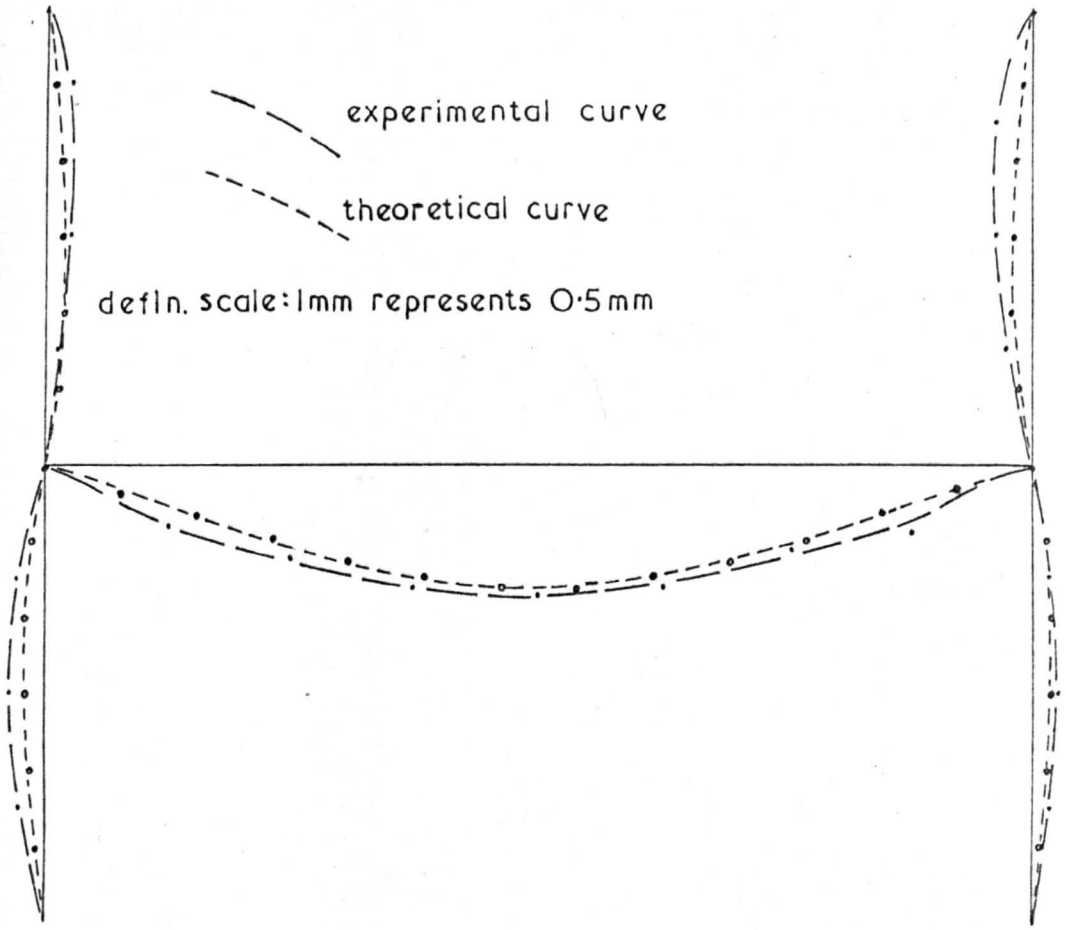

DIAGRAM 52: Deflection Profile of Frame 2 Immediately after Loading

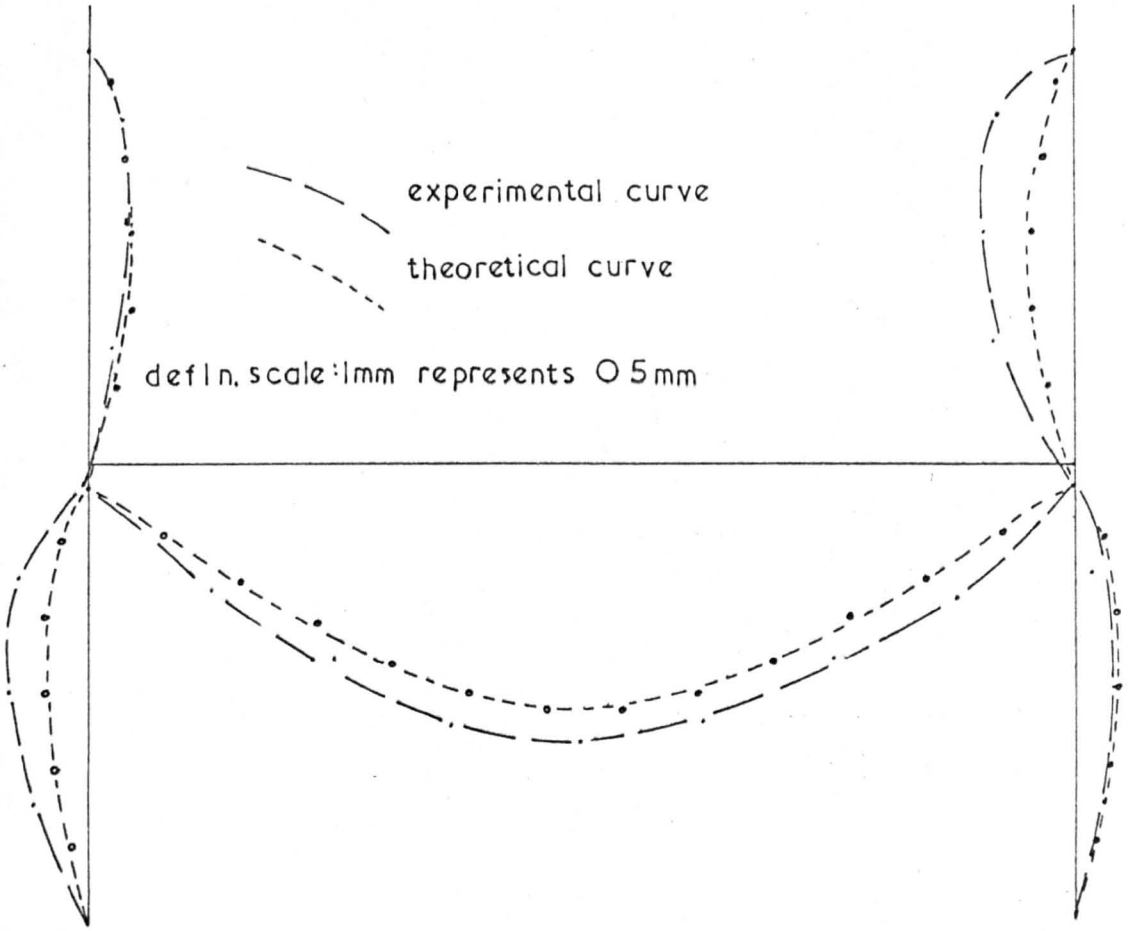

DIAGRAM 53: Deflection Profile of Frame 2 after 550 days of Sustained Load

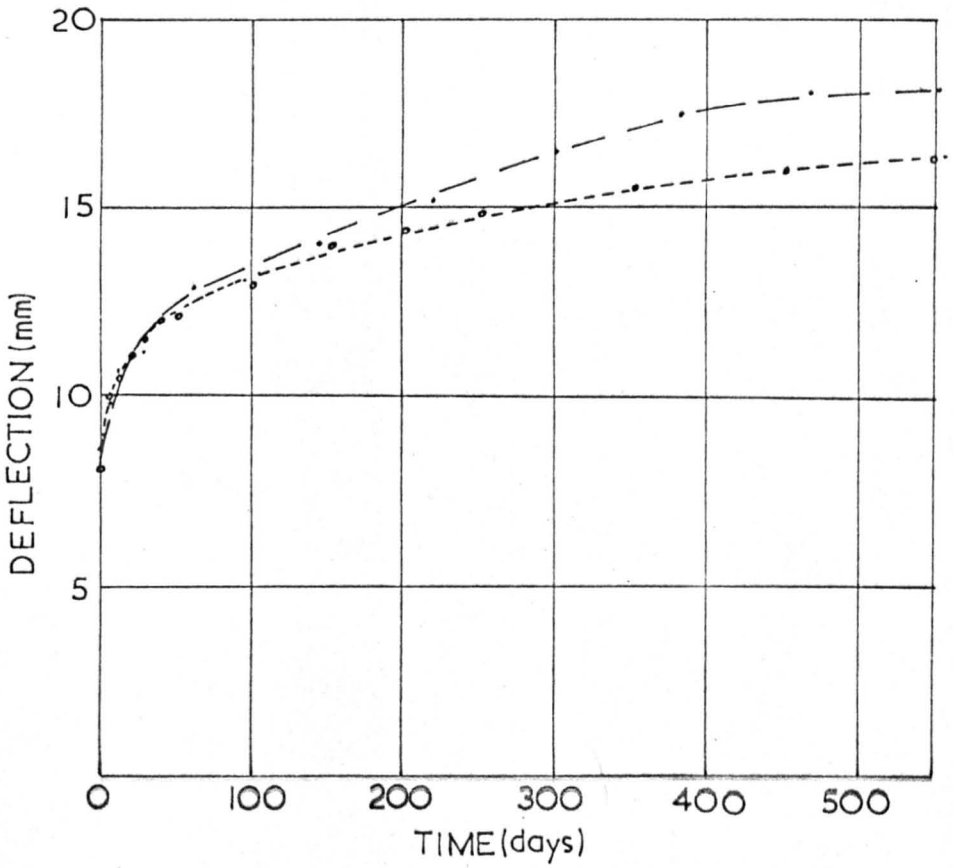

DIAGRAM 54: Beam Centre Line Deflections of Frame 2 under Sustained Load

probably under estimated this effect due to the influence of previous loading on the basic data it was using in the computation of column deformation.

However, another interesting point is that the computer analysis gave a support moment of 22.3 KNM immediately after loading; analysis based on the concrete section throughout gave a value of 19 KNM. This is due to the fact that there was less cracking in the columns than in the beam and this cracking occurred later in the loading history. Consequently use of the concrete section throughout leads to an underestimate of the support moment.

The computer analysis seriously underestimated the lateral deformation of the columns. This is probably due to the fact that the computer analysis makes no allowance for out of straightness, non symmetric placing of reinforcement or the secondary moments produced by lateral deformation as well as using the data from previously loaded specimens. In the most severe case the final moment produced by lateral deflection of a column was about 1.25 KNM which is about 22% of the moment at the centre of the column arising from primary analysis. The influence of accidental eccentricities and moments due to lateral deflection are very much increased by time-dependent deformation.

The between column variation of the column lateral deflections suggests that they were influenced by out of straightness considerations. The observations also suggest that the loading arrangement permitted some sideway of the frame although it was designed to prevent this.

The removal of load produced an immediate response in the beam deflection of 10.8 mm whereas the deformation on the application of load was 8.51 mm. After 100 days of recovery the beam deflection reduced by a further 1.65 mm.

The beam section moment-curvature specimens and in particular the column section moment-curvature specimens showed a response on removal of load greater than the response on load application.

(iii) Continuous Beam.

The deflection of the long span immediately after loading was 14.34 mm (span/488) and this increased to 24.34 mm (span/288) after 18 months of sustained load. The computer analysis gave a value of 13.27 mm (approximately 7.5% error) for immediately after loading and 23.44 mm (approximately 4% error) after 18 months of sustained load, see diagram 21, 55 and 56.

These figures should be compared with the deflection of 7.6 mm calculated using the concrete section flexural rigidity and 17.6 mm calculated using the cracked transformed flexural rigidity.

The agreement between theory and experiment is good although the influence of shear is again apparent. The effect of shear on cracking can be seen in diagram 18 and this probably caused the discrepancy between theory and experiment. It should be noted that the theoretical analysis under estimated the deflection of the long span and over estimated the deflection of the short span. This is entirely consistent with the view that shear caused the centre support zone to be less stiff than the pure moment data implied.

As the beam had the same cross section throughout, significant moment redistribution was not expected and this was confirmed by the computer solution shown in diagram 21.

The immediate response on load removal was 17.71 mm at the centre of the long span whereas the deflection on application of load was 14.34 mm.

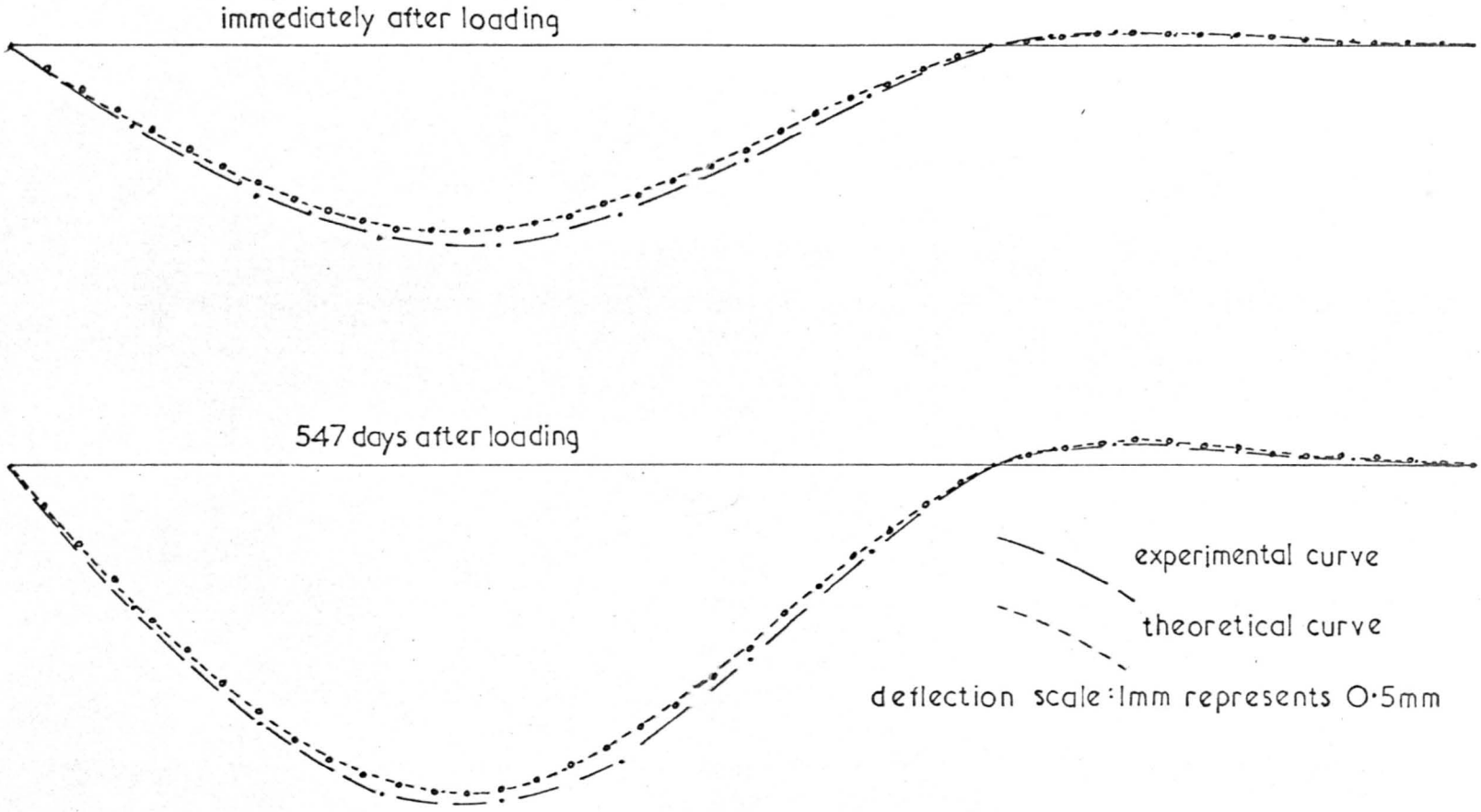

DIAGRAM 55: Deflection Profiles of the Continuous Beam

DIAGRAM 56: Deflections during Loading and under Sustained Load of the Centre Line of the Long Span of the Continuous Beam

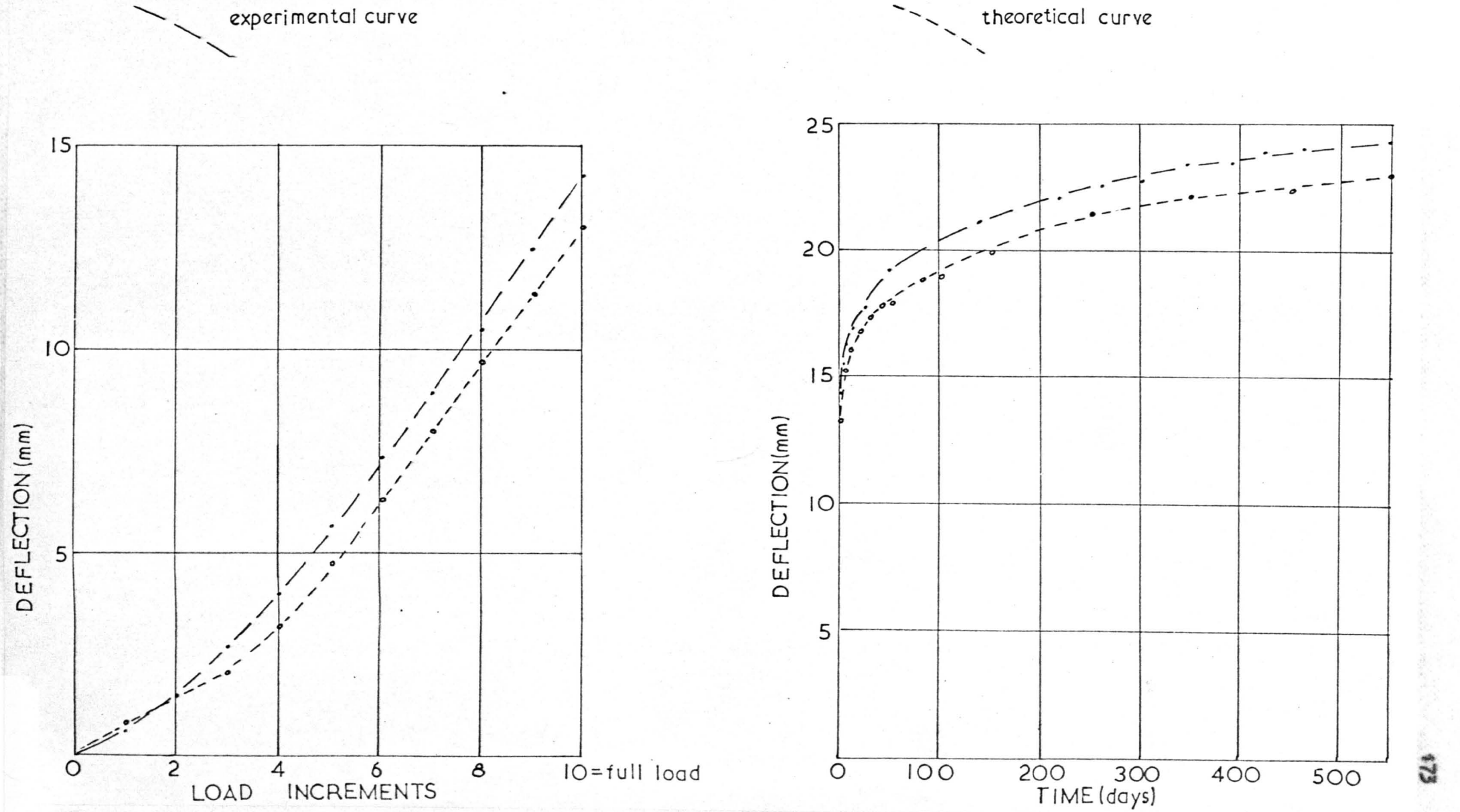

D. General Conclusions and Comments on Future Research

(i) Creep and Shrinkage in plain concrete.

It is hoped that the theoretical arguments leading up to the justification of a simple power law relationship between time strain and time and the good correlation with experimental data will lead to a greater fundamental understanding of the behaviour of concrete under sustained load. However, future experimental data is required to support this theory. It is important to establish what influences the two constants defining this law and the existence or otherwise of discontinuities. In short, it is desirable to have some information on the influence of mix proportions, environmental conditions, size and stress level on the form of the relationship. It is important to establish when discontinuities occur and how many are likely to occur in the probable life of a structure. If many discontinuities occur then the fact that the relationship is linear over short ranges will be of little value. For this purpose, it is important to take a great many observations during the sustained load tests and to perform the tests under closely controlled conditions. All the data so far considered had been obtained from tests in which the age at loading was so great that marked shrinkage and ageing were not present; it would be interesting to investigate the influence of these two effects on the relationship.

One wonders whether reinforced concrete exhibits a similar type of behaviour. The difficulty here is that reinforced concrete exhibits very much less strain than plain concrete (owing to the restraining influence of the reinforcement) and full scale tests inevitably introduce some scatter into the results owing to the increased difficulty of maintaining close control. However diagrams 57 and 58 show that reinforced concrete exhibits similar behaviour.

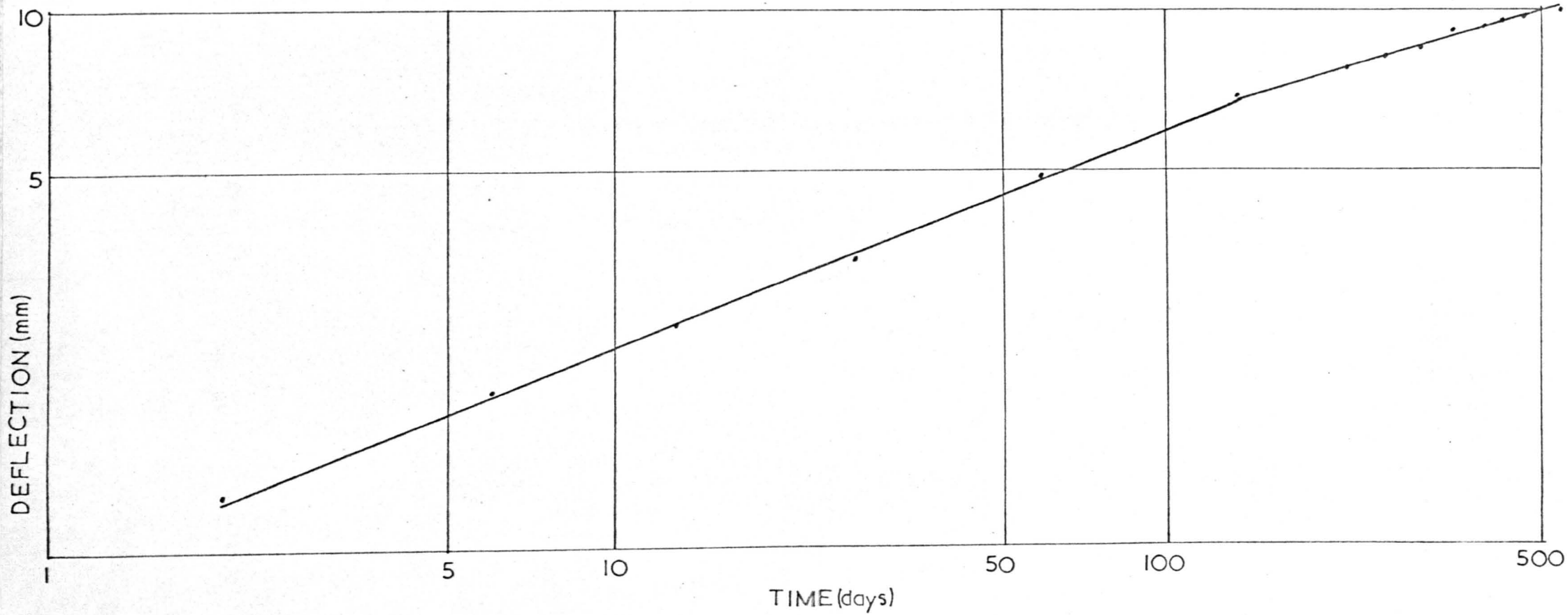

DIAGRAM 57: Time Dependent Deflection of the Centre Line of the Long Span of the Continuous Beam

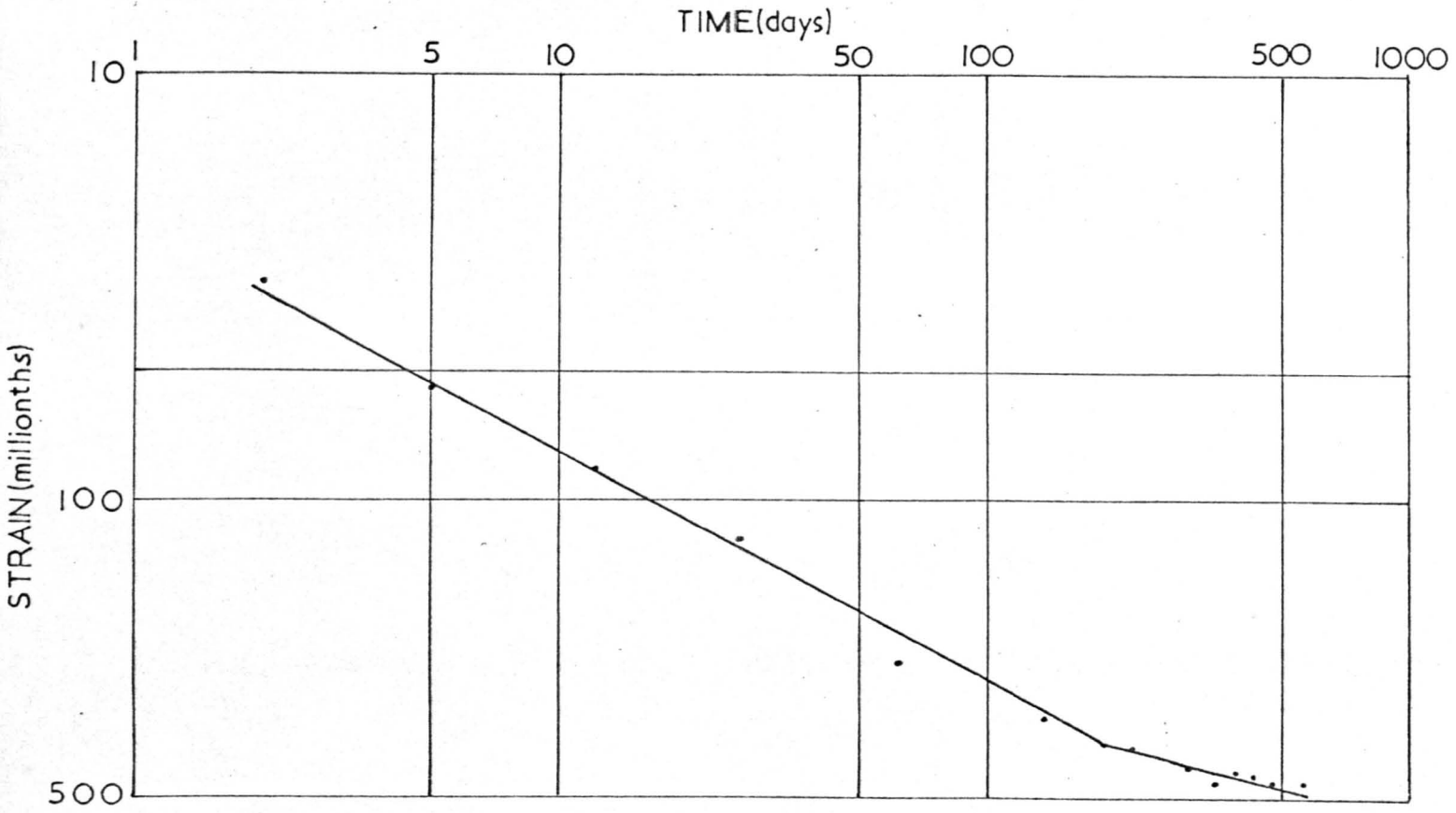

DIAGRAM 58: Axial Time Strain in Specimen C3

The analysis of experimental data in this way can now be seen as a rival to the computer analysis of structures and some comments on the relative merits of the two techniques is justified. It has long been recognised that classical analysis of materials involving following the history of each particle is impossible even with the aid of modern computers. Consequently the techniques of statistical physics coupled with experimental analysis offer the only realistic approach to the behaviour of plain concrete. However, in order to obtain the influence of the many relevant variables on the form of the relationship for plain concrete it is clear that a large amount of laborious and expensive experimental work is necessary. The extension of these techniques to reinforced concrete would in general require an impractical amount of experimental data. The development of computer programs may be laborious for the particular individuals concerned but it is generally more realistic economically than the alternative largely experimental approach. It is therefore felt that classical methods coupled with the brute force of the computer offer the most promising approach to the time dependent analysis of structures. Local strain patterns in a material are generally unimportant and a high level statistical approach will generally provide all the necessary information but in a full scale structure we generally require to calculate the deflection of each individual member and consequently a more detailed approach is necessary. It must also be appreciated that computer based classical techniques are now producing solutions to a meaningless accuracy from the practical point of view and the introduction of statistics into these techniques is overdue.

(ii) Behaviour of full scale structures

The influence of shear on flexural stiffness is apparent throughout this investigation. The latest draft of the Unified Code generally requires the provision of much less shear reinforcement than CP 114, frequently less

than half. In view of this and the increased importance of deflection under service loads the influence of shear on stiffness is clearly an issue which requires further investigation. The influence of shear on crack width is also neglected by the draft Unified Code. This point is not only a service load consideration; the influence of shear on stiffness as collapse is approached may have an appreciable effect on the force field.

Also, it must be emphasised that local cracking around joints may significantly affect midspan deflections. Whenever deflection is critical attention must be paid to reinforcement detailing at joints and both bending and shear stresses at the joint should be minimised.

The calculation of the bending moment distribution by using the concrete section throughout is likely to introduce appreciable error as in general beams will be cracked and columns uncracked. This effect is significant in a deflection calculation although generally unimportant in design against collapse. If this point is neglected an over estimation of deflection will generally result when initially out of balance moments are significant.

The effects of time dependent moment redistribution were revealed by the computer analysis to be less than anticipated. The estimation of moment redistribution by considering the stiffness changes of statically determinate components leads to an exagerated result. When the process is incremented by computer it can be seen that, in the first time increment, the extra deformation at, say, the support zone leads to a reduction in moment there and an increase in moment at midspan. Consequently in the next time increment the situation is reversed and a backwards and forwards moment redistribution occurs unless there is a very marked difference in behaviour between the midspan and support zones or between members. Thus in general moment redistribution effects will be small unless the arrangement of

compression reinforcement leads to significant differences in behaviour between parts of the structure. The tests performed by Washa and Fluck (20) would seem to have been very critical situations. The differences in behaviour between support and midspan zones are more serious than between span differences as moment redistribution will occur regardless of the existence of out of balance moment. Washa and Fluck's tests appear to be the only evidence of the magnitude of this form of redistribution. The computer program for continuous beam analysis is capable of dealing with this situation but as experimental data on the time dependent behaviour of only one beam cross section is currently available a meaningful test cannot be run. It is desirable to collect further information on this either by testing a series of suitable two span beams or by investigating the behaviour of a second beam cross section, to enable computer analysis.

The computer programs were written with service load analysis in mind but they could in principle be extended to cover loading to collapse if shear and buckling effects were included. The influence of time on collapse of reinforced concrete frames is a little investigated topic. In their current forms the computer programs perform incremental loading followed by incremental time. As rates of loading in practice are low, it would be interesting to consider incremental loading and incremental time simultaneously. It is felt that the influence of sustained load and slow application of load on reinforced structures is of considerably more importance than the effects of dynamic loads such as wind.

BIBLIOGRAPHY

BIBLIOGRAPHY

1. Report of the Reinforced Concrete Structures Committee of the Building Research Board with Recommendations for a Code of Practice for the Use of Reinforced Concrete in Building. DSIR: HM Stationery Office, 1934.

2. British Standard Code of Practice, CP 114: 1948 - The Structural Use of Normal Reinforced Concrete in Buildings: BSI 1948.

3. British Standard Code of Practice, CP 114: 1957 - The Structural Use of Reinforced Concrete in Buildings: BSI 1957 (amended in 1965 and 1967).

4. Why Limit State Design?: Bate S C C: Concrete, March 1968.

5. New Concepts in the Design of Structural Concrete: Rowe R E, Cranston W B and Best B C: The Structural Engineer, December 1965.

6. Proposals for the Control of Deflection in the New Unified Code: Beeby A W and Miles J R: Concrete, March 1969.

7. An Investigation of the Crack Control Characteristics of Various Types of Bar in Reinforced Concrete Beams.

8. Symposium on Design for Movement in Buildings: The Concrete Society, October 1969.

9. Studies in Reinforced Concrete. II - Shrinkage Stresses: Glanville W H: Building Research Technical Paper No 11, DSIR 1930.

10. Studies in Reinforced Concrete. III - The Creep or Flow of Concrete under Load: Glanville W H: Building Research Technical Paper No 12, DSIR 1930.

11. Creep of Concrete under Load: Glanville W H and Thomas F G: The Structural Engineer, February 1933.

12. Studies in Reinforced Concrete. IV - Further investigations on the Creep or Flow of Concrete under Load: Glanville W H and Thomas F G: Building Research Technical Paper No 21, DSIR 1939.

13. Concrete Creep Data: Ross A D: The Structural Engineer, August 1937.

14. The Effects of Creep on Instability and Indeterminacy Investigated by Plastic Models: Ross A D: The Structural Engineer, August 1946.

15. A New Aspect of Creep in Concrete and its Application to Design: McHenry D: Proc. ASTM 1943.

16. Shrinkage and Creep in Concrete: Lea F M and Lee C R: Symposium of The Society of Chemical Industry, May 1946.

17. Theories of Creep in Concrete: Neville A M: Journal of American Concrete Institute, September 1955.

18. Sustained load Strength of Eccentrically Loaded Short Reinforced Concrete Columns: Viest I M, Elstner R C and Hognestad E: Journal of American Concrete Institute, March 1956.

19. Effect of Compressive Reinforcement on the Plastic Flow of Reinforced Concrete Beams: Washa G W and Fluck P G: Journal of the American Concrete Institute, October 1952.

20. Plastic Flow (Creep) of Reinforced Concrete Continuous Beams: Washa G W and Fluck P G: Journal of American Concrete Institute, January 1956.

21. Creep of Concrete Under Variable Stress: Ross A D: Journal of American Concrete Institute, March 1958.

22. Creep and Creep Recovery of Concrete under High Compressive Stress: Freudenthal A M and Roll F: Journal of American Concrete Institute, June 1958.

23. Long-time Creep and Shrinkage Tests on Plain and Reinforced Concrete: Troxell G E, Raphael J M and Davis R E: Proc of American Society for Testing of Materials, 1958.

24. Role of Cement in the Creep of Mortar: Neville A M: Journal of American Concrete Institute, March 1959.

25. Recovery of Creep and Observations on the Mechanism of Creep of Concrete: Neville A M: Applied Scientific Research, 1960.

26. Instantaneous and Long Time Deflections of Reinforced Concrete Beams under Working Loads: Yu W and Winter G: Journal of American Concrete Institute, July 1960.

27. Shrinkage and Creep Influence on Deflections and Moments of Reinforced Concrete Beams: Gesund H: Journal of American Concrete Institute, May 1962.

28. Some Problems in the Theory of Creep: Arutyunyan N: Pergamon Press, 1966.

29. Creep of a Cracked Reinforced Beam: Sackman J L and Nickel R E: Journal of Structural Division, Proc of American Society of Civil Engineers, 1968.

30. Creep and Shrinkage Effects in Reinforced Concrete Beams: Leong T W and Warner R F: University of New South Wales, Australia UNICIV Report No R.40, February 1969.

31. Methods of Computing Stress in Concrete from a History of Measured Strain: England G L and Illston J M: Civil Engineering and Public Works Review, April, May and June 1965.

32. The Components of Strain in Concrete under Sustained Compressive Stress: Illston J M: Magazine of Concrete Research, March 1965.

33. Instantaneous and Time Dependent Deflections of Simple and Continuous Reinforced Concrete Beams: Branson D E: Alabama Highway Research Report No 7.

34. Tests on Beams with Sustained Load: Hajnal-Konyi K: Magazine of Concrete Research, Vol 15, March 1963.

35. Time dependent deflections of Reinforced Concrete Beams: Corley W G and Sozen M A: Journal of American Concrete Institute, March 1966.

36. Components of Creep in Mature Concrete: Illston J M: Journal of American Concrete Institute, March 1968.

37. Numerical Creep Analysis Applied to Concrete Structures: England G L: Journal of American Concrete Institute, June 1967.

38. British Standards Institution: Unified Code of Practice for Structural Concrete. (In draft) 1969.

39. Deformation, Strain and Flow: Reiner M: H K Lewis & Co Ltd, 1960

40. The Inelastic Behaviour of Engineering Materials and Structures: Freudenthal A M: John Wiley, New York, 1950.

41. Progress in Understanding High Temperature Creep: Dorn J E: H W Gillet Memorial Lecture, American Society for Testing and Materials, 1962.

42. Deflections of Reinforced Concrete Beams: Stevens R F and Bryden-Smith D W: Building Research Station Seminar on Deformed Bars in Concrete, April 1970.

43. Creep of Lightweight Concrete: Best C H and Polivka M: Magazine of Concrete Research, November 1959.